GA–A23328

DIII–D THREE-YEAR PROGRAM PLAN 2000–2002

by
R.D. STAMBAUGH and RESEARCH STAFF OF THE DIII–D TEAM

JANUARY 2000

DISCLAIMER

GA–A23328

DIII–D THREE-YEAR PROGRAM PLAN 2000–2002

by
R.D. STAMBAUGH and RESEARCH STAFF OF THE DIII–D TEAM

Work supported by
the U.S. Department of Energy
under Contract No. DE-AC03-99ER54463

GA PROJECT 30033
JANUARY 2000

ABSTRACT

This three year program plan presents a summary of the research planned on the DIII–D tokamak in the years 2000–2002. Reference is made to GA–A22950, "The DIII–D Five-Year Program Plan," which is a comprehensive discussion of research planned for DIII–D in the period 1999–2003.

CONTENTS

CONTENTS (Continued)

LIST OF FIGURES

LIST OF TABLES

1. EXECUTIVE SUMMARY

1.1. MISSION OF THE DIII–D NATIONAL FUSION PROGRAM

The overall mission statement of the DIII–D Program is "To establish the scientific basis for the optimization of the tokamak approach to fusion energy production."

The main output of the DIII–D Research Program is a scientific basis. "Scientific" means developing a solid understanding of the underlying physical principles and incorporating it into useful predictive modeling tools. "Optimization" means experimentally demonstrating performance parameters at the theoretically predicted limits for the tokamak magnetic confinement system and achieving to the greatest degree possible an integrated, steady-state demonstration of optimized performance that projects to an attractive fusion power system. The integrated optimization sought and the scientific basis established will allow the definition of optimal paths to fusion energy using the tokamak approach.

1.2. DIII–D NATIONAL PROGRAM RESEARCH GOALS

This mission has been elaborated by the DIII–D Research Council in three additional research goal statements.

1. The DIII–D Program's primary focus is the Advanced Tokamak (AT) Thrust that seeks to find the ultimate potential of the tokamak as a magnetic confinement system.
2. Where it has unique capabilities, the DIII–D Program will undertake the resolution of key enabling issues for advancing various magnetic fusion concepts.
3. The DIII–D Program will advance the science of magnetic confinement on a broad front, utilizing its extensive facility and national team research capability.

Determining the ultimate potential of the tokamak as a confinement system is a complex scientific endeavor. The integration of advanced tokamak elements into achievable single discharges requires programmatic compromise and tradeoffs evolved over a multi-year period.

In order to provide more focus on critical issues in the DIII–D Program, the method of organization of the experimental research was changed in 1998. The main motivation for the new scheme was the desire to gain a more purposeful and visible path to the eventual AT integrated plasma scenarios targeted in the Five-Year Plan. This new scheme also makes it natural to create cross-disciplinary teams to pursue integrated plasma scenarios. The new scheme is a matrix type of approach in which one dimension of the matrix is a set of Thrusts. A Thrust is aimed at a key objective of the research and is given a significant block of run time in which to realize its objectives. The research thrusts and their leaders will change year-to-year to keep up with the evolution of the experimental program. Most of the thrusts in the 2000 run plan relate to the AT goal of the DIII–D Program. The AT Program in its broad outlines is described in Section 2.2 of the Five-Year Plan. This work pursues Goal 1 above.

The second dimension of the experimental planning matrix is comprised of the four enduring topical areas of fusion energy science: stability, confinement and transport, divertor/edge physics, and heating and current drive. The DIII–D Facility and the DIII–D National Team is a resource of immense value to the U.S. Fusion Program in terms of advancing the science of magnetic confinement on a broad front. DIII–D has a superb diagnostic set, increasingly flexible and capable plasma control systems, an excellent research staff, and a comprehensive set of analysis codes and theory support that enable real learning in depth from the experiments done. The staff recognizes and embraces a responsibility to the greatest extent possible to use that resource to advance the state of fusion energy science knowledge generally.

The managers of these topical areas implement this second dimension of the matrix and have responsibility for the work supporting Goal 3 above. Their continuing leadership of these topical areas over a period of years assures the continued scientific focus of the DIII–D research. A thorough discussion of the scientific topics being pursued in the DIII–D Program can be found in Section 2.3 in the Five-Year Plan.

The DIII–D Research Staff also are strongly motivated to see magnetic confinement progress to future next-step devices. The AT work and the broader scientific work on DIII–D can contribute greatly to the definition and the support for these future machine initiatives. Some of those possible next step options are:

An international D-T burning plasma experiment such as the RTO-RC ITER which plans more exploitation of and/or reliance on AT physics.

An advanced performance superconducting tokamak (JT–60SU, ARIES-RS) which exploits AT physics toward steady-state.

A copper-coil ignition experiment about the size of JET and using gyroBohm scaling of H–mode, relying on more conventional tokamak physics.

A compact, high magnetic field copper-coil ignition experiment (as exemplified by CIT/BPX/IGNITOR) but enabling studies of or relying on AT physics (FIRE).

A next-step spherical torus which relies on most elements of AT physics to enable the study of burning plasma physics in long pulse or steady-state.

Research toward Goal 2 can appear either as thrusts or as elements of the Topical Science Area plans. A discussion of how DIII–D research relates to the various future machine possibilities can be found in Section 2.4 of the Five-Year Plan.

Competition for experimental time on DIII–D is intense. Priority goes to the Advanced Tokamak work, which occupies most of the thrusts. We seek to reserve about 30%–40% of the run time for the Topical Area Managers to allocate to more broadly motivated studies. The work to support Goal 2 has to find time either as a thrust or in the Topical Areas.

1.3. DIII–D AND FESAC FIVE-YEAR GOALS

In this section, we outline how in the next five years the DIII–D National Program will make major contributions to the newly defined FESAC Goals and Objectives for Magnetic Fusion Energy (see Table 1: Goals and Near-Term/Long-Term Objectives for MFE, "Report of the FESAC Panel on Priorities and Balance," September 1999).

FESAC Goal 1

Goal: • Advance fundamental understanding of plasma, the fourth state of matter, and enhance predictive capabilities, through comparison of experiments, theory and simulation.

In the area of high temperature plasma science the DIII–D combines an internationally unexcelled capability for reproducibly producing high temperature plasmas in a wide range of plasma shapes, a unique ensemble of plasma diagnostics with outstanding spatial and temporal resolution, and close coupling to the exceptional U.S. MFE theory and modeling community. The FESAC 5-year objectives and specific DIII–D 5-year research directions are:

- **Turbulence and Transport:** *Advance understanding of turbulent transport to the level where theoretical predictions are viewed as more reliable than empirical scaling in the best understood systems*.

  An overall goal for the DIII–D program is to work towards a predictive understanding of tokamak transport. Achieving this goal requires the combined efforts of theorists, modelers, and experimentalists to develop the fundamental theories, include them in numerical models, compare those models with the results of experiments and then iteratively improve them. The key issues here are understanding turbulent transport in both the electron and ion channels. Our work over the next few years will include fundamental investigations of the nature of tokamak turbulence, comparison of those turbulence measurements with predictions of gyrokinetic and gyrofluid codes, and definitive tests of present-day transport models in well-diagnosed plasmas using both steady-state and modulated techniques. In addition, we will be further testing the model of $E \times B$ shear suppression of turbulence by utilizing various techniques (e.g. impurity injection, electron heating) to investigate the functional dependence of the turbulence growth rates on these plasma parameters. Finally, by use of $E \times B$ shear to stabilize the longer wavelength, ion temperature gradient modes, we will attempt to isolate and investigate the shorter wavelength modes which primarily affect electron transport.

- **Macroscopic Stability:** *Develop detailed predictive capability for macroscopic stability, including resistive and kinetic effects*.

  DIII–D is conducting experiments aimed at validating theoretical models for ideal, resistive, and kinetic plasma instabilities using experimental measurements adequate for quantitative tests of the theoretical calculations. The goal is to extend the DIII–D performance to the theoretical limits of stability and to develop the intellectual, computational, and laboratory tools necessary to apply these results to other devices.

- **Wave-Particle Interactions:** *Develop predictive capability for plasma heating, flow and current drive, as well as energetic particle driven instabilities, in power-plant relevant regimes.*

  The DIII–D Program will develop methods of plasma current generation (initiation, rampup, sustainment, and profile control) to provide future devices the basis for full steady-state transformerless operation. DIII–D is developing the physics basis being embodied in predictive codes for electron cyclotron, fast wave, and neutral beam current drive and for maximal use of the self-driven bootstrap current.

- **Multi-Phase Interfaces:** *Advance the capability to predict detailed multi-phase plasma-wall interfaces at very high power- and particle- fluxes.*

  DIII–D will bring 2-D measurements of divertor plasma properties into comparison with 2-D predictive code calculations of those properties. The DIII–D principal research direction will be to maximize the degree of recombination and radiation in the divertor plasma in order to minimize heat fluxes to and erosion of plasma facing surfaces. Detached plasma states with high recombination fractions have been found and successfully simulated in the 2-D codes. The frontier task is to achieve these regimes in the lower density plasmas optimal for current drive and high bootstrap fractions.

FESAC Goal 2

Goal: • *Resolve outstanding scientific issues and establish reduced-cost paths to more attractive fusion energy systems by investigating a broad range of innovative magnetic confinement configurations*.

The Advanced Tokamak vision of the ultimate potential of the tokamak as defined by theory work has extremely hollow current profiles and nearly 100% self-organized bootstrap current produced by high quality transport barriers near the plasma edge. These equilibria are certainly highly innovative and are so different from normal tokamak experience as to essentially constitute an alternate concept. Studies have shown that these modes, if realized, can halve the cost of electricity in tokamak fusion power systems.

The experimental and theoretical research DIII–D carries out in pursuit of the AT vision has many elements of generic value across magnetic confinement concepts:

- **Electrostatic Turbulence Suppression:** The mechanism of stabilization of at least electrostatic turbulence by sheared E×B flows, pioneered by DIII–D, appears to be universal across magnetic confinement concepts and is a continuing focus of DIII–D research.

- **Wall Stabilization:** The physics and technology of stabilization of modes by a nearby conducting wall and feedback coil system being investigated on DIII–D is a development necessary for the spherical torus, RFP, spheromak, and FRC.

- **Energetic Particle Density Gradient Driven Instabilities:** The study of these instabilities was identified as having generic value across concepts at the Snowmass Summer Study. Such modes, excited by the fast ions from the neutral beams, are an important subject of study in DIII–D.

- **Current Drive by Waves and Beams:** The wave-particle and beam-plasma interaction physics, developed in the tokamak generally and DIII–D in particular, for driving current is largely generic across magnetic concepts.

- **Parallel Field Line Physics:** The physics investigations in the scrape-off layer and divertor plasmas is largely generic across concepts because of the dominant role of the parallel heat and particle flows and the prominence of concept non-specific atomic physics. The DIII–D divertor research emphasis on systematic experiments, 2-D diagnostic measurements, and modeling enables transfer to other concepts of the understanding gained.

FESAC Goal 3

Goal: • *Advance understanding and innovation in high-performance plasmas, optimizing for projected power-plant requirements; and participate in a burning plasma experiment.*

The DIII–D National Program was instrumental in defining the Advanced Tokamak concept. This vision of the ultimate potential of the tokamak as defined by theory work has extremely hollow current profiles and nearly 100% self-driven bootstrap current produced by high quality transport barriers near the plasma edge. Theory predicts that with wall stabilization of ideal modes the beta limit in the tokamak can be about twice the free boundary limit. Transport rates as low as neoclassical in the ions are envisioned and have been seen in experiments. Detached, highly recombining divertor operation needs to be combined with these advanced core plasma modes. Studies have shown that these modes, if realized, can halve the cost of electricity in tokamak fusion power systems and enable modest sized burning plasma experiments reaching for high gain and steady-state.

The FESAC 5-year objectives and specific DIII–D 5-year research directions are:

- *Assess profile control methods for efficient current sustainment and confinement enhancement in the Advanced Tokamak, consistent with efficient divertor operation, for pulse length >>* τ_E.

  Efficient current sustainment will be achieved on DIII–D by maximizing the bootstrap current and supplementing that with electron cyclotron, fast wave, and neutral beam current drive. Near term scenarios being pursued aim at bootstrap fractions over 50% and sustained with current profile control (for up to 5 seconds) by microwave ECH power in a divertor plasma with a normalized beta of 4 and an energy confinement enhancement 2.5 times L–mode. Parallel lines of research on transport barrier physics and divertor physics in closed, pumped divertors are laying the groundwork for eventual long pulse integrated scenarios beyond the near term work.

- *Develop and assess high-beta instability feedback control methods and disruption control/amelioration in the Advanced Tokamak, for pulse length >> τ_E.*

DIII–D is developing the physics and the technology of stabilization of kink modes by a conducting wall backed by non-axisymmetric feedback coils. Stabilization of neoclassical tearing modes by direct application of ECCD and indirect methods of current profile alteration by ECCD will be researched. DIII–D has an extensive program of stability studies and plasma control development aimed at enabling disruption free operation close to stability limits. The injection of impurity pellets, massive gas puffs, or liquid jets shows promise of success at providing a means of ameliorating the consequences of disruptions.

FESAC Goal 4:

Goal: • *Develop enabling technologies to advance fusion science; pursue innovative technologies and materials to improve the vision for fusion energy; and apply systems analysis to optimize fusion development.*

The DIII–D will deploy, and thereby foster, the development of a number of enabling and innovative technologies. Most notable are advanced methods for plasma heating and current drive (microwave ECRF); disruption mitigation by solid, liquid, or gas injection; plasma fueling (inside pellet launch); plasma flow control (neutral beam, ECRF, ICRF); investigation of novel divertor concepts; feedback technologies for wall stabilization; studies of surface erosion; and small-sample testing of low activation materials in plasma environment.

Summary

Within world fusion science research, the DIII–D National Program aims to retain leadership in advanced tokamak research and in high temperature plasma science. In so doing, results from DIII–D research will be of benefit to other magnetic confinement configurations and will serve as a test bed for several enabling and innovative technologies.

1.4. THE DIII–D PROGRAM INTERNATIONAL ROLE

DIII–D advanced tokamak research is carried out with extensive international collaboration to provide opportunities for scientific confirmation and joint experiments. Worldwide tokamaks (with characteristics listed in Table l) have research programs which differ and complement each other; a summary of research capabilities is given in Table 2. International databases enable documenting accomplishments, comparing results of experiments and theory, and coordinating research. U.S. tokamaks make vital contributions to the world program with a focus on concept innovation and optimization.

Table 1
Characteristics of Operating World Tokamaks

	Plasma Current (MA)	Magnetic Field B(T)	Major Radius R (m)	Comment
Performance Extension Tokamaks				
JET	6.0	4.0	3.0	E.U.
JT–60U	3.0	4.4	3.3	Japan
DIII–D	3.0	2.1	1.7	U.S.
Alcator C–Mod	2.0	9.0	0.65	U.S.
Tore Supra	1.7	4.0	2.3	France (superconducting)
ASDEX Upgrade	1.6	3.1	1.7	Germany
Proof-of-Principle Tokamaks				
FT–U	1.6	8.0	0.93	Italy
TCV	1.2	1.4	0.88	Switzerland
TEXTOR	1.0	3.0	1.75	Germany
JFT–2M	0.5	2.2	1.3	Japan
T–10	0.4	3.0	1.5	Russia
Compass-D	0.4	2.1	0.55	England
Triam-1M	0.15	8.0	0.84	Japan (superconducting)
Concept Exploration Tokamaks (partial list)				
JFT–2M	0.5	2.2	1.3	Japan
ET	0.3	0.25	5.0	U.S./UCLA
Truman-3M	0.18	1.2	0.5	Russia
HBT–EP	0.025	0.35	0.95	U.S./Columbia U.
Steady State Tokamaks (under construction)				
KSTAR	2.0	3.5	1.8	Korea (2004)
HT–7U	1.0	3.5	1.7	China (2004)
SST–1	0.22	3.0	1.1	India (2002)

Table 2
World Advanced Tokamak Research Capabilities

Research Facility	Unique Research Capability
Performance Extension Tokamaks	
JET (E.U.)	DT capability at large size
JT–60U (Japan)	Long pulse high performance physics at large size
DIII–D (GA)	High shape flexibility, high beta, divertor, ECH
Alcator C–Mod (MIT)	High field, high density divertor
Tore Supra (France)	Long pulse superconducting
ASDEX Upgrade (Germany)	AT physics
Proof-of-Principle Tokamaks	
FT–U (Italy)	High field, IBW
TCV (Switzerland)	High elongation
Concept Exploration Tokamaks	
ET (UCLA)	High beta via omnigeneity
HBT–EP (Columbia U.)	High beta via feedback

Comparing results from DIII–D with the two larger higher-temperature European and Japanese devices provides an opportunity to extend DIII–D research results and understanding to a larger scale. The European JET can operate with D-T plasmas, while the Japanese JT–60U research focuses on steady-state high-performance plasmas. Three mid-size divertor tokamaks are equipped with sufficient plasma heating, control, and diagnostic systems to carry out advanced tokamak research on a broad front. DIII–D is a low-field tokamak with high power heating including ECH for high-beta advanced tokamak research. DIII–D is unique worldwide with its poloidal field magnet capability for extensive research in plasma shaping and to emulate other tokamak shapes for coordinated joint research. Alcator C–Mod is the world's highest-field tokamak, capable of very high-density operation with equal electron and ion temperatures, with plasma pressure equal to that expected in a reactor. Its compact size and closed divertor configuration offer unique capabilities for studying high power-density plasma exhaust physics. Together DIII–D and Alcator C–Mod provide data from two plasmas with very different physical parameters but similar dimensionless parameters. The German ASDEX-Upgrade has external plasma shaping control coils of more reactor relevance but with less shape flexibility than DIII–D. Three non-divertor tokamaks, TEXTOR, FTU, and Tore Supra address pumped limiter, high field physics and steady-state current drive, and heat removal respectively. Korea is constructing a superconducting advanced tokamak (KSTAR), and China is engineering the design of a superconducting tokamak (HT-7U). DIII–D collaborates with all these international tokamaks.

Two U.S. experiments contribute to tokamak concept exploration. The Columbia University high beta tokamak (HBT-EP) is addressing wall stabilization and active mode control, issues critical for advanced tokamak operation now being extended to DIII–D. The UCLA Electric Tokamak (ET) is a low-curvature electric tokamak built to explore the possibility of achieving classical confinement and unity beta in tokamaks.

The National Academy has suggested research program strengths can be classified as to their leadership uniqueness in the context of related world programs. In this respect, DIII–D is unique in its plasma shape flexibility, its high beta research including feedback stabilization, its comprehensive transport diagnostics, its ECCD profile control capability, and its advanced tokamak divertor program. DIII–D pioneered advanced tokamak concepts through an integrated approach to fusion energy science and is a leading supplier of results to international physics databases. DIII–D is among world leaders in ICRF (having pioneered fast wave current drive), in the study of neoclassical tearing modes (collaborating with AUG and JET), and in pellet fueling. DIII–D does not commit significant resources to a number of research areas where others have strong leads. These areas include large scale facility size, D-T capability, LHCD, and metallic divertor. From the above classification it is evident that DIII–D strives for leadership in several areas of fusion science and physics innovation rather than in fusion technology where other world facilities lead.

1.5. RESEARCH PLAN LOGIC

Our long range AT Program will evolve in two phases. First to establish the credibility of the AT approach, we have set out on a three year (1999–2001) focus on demonstrating intermediate AT scenarios for 5 seconds. Two intermediate scenarios, are described in Sections 2.2.1 and 2.2.2 and will be carried out with lower toroidal field, plasma current, and EC power less than our ultimate objective. Achievement of this intermediate objective in 2001 will provide a basis point for pressing on to the second phase of our AT program, developing deeper scientific understanding of AT physics, and exploring the ultimate potential of the tokamak. That potential, as defined by theory calculations of stability and the residual transport after ITG turbulence is suppressed involves very broad pressure profiles, transport barriers near the plasma edge, nearly 100% bootstrap current in a peak near the edge, and very high normalized beta supported by effective wall stabilization systems. These more challenging investigations as well as our intermediate scenarios will be extended to 10 second pulses at full (2.1 T) toroidal field in DIII–D. These ultimate scenarios are described in Section 2.2.3.

The logic diagram for the DIII–D Advanced Tokamak Program has been revised to take account of progress in 1999 and is shown in Fig. 1. The main line is the pursuit of

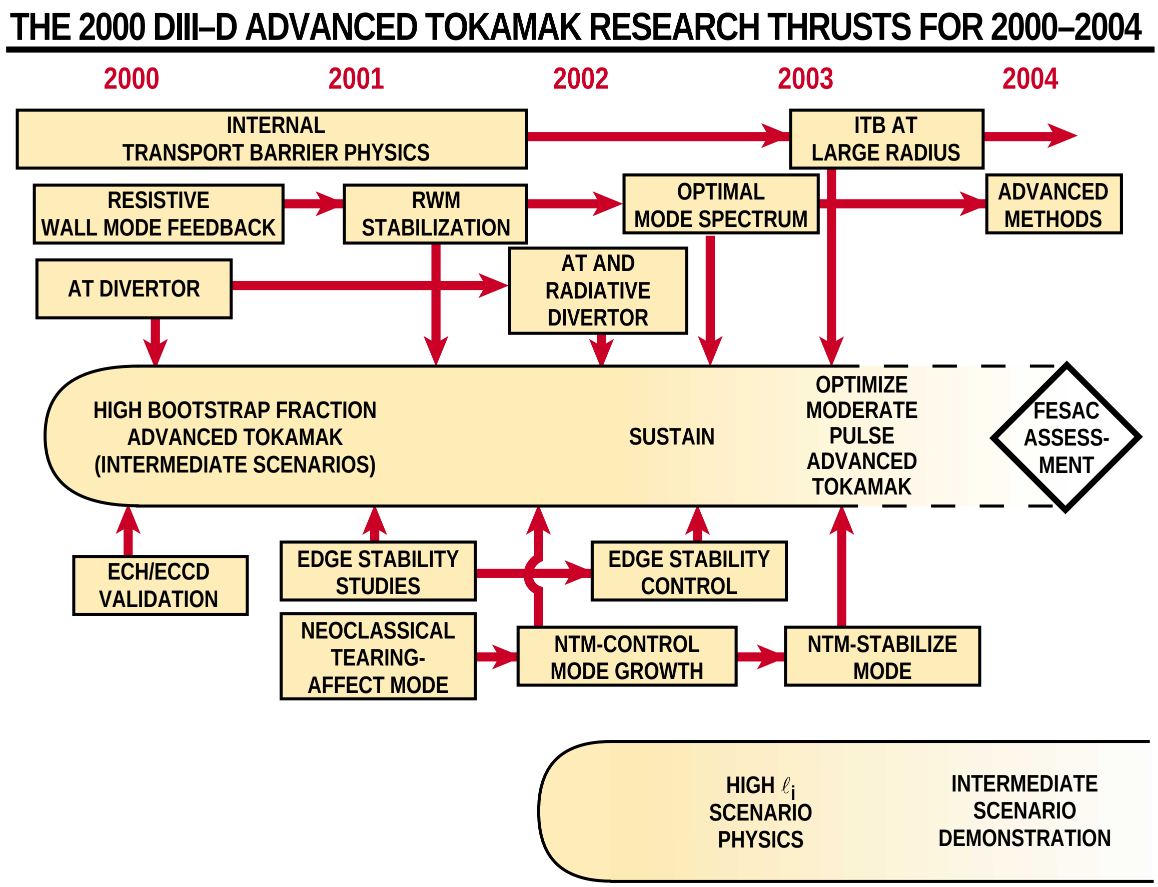

Fig. 1. Logic diagram for the DIII–D Advanced Tokamak Program.

the high bootstrap fraction AT scenario. This scenario was described as the negative central shear scenario in Section 2 because it derived from the exciting negative or reversed shear discoveries in tokamaks in the last few years. However, since our results to date have been most positive with weak or slightly positive shear, we have called this line of AT research simply the high bootstrap fraction scenario in this diagram and in our research thrust lists. The matter of whether the optimal shear is negative or weakly positive will be decided by the research. Good progress was made on this scenario in 1999. To prepare for the new but limited ECCD power in 2000, this scenario begins at the reduced current and field of 1.2 MA and 1.6 T. In 1999, without any active current profile control, discharges with $\beta_N H_{89} \sim 9$ for 2 seconds (16 energy confinement times) were achieved, exceeding our expectations for 1999 preparatory work. The duration of these discharges was limited by the uncontrolled inward diffusion of the current profile which resulted in the growth of a resistive wall mode. Hence the next order of business in this research line is to apply ECCD power in 2000 to counteract the resistive diffusion of the current. Success in that endeavor will set the basis for longer pulse sustainment of these discharges, but owing to the limited pulse length of the gyrotron set in 2000, the actual longer pulse sustainment will be sought in 2001 and 2002 when most of the EC power is available from the long pulse tubes. As more ECCD power becomes available throughout 2000–2002, we will increase the field and the current at which this scenario is developed with the intent of reaching 1.6 MA current at full field (2.1 T) in DIII–D in 2002. Further increases in long pulse EC power and the magnet pulse length will culminate in DIII–D being the laboratory for the study of the moderate pulse advanced tokamak called for in the FESAC goals.

Two research thrusts in 2000 should be of one year duration and are in direct support of our AT scenario thrust. The thrust on ECH/ECCD validation provides specific runtime to bring into physics operation the new gyrotron systems. Our commitment is to have four gyrotron physics operation in 2000; we have six gyrotrons in-house and are working to get at least five operational. Work in this thrust will demonstrate that local heating and current drive can be obtained from these gyrotrons and some physics experiments using them will be carried out under this thrust. This thrust should be of one year duration with the EC physics studies reverting to the Heating and Current Drive Topical Area in 2001 and thereafter.

The AT divertor thrust will bring into operation the now highly baffled and fully pumped upper divertor that enables increased pumping of the high triangularity plasmas to be studied in the AT scenario work. This thrust will develop the basic understanding of particle control preparatory for the AT scenario, including a first look at impurity control by means of strong fuel ion flows in the scrape-off layer. Further research using this divertor will probably be carried out in the Edge and Divertor Physics Topical Area in 2001. In 2002, we anticipate a strong effort to explore coupling the AT scenario with a radiative divertor, work essential to eventual integration of the core and divertor physics efforts.

In the pursuit of this scenario in 1999, results learned about the instabilities which can terminate AT modes have affected the choice of research thrusts in 2000. Since the mode this primary scenario has encountered as limiting is the resistive wall mode, the research thrust on the resistive wall mode will continue in 2000. The necessary feedback amplifiers for the present six coil system were made operational a year ahead of schedule in 1999 to get a first look at feedback interaction with the RWM. However much work remains to be done on the basics of the physics and the feedback methodologies and so the RWM work will proceed in parallel with the AT scenario work. Application of the RWM system to stabilization of the RWM is anticipated in 2001. A substantial increase in the stable normalized beta is predicted if the present six coil RWM system is expanded to 18 coils to optimize the mode spectrum. Research using this optimized 18-coil system will begin in 2002. More advanced wall stabilization approaches using systems internal to the DIII–D vacuum vessel may be studied later.

Our AT scenario in 1999 surprisingly went smoothly into an ELMing H–mode edge without encountering the terminations of high performance from edge instabilities prominent in most previous AT efforts on DIII–D. We have developed a detailed understanding of the edge instabilities involving second stable ballooning access afforded by the edge bootstrap current. In 1999, our research thrust on edge instabilities made progess on developing methods to actively intervene in the edge stability situation. However, since our primary scenario was not limited by edge instabities in 1999 and since runtime is very limited, we have not allocated specific runtime to the Edge Stability Thrust in 2000. Another factor in this decision was that we are developing a lithium beam based diagnostic to measure the edge current density and the availability of that diagnostic will illuminate the further study of the edge instabilities in 2001 and 2002. This course runs the risk that our primary AT scenario will reencounter the edge instabilities as the field and current are raised. A preliminary search for such future problems may be made in the AT scenario thrust in 2000. Some work also continues on the Edge Stability in the Stability Topical Area in 2000.

Our AT scenario in 1999 was also not limited by neoclassical tearing modes. Hence we have also have not allocated specific runtime to the Neoclassical Tearing Mode Thrust in 2000. This decision was somewhat difficult since the ECCD power will be available in 2000 to begin the very interesting research in stabilizing NTMs with local ECCD. Some work on this research line using the ECCD has been planned in the Stability Topical Area in 2000. We anticipate returning to a focus on this NTM work in 2001 with an emphasis on studying how to use ECCD to affect the modes, followed by work in 2002 on shrinking the magnetic islands and work in 2002 on stabilizing the NTM. If our AT scenario reencounters the NTM limitation, we may have to accelerate the work on NTMs and can do so.

Our research thrust on Internal Transport Barriers is aimed at longer term optimization of AT scenarios. Theory work has pointed to ultimately very advanced states of tokamak performance with nearly 100% bootstrap current in a very hollow profile with a peak near the outer edge of the plasma produced by a broad pressure profile with a transport barrier near the plasma edge. In the long run, it will be desirable to move the transport barrier location to a large radius. Very exciting exploratory work on ITBs was done in 1999 using counter injection to alter the radial electric field profile to affect the E×B turbulence shearing rate with the result of moving the radius of the foot of the transport barrier from $\rho \sim 0.4$ using co-injection to 0.6 using counter injection. Favorable results were also obtained using neon to lower turbulence growth rates. Exploratory results on using inside-launch pellet injection to form transport barriers were also obtained. This work is important to the long term since relatively more bootstrap current can be obtained from a density gradient than from a temperature gradient, within an overall stability constraint on the pressure gradient. This important work for the long term will continue (albeit at a reduced level) in 2000 with an eventual goal (~2002) of contributing the knowledge base to further optimize the AT scenarios we will have developed by that time.

Another longer term AT research objective is to open a second major line of AT work, the High l_i Thrust, starting in 2002. Limited runtime forced a choice between the NCS and High l_i AT lines in 1999. We have placed our primary effort on the NCS or high bootstrap fraction line in the near term. But the high l_i scenario is also a credible path to an Advanced Tokamak future. We intend to restart work on this scenario in 2002 with the initial physics investigations of active stabilization of the sawtooth instability by fast waves followed by the development of scenarios using fast wave, electron cyclotron, and neutral beam heating and current drive power in later years. This next major research line can be expected to develop a logic diagram as complex as that shown in Fig. 1 for the high bootstrap fraction scenario.

Facility Capabilities

The Advanced Tokamak facility capabilities needed to accomplish this research are shown in Fig. 2. The key hardware capability being implemented is high power, long pulse gyrotrons. The new gyrotrons are nominal 1 MW output power and are equipped with diamond windows for 10 second operation in DIII–D. Experiments in the year 2000 will be conducted with four gyrotrons. Two gyrotrons have the new diamond windows. One is an old developmental prototype and the other is the first production tube of the new diode gun design. The other two gyrotrons will be older units limited to 2 second pulses. This complement of EC sources will enable us to attempt the high bootstrap fraction scenario identified as four tubes (2000) in Table 3. Two additional new production tubes will become available in the year 2001, so we can then begin experiments attempting the high bootstrap fraction scenario at the higher parameters identified as six tubes (2001) in Table 3. To enable the AT studies at longer pulses and full field and beyond our intermediate scenarios, two more production unit gyrotrons will become available in 2002. In 2003, the EC system power will be brought to the full power called for in the scenarios described in Section 2.2.3 by the installation of three higher power (1.5 MW) gyrotrons being developed by the Virtual Laboratory for Technology.

For density control, the upper divertor private flux baffle and inner leg pump which were installed at the end of 1999 are expected to give us the required density control for high triangularity plasmas using the upper pumps or for low triangularity plasmas using the lower pump. Because of the importance of triangularity, the upper divertor density control capability is an essential element of the AT scenario thrust in the 2000 campaign.

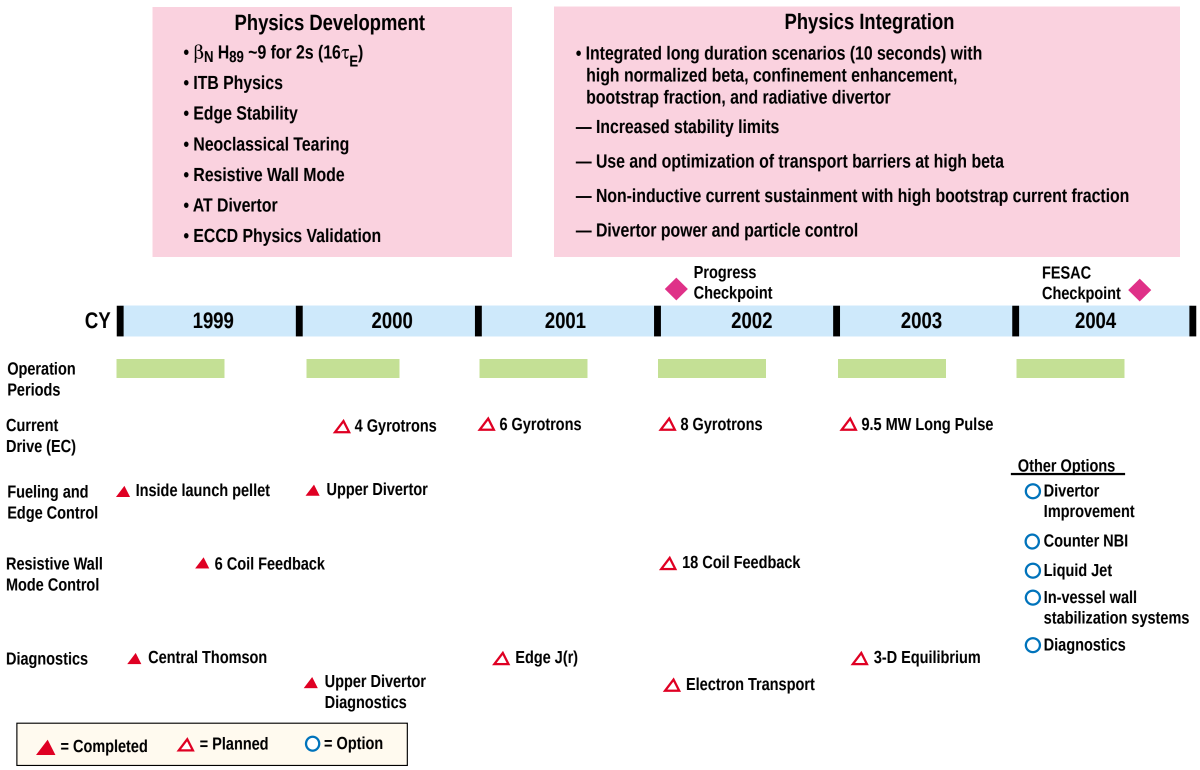

Fig. 2. DIII–D Advanced Tokamak Five-Year Research Plan.

The new upper divertor will also allow resumption of the studies of optimizing the core/divertor plasma performance balance by better retaining neutrals and impurities in the divertor using copious flows in the scrape-off layer (puff-n-pump in DIII–D jargon). This effort to make a divertor compatible with an AT core may be also applied to the NCS scenario effort in 2001.

The pellet fueling capability, extended to inside launch in 1999, proved valuable in The pellet fueling capability, extended to inside launch in 1999, proved valuable in triggering internal transport barriers in the density channel. This pellet fueling capability will be further utilized to explore transport barriers and to extend the AT thrust beyond the intermediate scenarios (post 2001).

The wall stabilization work made a good beginning in 1999 with initial development of feedback control using a six-coil system and by accelerating three power supplies originally planned for 2000. Studies in 2000 and 2001 will focus on the basic physics of wall stabilization and on validation of quantitative models for feedback stabilization. Modeling results indicate that such an extension of the system to 18 coils could significantly increase the margin over the no-wall stability limit which can be achieved with feedback stabilization. Two new toroidal arrays of 12 saddle loops each, above and below the midplane, will be available in 2000 to improve our measurements of resistive wall mode structure. These loops are also expected to serve as the sensors for the 18-coil system. The 18-coil resistive wall mode (RWM) feedback system is planned for the 2002 campaign to optimize the normalized beta that can be held by wall stabilization in DIII–D.

Enhanced diagnostic capabilities will support the evolving AT research plan. A lithium beam diagnostic will be added for the 2001 campaign to enable measurement of the edge current density profile to significantly enhance the scientific understanding of edge MHD instabilities related to the edge bootstrap current, which we believe opens second regime access. This increased understanding will be important in developing techniques for preventing edge MHD instabilities from terminating high performance AT phases. Although important work remains to clearly identify ITG modes in a plasma, the transport frontier is moving on to the yet smaller wavelength turbulence probably responsible for the residual anomalous electron transport when the longer wavelength turbulence has been suppressed by sheared E×B flows. An initiative in diagnostics for this electron transport is planned. After the complete installation of the resistive wall mode feedback system is completed, a set of diagnostics to enable reconstruction of 3-D, non-axisymmetric equilibria is planned.

Over the three year period 2001–2003, as physics progress pushes out to longer duration AT phases, a set of modest modifications to the thermal capacity of the DIII–D toroidal coil connections and poloidal coil power supplies will be made to bring the pulse length to 10 seconds. The radiative divertor physics will be called upon then to provide sufficient radiative heat dispersal in the divertor to enable 10 second pulses and thereby, to fully integrate AT operation with effective divertor operation.

2. ADVANCED TOKAMAK PROGRAM PHYSICS

2.1. PHYSICS ELEMENTS OF THE PRINCIPAL AT SCENARIOS

The goal of the DIII–D program is to establish the scientific basis for the optimization of the tokamak approach to fusion energy production. This scientific research has many elements, but the principal focus of the DIII–D program toward achieving this optimization is the advanced tokamak program. The advanced tokamak program is aimed at improvement of the tokamak concept towards higher performance and steady-state operation through internal profile modification and control, plasma shape, and MHD stabilization. The dependence of the core performance on the boundary conditions, and the operational regimes envisioned, put more stringent requirements on the divertor and edge plasma, leading to inclusion of divertor optimization and control in any tokamak optimization program.

Two characteristics make the optimization of tokamak performance "advanced": the inherent one and two dimensional dependence of tokamak performance on the plasma profiles, shape, and boundary; and the requirement to develop solutions that are both multidimensional and self-consistent. The performance capabilities and limitations of the tokamak, and requirements for an energy producing tokamak have long been communicated in terms of global zero-dimensional parameters and largely empirical scaling relations. Chief among these scaling relations are the confinement scaling relations and the scaling of beta with normalized current, known as Troyon scaling. More recently we have discovered, both experimentally and theoretically, that the performance of the tokamak plasma also depends largely on the details of internal plasma profiles, details of the plasma shape, and details of the plasma boundary.

This improvement in our understanding depended critically on the development of new diagnostics to measure the important profile parameters, such as the motional Stark effect diagnostic for measuring the internal magnetic field structure, the charge exchange recombination system to measure toroidal and poloidal plasma flows, and many new turbulence measurements. These new measurements lead to discovery and appreciation of new and important physics phenomena in the tokamak, such as the role of sheared $\mathbf{E}\times\mathbf{B}$ flow, and neoclassical tearing modes.

Equally important to new diagnostic capability is the development of new theories and modeling capabilities to put the transport, stability, and current drive projections on a firmer physics basis. An excellent example of the modeling and theory progress is in gyro-kinetic and gyro-fluid approaches for physics based transport calculations, and the appreciation of the importance of sheared **E**×**B** flow in the predictions.

The self-consistency of the parameters and profiles of high performance plasmas is one of the leading challenges of the advanced tokamak program. As well as the details of both the current density and pressure profile impacting the ideal stability limit and stability to non-ideal modes, at high beta the self-generated bootstrap current is necessarily a major component of the total current. Since the profile of the bootstrap depends on not only the profile of the pressure but of its individual constituents (density, electron temperature, ion temperature, …), the pressure profile and the current density profile are not separable. But, the pressure profile is determined by the transport profiles. In turn, the details of the pressure profile and the current density impact the turbulence growth rates and sheared **E**×**B** flow which predominantly determine the transport. In a final advanced tokamak scenario, these interdependencies and complex non-linear relationships must be fully taken into account and fully integrated. This process greatly benefits from and contributes to the development of a strong fundamental (first principal) physics basis for fusion science.

The DIII–D Advanced Tokamak program aims to develop the best possible operational scenario for fusion energy production using the tokamak. There are many opportunities to make improvements, and many complex interdependencies that allow for a multitude of possible advanced tokamak solutions. In this context it is important to recognize that our rapidly developing understanding and new innovations can lead to scenarios that we do not now envision. So, in developing the “scientific basis for optimization of the tokamak’’ we consider of paramount importance to maintain an attitude of research that is open to new discoveries and continual improvements. We therefore try to plan a DIII–D program that is not only targeted toward testing specific scenarios, but is also optimally positioned to take advantage of new discoveries and innovations. This translates directly into developing diagnostic and control capabilities that are flexible and versatile.

To make significant progress in our research, it is important nevertheless to focus on testing specific scenarios while being alert for discovery. It is important to set aggressive and measurable goals (targets) toward which to focus our efforts. We take our best present understanding of the physics and our best vision of the future embodiment in an energy producing system and develop scenarios, which we can test experimentally in the DIII–D device.

Consideration of physics and energy production lead us naturally to two principal steady-state advanced tokamak scenarios. These two scenarios are negative central magnetic shear (NCS) and high internal inductance (high l_i). These two scenarios do not encompass all the known approaches to tokamak improvement, but rather provide some focus to the challenges that confront us. The profiles and conditions of the two scenarios are quite different, but it is recognized that a fully optimized scenario might lie somewhere in the space between the two.

The viability of a tokamak as an economically and environmentally attractive power plant requires both sufficient energy confinement time, τ_E, for ignition margin, and sufficient volume average toroidal beta, $\beta_T = 2\mu_0 \langle p \rangle / B_T^2$, for adequate fusion power density. Further improvements in the tokamak reactor concept can be made if these improvements in β_T^{max} and τ_E are obtained in steady-state discharge conditions (Kikuchi 1993). We are seeking scenarios that have the potential for high beta, high confinement consistent with steady state, and consistent with divertor scenarios that can provide adequate heat removal, particle and helium ash control, and impurity control.

A minimum necessary condition for an attractive fusion energy producing system is high energy gain. Some insight into possible operational scenarios is obtained by considering the energy gain for a steady state system, given by Eq. (1):

$$Q \propto \frac{P_{fus}}{P_{CD}} = \frac{P_{fus}}{\frac{n\,R\,I_P}{\gamma_{cur}}\left(1 - f_{BS}\right)} \propto \frac{\gamma_{cur}\,\varepsilon_{eff}\,\beta_N^2}{n\,q\,\left(1 - \xi\sqrt{A}\,q\,\beta_N\right)} \quad . \tag{1}$$

In Eq. (1), P_{FUS} is the fusion power, the P_{CD} is the current drive power, γ_{CUR} is the current drive efficiency, ε_{EFF} is the effective inverse aspect ratio, **A** is the aspect ratio, q is the safety factor at the plasma edge, β_N is the normalized beta and f_{BS} is the fraction of the total current that is the self-driven bootstrap current. In any steady state scenario, care must be taken to minimize the current drive power required. One can view two separate approaches (NCS or high-l_i) to minimizing this current drive power: (1) maximize the bootstrap fraction, or (2) maximize the efficiency of current drive (γ_{CUR}/nI). If the bootstrap fraction becomes a major fraction of the total current, the current profile becomes naturally hollow with the maximum off-axis and the central portion of the plasma has negative central shear, NCS. The bootstrap fraction is further increased by increasing the minimum value of q, q_{min}, and moving the radius of the q_{min} to larger radius. If the emphasis is placed on increasing the current drive efficiency, it is natural to drive the current on axis where the temperature is highest (current drive efficiency is proportional to electron temperature) and where the effects of trapping are minimal. Axial current drive leads naturally to peaked current densities, with large positive magnetic shear in the outer plasma region. A schematic of the resultant current profiles is shown in Fig. 3. The actual current profile for these two cases depends on establishing consistency among the profiles, stability, and transport.

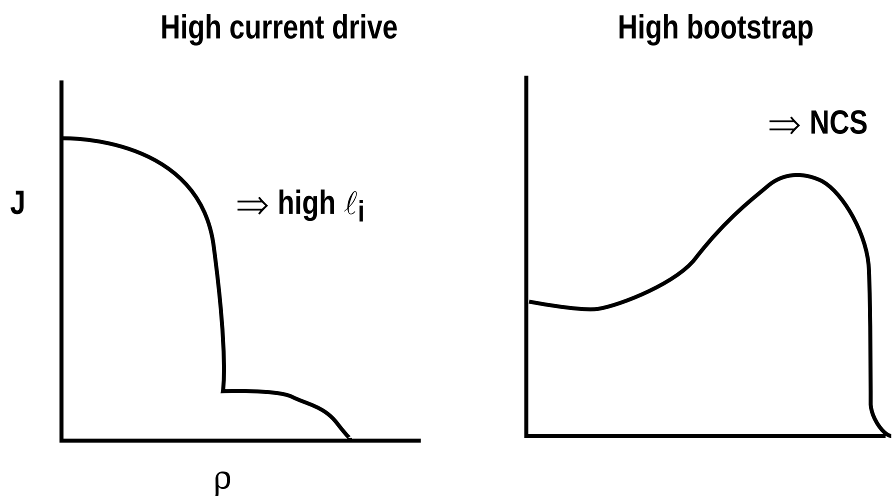

Fig. 3. Steady state considerations also lead to two "natural" current profiles.

Unless the NCS scenario has fully 100% bootstrap driven current, it is important to maintain relative high current drive efficiency in both the NCS and high ℓ_i scenarios.

The need for high current drive efficiency pushes steady state operational regimes to higher temperature and lower density than might otherwise be the optimal in a Ohmically pulsed scenario. The higher temperature and lower density, impose new challenges for heat removal and impurity control for the divertor. This lower density, higher temperature operation motivates the inclusion of divertor optimization as an important element in the DIII–D AT program.

Simple physics considerations also lead to the same operational scenarios, (1) NCS and (2) high ℓ_i. We show in Fig. 4, the general dependence of ideal ballooning stability and ion temperature gradient (ITG) driven instabilities on the magnetic shear, $S_M = \rho/q\ (\partial q/\partial \rho)$. These general dependencies, known for a long time, clearly show that both low or negative magnetic shear and high magnetic shear are favorable for stability of ballooning modes and ITG modes. These physics considerations lead to the same two general classes of scenarios given above; (1) low or negative shear → NCS, and (2) high positive shear → high ℓ_i. It is worth noting that the magnetic shear (in the large aspect ratio circular limit) observed experimentally in Ohmically driven discharges is near 1, nearly the most unfavorable value for ballooning and ITG mode stability. So one might expect that the ability to modify the current profile toward either larger positive or negative magnetic shear would lead to positive benefits.

2.1.1. General NCS Considerations

The NCS scenario has the potential for a high bootstrap fraction at moderate q: the bootstrap fraction can approach unity at q_{95} = 5–6. Furthermore, there is the potential for the bootstrap current to be well aligned with the total current, resulting in low, total current drive requirements. The hollow current profile, and the resultant region of negative central magnetic shear derive naturally from the bootstrap current. The bootstrap current is proportional to the square-root of the local aspect ratio times the pressure gradient, both of which go to zero on axis, so that the bootstrap current profile is naturally hollow. In addition, the higher axial q and lower poloidal field in the core have the effect of increasing the total bootstrap fraction. The high bootstrap fraction results in lower total current drive, but highly localized, off-axis, precision current drive is needed. Electron cyclotron current drive is well suited for the precise off-axis current drive needed. Because of the potential of the NCS scenario with respect to fusion energy, we have chosen it as the leading scenario on which to focus.

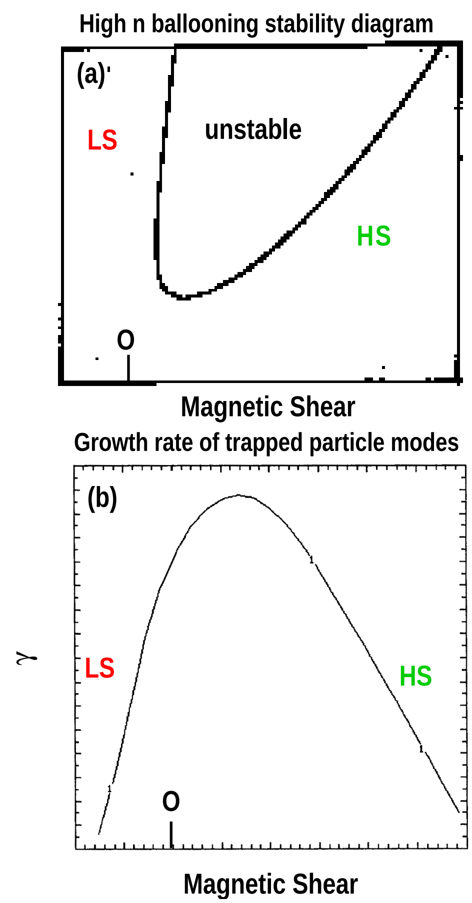

Fig. 4. Both low magnetic shear (LS) and high shear (HS) are favorable for: (a) higher beta, (b) reduced turbulence and reduced transport. Magnetic shear is $s \propto R/B_T^2 q^2\, d\rho/dr$.

The NCS scenario does have some very specific challenges. The first challenge is stability. Stability to ballooning modes is a necessary condition for achieving high beta, and therefore an important consideration. The NCS scenario avoids ballooning mode limitations because the region of high pressure gradient is in the region of low or negative shear, where there is access to the second regime and no limiting pressure gradient is calculated. Furthermore, the negative shear region is stabilizing to neoclassical tearing modes where the pressure gradient is expected to be large, and if the minimum value of q is above 2, the absence of low order rational surfaces should further diminish the importance of the modes.

There are several MHD instabilities that remain a challenge to the NCS scenario. Strong pressure gradients in the region of negative shear can be destabilizing to resistive interchange modes. Modeling indicates that these modes are stable if the magnitude of the negative shear is kept modest. Double tearing modes are calculated to be unstable as a consequence of the double value of q. However, these are rarely observed in the experiment, and modeling indicates modest rotational difference in the plasma between the two surfaces (as observed in the experiment) is sufficient for stabilization.

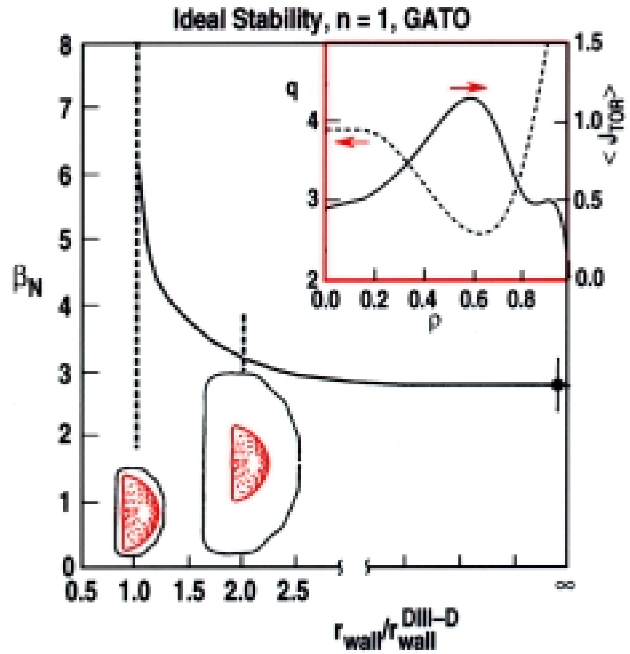

Fig. 5. Maximum stable beta increases for closer wall position: ideal n=1 stability using DIII–D plsma shape and DIII–D wall. Insets are typical current density and q profile (Taylor1995).

The NCS scenarios have quite low l_i and are generally unstable to the external/global kink, in the absence of a conducting wall. However, the broad current density profile, broad pressure profile, and strongly shaped plasmas couple very strongly to a nearby wall. Modeling indicates that $\beta_N > 5$ stable to n=1 and 2, is easily obtained if a conducting wall is located at $r_W/a <$ ~1.5. The modeling calculations for n=1 are shown in Fig. 5. However, the real wall is resistive and the plasma is subject to the resistive wall mode. The stabilization of the resistive wall mode then is key part of validating and optimizing the NCS scenario. The DIII–D program is taking twoapproaches to stabilization of the resistive wall mode; passive stabilization with a rotating plasma in the presence of a resistive wall, and active feedback stabilization with non-axisymmetric external coils.

It is important to note that reasonably high beta values can be calculated for the NCS scenario without a conducting wall; β_N values <4 are calculated, very similar to the high l_i scenario. So if wall stabilization proves not to be so attractive in a reactor embodiment, there remain attractive NCS and high l_i scenarios.

For the NCS scenario, perhaps the most challenging physics lies in the consistency of the profiles. A range of current density and pressure profiles can be identified that are consistent with high beta stability. In particular, it can be shown that broad pressure profiles are required for high beta stability and alignment of the bootstrap current (Fig. 6). However, the combination of the q profiles, pressure profiles, and rotation (E×B) profiles often result in transport reduction and often the formation of a clear internal transport barrier that leads to pressure peaking that are not compatible with high beta.

Discharges in DIII–D can have an internal transport barrier, ITB, with no edge transport barrier (L–mode NCS), a strong edge transport barrier, (H–mode NCS), and a self-regulating edge barrier with an internal transport barrier (ELMing H–mode NCS). These three cases have different challenges with respect to high beta and self-consistent solutions. The L–mode NCS has a very weak pressure gradient in the outer portion of the plasma. The key challenge for L–mode NCS is to move the transport barrier to larger major radius to achieve higher beta [as shown in Fig. 6(a)] and to obtain good bootstrap alignment. It is also important that for stability, the width of the transport barrier region not become too narrow as indicated in Fig. 6(b). In general, peaked pressure profiles that result from an ITB at small radius result in a low stability limit as shown in Fig. 7. The ELMing H–mode NCS and the H–mode NCS both lead to broader pressure profiles and the potential for high beta with an ITB. For the ELMing case, the repetitive ELMs provide a seed for neoclassical tearing modes, and the higher pressure gradient in the positive shear region make the neoclassical tearing modes unstable. For H–mode NCS, a clear strong barrier exists near the boundary, and the plasma is subject to low n kinks associated with the high edge pressure gradient and high edge current density. High beta, broad profiles, and strong shaping cause strong harmonic coupling and these edge driven modes are no longer localized to the edge. The key challenge for the H–mode NCS scenario is to understand how to moderate the edge and avoid the edge instability or its strong coupling to the core.

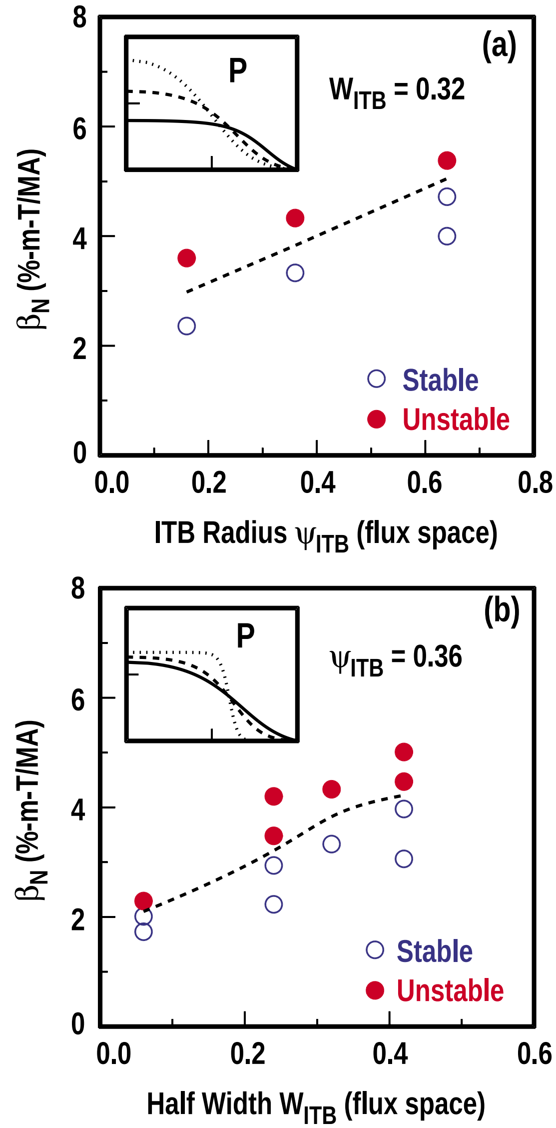

Fig. 6. Stability limit improves with internal transport barrier width and radius. Fixed shape DND, q_{95} = 5.1, q_0 = 3.2, q_{min} = 2.2; hyperbolic tangent pressure representation; ideal n = 1, wall at 1.5a.

A physics understanding of the edge instability is unfolding and we are developing techniques to modify and control these instabilities. In DIII–D the edge pressure gradient is limited by moderate n ($2 \lesssim n \lesssim 9$) kink/ballooning instabilities. These modes are driven by both the locally high pressure gradient and the locally high edge current density (the edge current density is the bootstrap current driven by the edge pressure gradient). The edge region is typically in the region of second stable access to infinite n ballooning modes, and local pressure gradient is significantly higher than that expected from the first regime limit. High squareness shaping eliminates the access to second regime stability and leads to much smaller and more frequent ELMs (presumably at higher n) more compatible with an internal transport barrier. Edge impurity radiation reduces both the edge pressure gradient and the edge current density and also gives smaller and more frequent ELMs. Both plasma shaping and edge impurity radiation are being evaluated as techniques to control the edge instabilities, and better measurement of the edge current density with Li beam polarimetry is being pursued in order to better quantify the edge stability models.

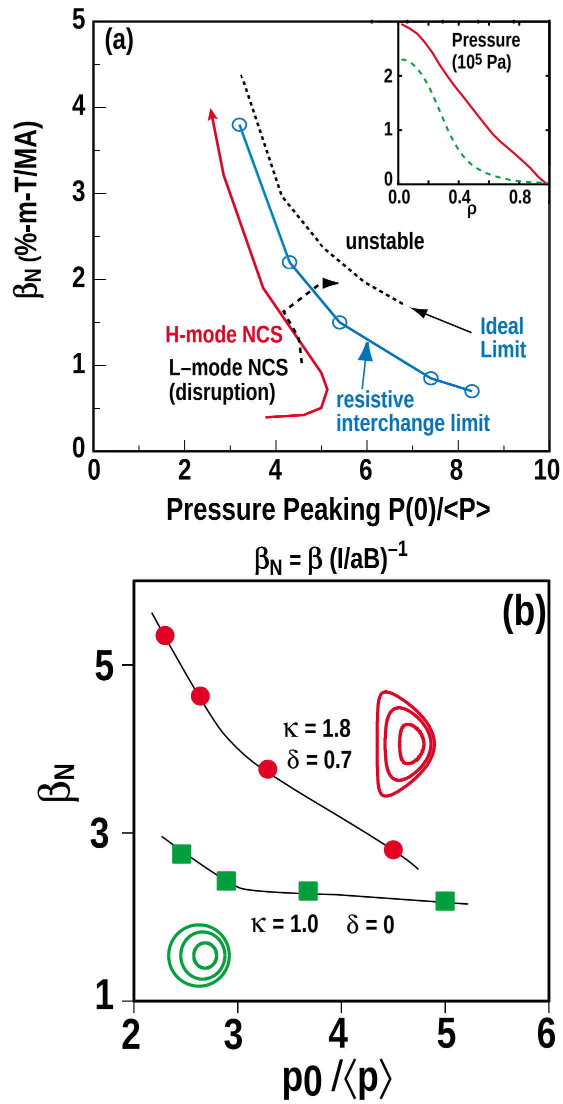

Fig. 7. Higher β is obtained with broad pressure profile (a) normalized beta vs. pressure peaking. Ideal and resistive limits are from generated equilibria similar to the experimental. Dashed trajectory is for an L–mode NCS discharge, solid trajectory is for H–mode NCS discharge (Lao 1996). Insets are exp. pressure profile just prior to disruption.(b) β_N vs. pressure peaking for D shaped and circular shaped equilibria, q_0 = 3.9, q_{min} = 2.1, q_{95} = 5.1, rw/a = 1.5 (Turnbull 1996).

A sound physics understanding of the reduced transport in the NCS discharges, and of the transport barrier formation, is developing based on sheared E×B flow stabilization of microturbulence. An extremely rich variety of physics effects provide for exciting and interesting fusion science research, as well as opportunities for control of the transport and transport barrier. The ability to vary the location of the internal transport barrier and to control the magnitude of the local pressure gradient can allow us to generate pressure profiles consistent with high beta stability and bootstrap alignment; see Fig. 6.

2.1.2. General High-l_i Considerations

A significant experimental basis for a high l_i high performance scenario exists. A number of tokamaks have observed experimentally that the maximum achievable beta increases with internal inductance, and the DIII–D experimental program has established the scaling relation $\beta_{max} = 4\ l_i * I/aB$.(Taylor 90 IAEA). This relation has been supported by a large number of experimental results from other tokamaks. It has also been shown to be consistent with theory and modeling results (Lao 1991), at least for a class of equilibria generally consistent with Ohmically driven current profiles. It has also been shown in a wide range of experiments that the energy confinement time increases with l_i. The increase in confinement has been shown to be a consequence of an increase in magnetic shear and a consequence of an increase in the E×B flow shear. There exists a positive feedback mechanism between the two effects. These high confinement and high beta results have to date been achieved transiently by ramping down the plasma current or by expanding the plasma size.

Self-consistency of the profiles in steady state does place limitations on the high l_i scenario. Maintaining q_0 slightly above unity and avoiding the m/n = 1/1 sawtooth instability has been observed to be a necessary condition in achieving high performance in many tokamaks. We will make the most peaked current density profile possible (highest l_i) consistent with ballooning stability and resulting allowable pressure profiles in the following way. The current profile will consist of the driven seed current and the bootstrap current. The driven seed current will have a top-hat form and is located in the core, with the limitation that $q_0 > 1$. The total current density is equal to the maximum of the local current density and the local bootstrap current. The pressure gradient is limited to remain below the ballooning limit. The resultant current density profile is shown in Fig. 8, and the internal inductance is limited to $l_i \sim 1.1$. The maximum beta stable to ideal ballooning modes in such a case is $\beta_N < 4$ (for $\kappa = 1.8$, $\delta = 0.7$ equilibrium), and the maximum bootstrap fraction is limited to approximately 60% at $q \sim 7$. This scenario is an attractive advanced tokamak scenario, and we think the physics challenges are not very demanding. However, because of its bootstrap current limitations and implications on achievable steady state Q, the high l_i scenario is not our leading scenario.

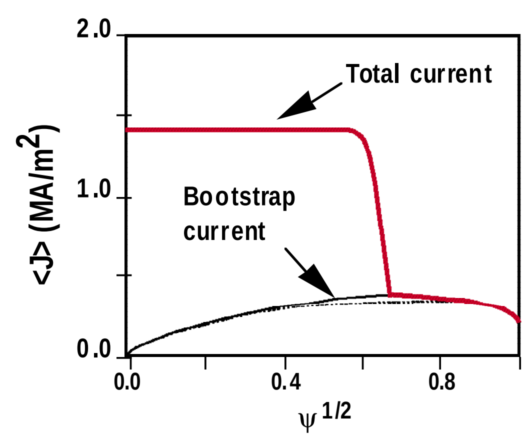

Fig. 8. Self-consistent current profile from high β, high l_i equilibrium $\beta_N = 4$, $l_i = 1.2$, $q_{95} = 8$, $q_0 = 1.05$.

2.2. THE NEGATIVE CENTRAL SHEAR (NCS) SCENARIO IN DIII–D

The principal approach to the AT in DIII–D is the negative central shear regime. This regime has the best set of characteristics to take forward to a steady-state fusion reactor. The hollow current profile is compatible with the high confinement arising from a transport barrier since the off-axis bootstrap current produced by the transport barrier will produce most of the required off-axis current peak. The rest of the non-inductive current can be either on-axis for central q control or off-axis to supplement and align the bootstrap current peak with the required total current profile. The negative central shear q profile and the broad pressure profile resulting from a transport barrier and q_{min} being at large radius are compatible with high normalized beta. Wall stabilization is also needed owing to the closer proximity of the current peak to the plasma edge. This scenario can be made with either the L–mode or H–mode edge. Which is best for stability and confinement is an active subject of ongoing research.

There is considerable flexibility in this scenario in regard to how the plasma edge is managed and how the interior current and pressure profiles are controlled. It is not clear, for example, how much magnetic shear reversal is needed, even to the limit of zero shear.

On three or four separate occasions in the last four years, different people from different viewpoints have constructed AT NCS scenarios for DIII–D using the ONETWO transport code, the stability codes GATO and BALOO, and the transport code CORSICA. We will summarize those scenarios below in order of increasing complexity of the transport modeling rather than in the chronological order in which they were done. They exhibit some different approaches and interests which provide pathways into the variations in experimental approach being currently pursued and we will comment on those pathways into the ongoing experimental program. Recent work on defining optimum scenarios for ARIES-AT also point to exciting long-term directions for the DIII–D research.

2.2.1. Scenarios Using Fixed Profiles

The purpose of this modeling exercise was to demonstrate the potential for intermediate advanced tokamak operation goals at intermediate values of plasma current and toroidal field with the view of a phased installation of a ten gyrotron system (nominal 1 MW/gyrotron source with 70% delivered to the plasma) for ultimate operation at full field and current in DIII–D. For this purpose scenarios with 3, 6, and 10 gyrotrons were developed from B_T = 1.6 T to full B_T = 2 T and I_p ranging from 1.0 MA to 1.6 MA.

The starting point in each case was a stable MHD equilibrium with boundary consistent with the full RDP installation. Only the total pressure is important for the equilibrium, but the non-inductive current density calculations require the pressure to beseparated into electron and ion density and temperature. This division is shown in Fig. 9 for the three gyrotron scenario with $\beta_N = 4$.

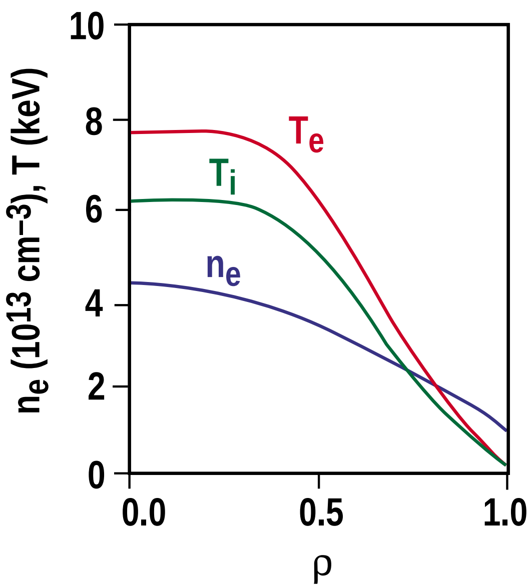

Fig. 9. NCS profiles of temperature and density.

The density profile was chosen to be consistent with pumped ELMing H–mode discharges at higher q_{95}. These are more peaked than the canonical H–mode density profiles normally shown. Very little effort was directed to make an H–mode edge pedestal or consistency between the edge bootstrap current density and the total current density from the equilibrium because the purpose was to show whether the off-axis ECCD was sufficient in these conditions. The lack of predictive capability of the edge conditions during ELMs would make any detailed reconciliation baseless in any case. The level of the line-averaged density was limited by the empirical rule-of-thumb on DIII–D that the ELMing H–mode density can be varied from n (10^{19} m^{-3}) = 3 I (MA) to 6 I (MA). The actual density was maximized consistent with full non-inductive current. The impurity density profile was chosen arbitrarily to give a constant $Z_{eff} = 1.5$ across the plasma.

The temperature profiles were chosen to be a constant fixed ratio across the entire plasma. The transport code was run in analysis mode to derive both the local transport coefficients and the global confinement relative to the ITER-89P scaling law. The local transport coefficients were checked to ensure the ion diffusivity was at or above neoclassical and near the electron diffusivity.

The same source calculations in the transport code also provide the non-inductive current densities due to NBI, bootstrap, and ECCD. The scenario was iterated to give zero net ohmic current, not zero ohmic current density at all radii. Again, the goal of our modeling at that time can be seen directly by examining Fig. 10 which shows the total current density from the equilibrium and the non-inductive current densities calculated using the profiles in Fig. 9. It is clear that 2.3 MW of EC power delivered to the plasma under these conditions supplies sufficient current at the half radius to maintain the off-axis current density in conjunction with the bootstrap current. A resistive evolution could have been done and would have resulted in a less reversed q profile, but the degree of negative central shear is not believed to be an essential feature of this scenario.

Fixing the profiles is obviously equivalent to fixing the target β_N and H factor for the scenario. These calculations do represent first principles evaluations of where to place the RFCD and the efficiency of the RFCD. These calculations are of value in determining the rf and NBI power levels needed to make the target scenario in terms of current drive and assuming the target values of β_N and H. Scenarios at increasing plasma current and field were developed.

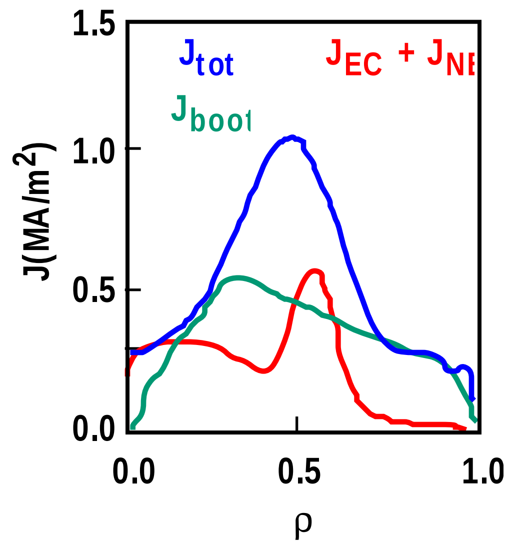

Fig. 10. Contributions to a hollow current profile.

Two scenarios are summarized in Table 3. We have labeled these scenarios by the number of gyrotron tubes we believe we will need to carry them out and also by the year in which we feel we can begin to attempt these scenarios. These scenario definitions have given focus to the effort in Thrust Area 2 in 1999 to develop transiently the plasma described in the year 2000 column. Good progress was made in 1999 on this scenario as shown in Fig. 11. This discharge is an ELMing H–mode as shown by the D_α trace, Fig. 9(f). The discharge is quasi-stationary for ~2 s or 16 τ_E and has a β_NH product of 9. β_N is just below 4 and is larger than the nominal no-wall limit of 4 x l_i, Fig. 11(c). Small recurring resistive wall modes were observed and are the course of the periodic drops in β_N. The plasma described in the year 2001 column is our principal target for the year 2001 demonstration of a sustained NCS AT mode, possibly with an integrated divertor solution.

In order to obtain sufficient current drive efficiency, these scenarios use low densities, a low fraction of the Greenwald limit. These low densities are below where detached divertor plasmas are found, setting the challenge to either raise the scenario density or to the divertor program to develop ways of making radiative divertors compatible with these AT core plasmas. Density control at least is required from the divertor program to meet these scenarios.

Table 3
Parameters of NCS Scenarios Using Fixed Profiles.

	4 Tubes (2000)	6 Tubes (2001)
P_{EC} (MW)	2.3	4.5
P_{FW} (MW)	3.6	3.6
P_{NBI} (MW)	4.1	3.8
I_p (MA)	1.0	1.3
I_{Boot} (MA)	0.65	0.9
I_{ECCD} (MA)	0.15	0.2
B_T (T)	1.6	1.75
β_T (%)	4.0	6.3
β_N	4.0	5.3
H_{89P}	2.8	3.5
n (10^{20} m^{-3})	0.32	0.5
n/n_G	0.3	0.4
$T_i(0)$ (keV)	6	8
$T_e(0)$ (keV)	8	9

2.2.2 NCS Scenario Simulations Using Diffusion Coefficients Derived From Discharges

MHD stability studies of discharges with an internal transport barrier (ITB) show that the stability limit improves with increasing width and radius of the ITB based on a systematic scan of simulated equilibria with model q and pressure profiles. The scenario modeling described in the preceding section began with a total pressure profile consistent with an MHD stable equilibrium and rather arbitrarily divided the total pressure into electron and ion pressure which were then portioned to density and temperature. The scenario modeling described in this section is based on transport coefficients determined from an existing ITB discharge with an L–mode edge which are then scaled to different parameter regimes. To date the studies have been focused on using this approach to achieve the discharge conditions chosen by the method of the previous section.

Time-dependent transport simulations were performed using the ONETWO and CORSICA transport codes. First, measured profiles from an ITB discharge from our 1999 campaign, very similar to that shown in Fig. 11, with B_T = 1.6 T, I_p = 1.2 MA, q_{95} = 5, β_N = 3.7 and H_{89P} = 2.9 were used to calculate thermal diffusivities $\chi_e(\rho)$ and $\chi_i(\rho)$. These calculated diffusivities, with the addition of the ion neoclassical diffusivity shown in Fig. 12, were the baseline model diffusivities used in the time-dependent ONETWO simulations. The target parameters for the simulations are exactly those of the ITB

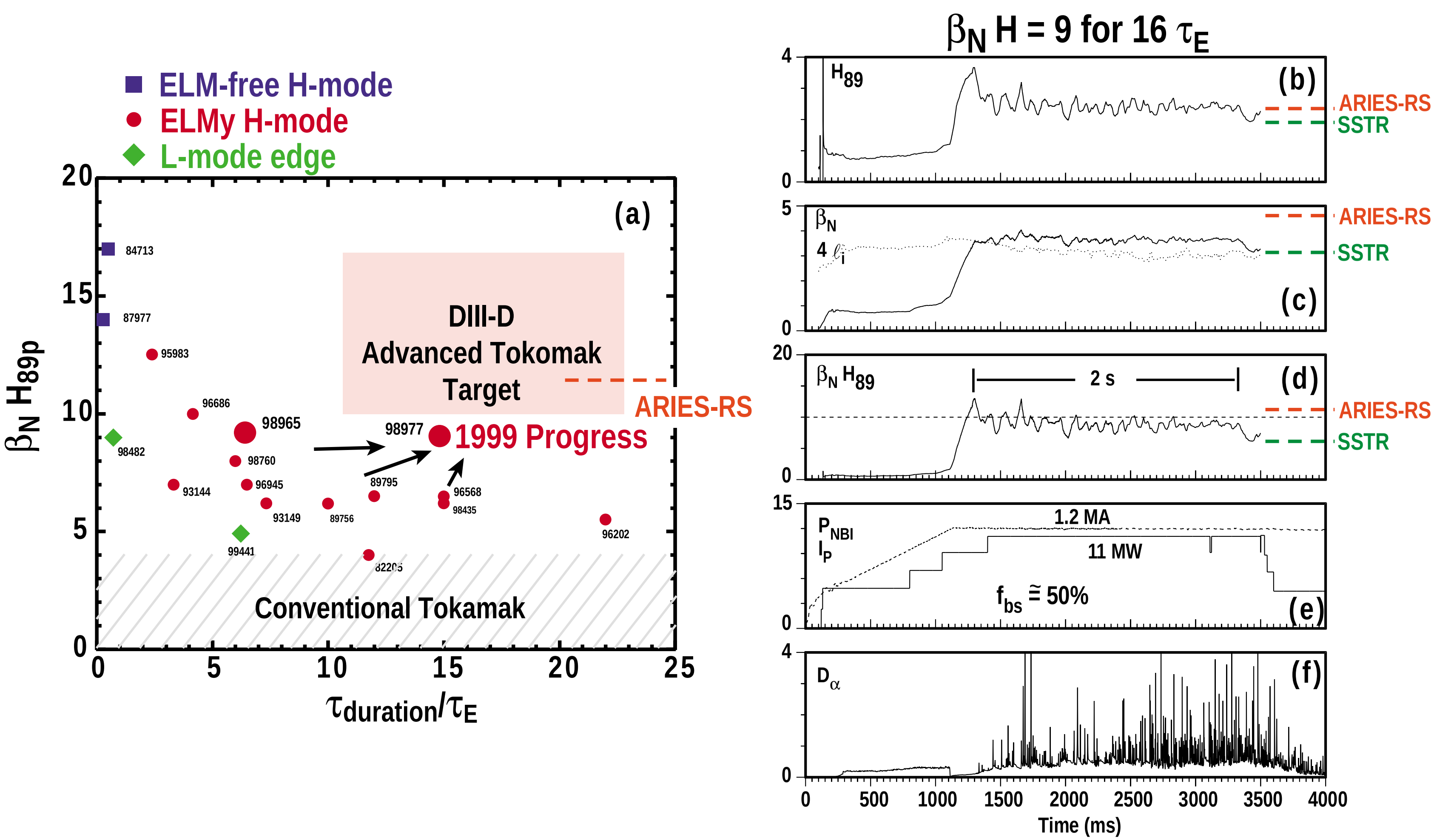

Fig. 11. (a) Recent progress in AT scenario development. Two large circles are 1999 results. (b) Confinement enhancement, H_{89P}; (c) normalized beta, β_N (solid) and 4 x internal inductance, ℓ_i; (d) product β_N, H_{89P}; (e) beam power (solid), plasma current (dashed); (f) divertor D_α.

discharge. CORSICA simulations have concentrated mostly on the sensitivity of results to other transport models.

In the process of performing the transport simulations, a number of iterations are carried out in order to optimize various choices. The ECH launching direction is optimized to align the electron cyclotron current drive (ECCD) profile with the off-axis bootstrap current profile, and to maximize the ECCD efficiency to overcome the dissipating ohmic current profile. We then evolve T_e, T_i, and current density with a fixed density profile for a period of 10 s. The transport profiles (χ_e, χ_i) remain fixed to those from the experiment. We iterate this transport simulation cycle three times, each with the starting profiles taken from those at the end of the previous cycle. In the last cycle, evolution of the MHD equilibrium is also performed. At the end of each cycle, we test the MHD stability with high-n (BALOO code) and low-n (GATO code) stability.

Figure 12 shows the summary of simulations for q(ρ), T_e(ρ), T_i(ρ), and individual components of the current density profile together with a tabulation of the parameters

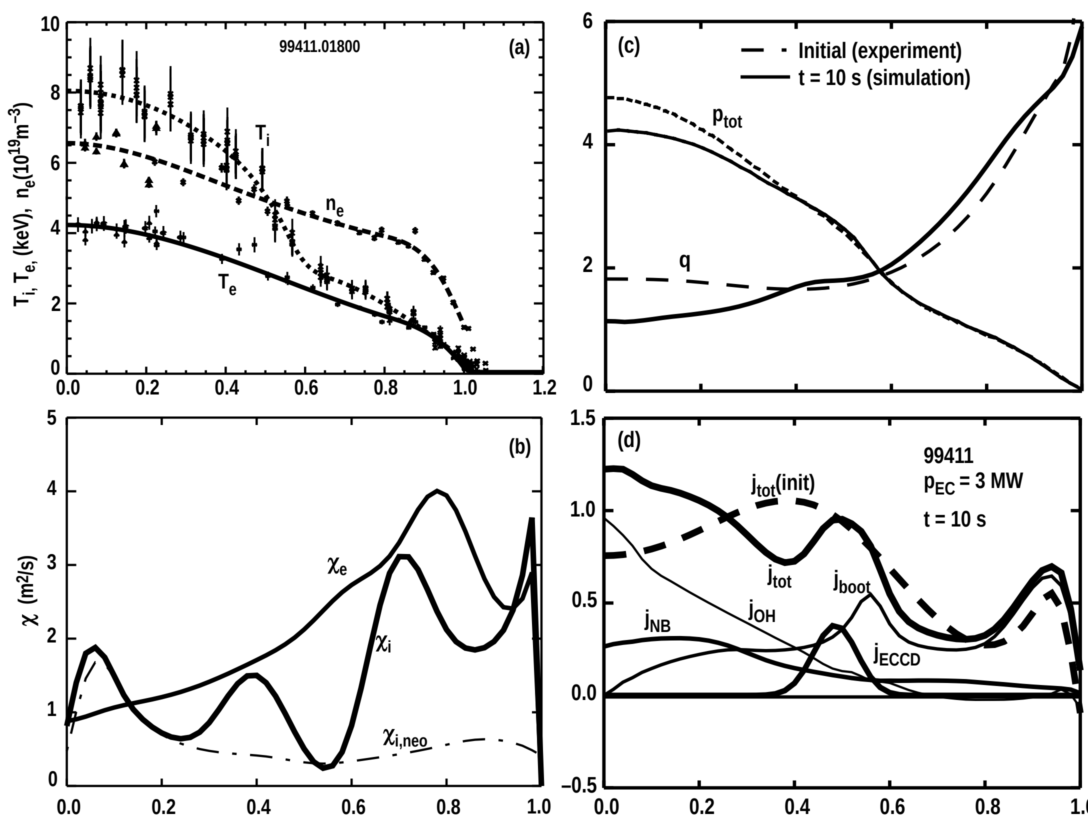

Fig. 12. NCS scenario using empirical transport coefficients. (a) Measured ion temperature, electron temperature, electron density; (b) experimental thermal diffusivities; (c) q profile, total pressure; (d) current profiles.

(Table 4), which can be compared with the case from the previous section. The detailed case shown in Fig. 12, illustrates that 3 MW of off-axis ECCD at $\rho = 0.5$ maintains $q_0 > 1$ and weak shear for 10 s and, we expect, sustains the high performance phase, allowing more detailed evaluation of AT physics. With the addition of density control with the two upper cryopumps, we expect significantly more electron cyclotron current and expect a quasi-stationary current profile.

Table 4
Parameters of L–Mode Edge NCS Scenarios Using Transport Simulations

	4 Tubes (2000)
P_{EC} (MW)	0→3.0
P_{FW} (MW)	0
P_{NBI} (MW)	9.2→6.2
I_P (MA)	1.2
I_{Boot} (MA)	0.67
I_{ECCD} (MA)	0.9
I_{OH}(MA)	0.24
B_T (T)	1.6
β_T (%)	4.3
β_N (%)	3.7→3.5
H_{89P}	2.9→2.6
n (10^{20} m^{-3})	0.48
n/n_G	0.48
$T_i(0)$ (keV)	8.4→6.9
$T_e(0)$ (keV)	4.2→4.5
q_{95}	5.0
J_{BS}	55%

2.2.3 NCS Scenarios Using Models of Transport Barrier Formation

Scenarios using models of transport barrier formation have been produced twice. A table of numbers for these scenarios is given in Table 5. These scenarios were constructed by 1-D simulations using the ONETWO code. All of the scenarios lie in the range β_T 5%–11% at full field in DIII–D. They are at plasma currents of 1.6–2.2 MA and employ strong shaping ($\kappa = 2.1$, $\delta = 0.8$). They employ a total of 15–20 MW of total heating and/or current drive power, made up of roughly equal contributions of NBI, ECH, and FW. They all employ fast wave heating to achieve a high core electron temperature.

Table 5
Parameters of Longer Range DIII–D Scenarios

Case	1	2	3	4	5
β (%)	7.5	5.0	8.1	8.7	11.5
β_N	5.7	3.8	6.2	5.8	6.0
I_p (MA)	1.6	1.6	1.6	1.8	2.2
$I_{bootstrap}$	1.07	1.45	1.85	1.92	2.1
I_{ECCD}	0.35	0.50	0.03	0	0
I_{FWCD}	0	0	0	0	0
I_{NBCD}	0.25	0.11	0	0	0
I_{OH}	–0.07	–0.46	–0.28	–0.12	–0.10
q_{95}	6.5	5.0	5.0	5.3	3.6
q_0	3.8	2.3	2.5	3.9	3.4
q_{min}	2.6	3.3	2.1	2.3	
$T_i(0)$ keV	15	12.3	18.5	14.5	19
$T_e(0)$ keV	8.5	9.7	7.0	12.7	13
$n_e(0)$ 10^{20} m^{-3}		0.59	0.89	0.72	0.88
$\bar{n}$ 10^{20} m^{-3}	0.57	0.35	0.54	0.48	0.53
n_{edge} 10^{20} m^{-3}		0.23	0.23	0.23	0.21
$\bar{n}/n_G$	0.4	0.26	0.4	0.32	0.3
P (MW)	20	14	12	14	14
P_{NBI} (MW)	6.5	4.0	4.0	4.0	4.0
P_{EC} (MW)	7.0	6.0	4.0	6.0	6.0
P_{FW} (MW)	6.5	4.0	4.0	4.0	4.0
W (MJ)		1.25	1.3	4.6	6.0
τ_E (s)		0.21	0.29	0.28	0.4
H_{89P}	3.5	3.4	4.4	4.0	4.95
ρ_{*e} at $\bar{T}_e$	2.3×10^{-4}	2.5×10^{-4}	2.1×10^{-4}	2.8×10^{-4}	2.9×10^{-4}
ρ_{*i} at $\bar{T}_i$	1.3×10^{-2}	1.2×10^{-2}	1.5×10^{-2}	1.3×10^{-2}	1.5×10^{-2}
ν_{*e} at $\bar{T}_e$	1.2×10^{-2}	4.2×10^{-3}	8.0×10^{-3}	2.9×10^{-3}	2.1×10^{-3}
ν_{*i} at $\bar{T}_i$	2.7×10^{-3}	1.8×10^{-3}	0.8×10^{-3}	1.6×10^{-3}	0.7×10^{-3}

Case 1: SSC-VH [Turnbull PRL 74, 718 (1995)]
Case 2: β = 5%, P = 16 MW, n & v_ϕ transported
Case 3: β = 8%, P = 15.2 MW, n & v_ϕ transported
Case 4: β = 8%, P = 17 MW
Case 5: β = 11%, P = 17 MW

Except for Case 2, all these cases require at least 6 MW EC power delivered to the plasma. These considerations lead us to believe that a 10 gyrotron EC system will ultimately be needed to form the NCS plasmas at full field and current in DIII–D.

They all seek steady-state negative central shear current profiles for stability at high β_N. They also seek high bootstrap fractions and make up any difference in the plasma current and the bootstrap current by use of RF current drive. The resulting plasmas have rather low ρ_* and very low ν_*, but they match up well along dimensionless parameter scaling paths to future tokamak devices (Section 2.4 of the Five-Year Plan). The scenarios all have rather low densities and high temperatures. The combination of low density (well below the Greenwald limit) and high power will make it particularly challenging to obtain radiating, detached divertors in these scenarios.

For reference, the first scenario is that published by (Turnbull, 1995, see also St. John IAEA 1994 and Taylor EPS 1994). At that time, DIII–D had seen plasmas with hollow current profiles, very high central betas (calculated to be second stable) and had also seen in other discharges the VH–mode, a transport barrier formed around $\rho = 0.8$. The scenario described considered combining these two features into what was called then Second Stable Core VH–Mode (SSC-VH). The inverted q profile and suitably broad pressure profile was shown through stability calculations to give β_N of 5.7 assuming wall stabilization. Various transport models were used for the electrons including INTOR scaling, the Rebut-Lallia-Watkins model and the Hsieh model for electrons. Essentially the ion diffusivity was taken to be neoclassical near the core (the transport barrier model here was a small multiplier times neoclassical ion transport inside the radius of q_{min}) and rising to 5 times neoclassical near the edge. A combination of bootstrap current which peaked off axis and off-axis ECCD were used to sustain the hollow current profile. On-axis NBCD was used to control the central current density. Fast Wave heating sustained the core electron temperature. A limitation of this scenario was the use of a fixed density profile; no density transport was considered. The rather broad density profile used still contributed a significant bootstrap current. Steady-state solutions were found with the required current profiles and pressure profiles for the high values of β_N in this scenario.

For the Five-Year Plan, we constructed transport simulations using a full but complex model of E×B shear stabilization of turbulence to dynamically form the transport barrier in the simulation. The current profile was evolved to steady state verifying the compatibility of the transport barrier with the second stable core. The model is diagrammed in Fig. 2.3–1 on page 2.3–4 of the Five-Year Program Plan. The model calculates the turbulence shearing rate with no free parameters from the Hahm-Burrell formula based on the evolving density, temperature and rotation speed profiles. Then the local value of $\omega_{E\times B}$ is compared to a model of the turbulence growth rate. This prescription for E×B shear suppression is based on gyrofluid turbulence simulations of

Waltz, 1994. The location where the transport barrier forms depends upon both the growth rate profile (which tends to rise from the center) and the source (heating, momentum and fueling) profiles. The barrier usually forms first at the edge due to the high power flux density and the strong density gradient (fueling). The H–mode edge can be suppressed (in the model) by a combination of high edge radiation and low recycling. We did so in order to concentrate on the core transport barrier properties and not on the more difficult to model edge L-H transition. A transport barrier then forms first in the core owing to the peaked heating and/or momentum sources. In the experiments, the reduction of the ITG mode growth rates due to hot ions and fast ion dilution have been found to aid internal transport barrier formation. The negative magnetic shear also eliminates MHD ballooning modes. Raising the power makes the internal transport barrier expand as the E×B shear pushes out against the rising growth rate. This model of transport barrier formation contains many feedback loops, since the radial electric field depends on all the profiles, and a very rich set of anticipated phenomena. It is also hard to run since both the model growth rate and $\omega_{E\times B}$ depend on local gradients.

The cases considered all model an L–mode edge. The transport barrier forms where the turbulence shearing rate from the radial electric field exceeds the local growth rate of the turbulence. When density transport is turned on, the strong local fueling source at the edge easily forms an edge transport barrier which can quickly lead to excessive edge pressure gradients. A large part of the NCS research thrust is aimed at controlling the edge pressure. To avoid this problem, we imposed a large edge growth rate to keep the edge in L–mode and fixed the edge density. The thrust to use an L–mode edge is one of DIII–D main AT thrusts but considering the high power flow through that edge, substantial mantle radiation or other means to suppress the L-H transition will have to be found. These are issues for future experimental and simulation work.

Despite the complexity of the model, the results in Table 5 represent another set of internally consistent numbers of target β_N and H factors with the required power levels and locations of current drive required to produce the necessary current profiles. The target β_N and H factors are large and represent ultimate goals for the DIII–D AT Program. Even with the high H factors, a 10 gyrotron system is needed and the total summed heating and current drive power of 20 MW will be a challenge to the divertor power handling capability in long pulse.

For the near term scenarios, perhaps some of the qualitative features seen in these transport barrier modeling efforts are worth noting. The density transport equation was turned on in Cases 2 and 3 and a transport barrier was allowed to form in the density channel (Fig. 13). Density gradients are more effective than temperature gradients in creating bootstrap current and for that reason, we obtain more bootstrap current than in the original SSC-VH scenario. Also, we have moved the transport barrier further out in radius and that also increases the total bootstrap current. We find it rather easy (in fact too easy in these simulations) to obtain full bootstrap current. It appears that with central fueling from beams or pellets and a longer time for the density to accumulate, we should see strong transport barrier formation in the future through density gradient with accompanying large bootstrap fractions. This research area has only just started on DIII–D. We completed the central Thomson scattering system and it is now operational on DIII–D. With it we will finally be able to see what is happening in the density channel when transport barriers form in the plasma interior. The UCLA group installed an x–mode interferometer on DIII–D about a year ago so we could get an early glimpse of a density transport barrier. One such profile (Fig. 14) shows a spectacularly high density gradient, showing us what exciting phenomena may lie ahead in these studies. We have a plan in the 1999 campaign in the Thrust 7 on ITB control to use the inside launch pellet injection together with the counter beam injection to stimulate the formation of transport barriers in the density profile.

Another interesting but not fully understood result was that the ECH was very effective at moving the location of the transport barrier. To see such dynamics was a principal reason for using the complex E×B shear model. The ECH deposition profile is about as narrow as the gradient regions of the transport barrier, and so the ECH is a precision tool

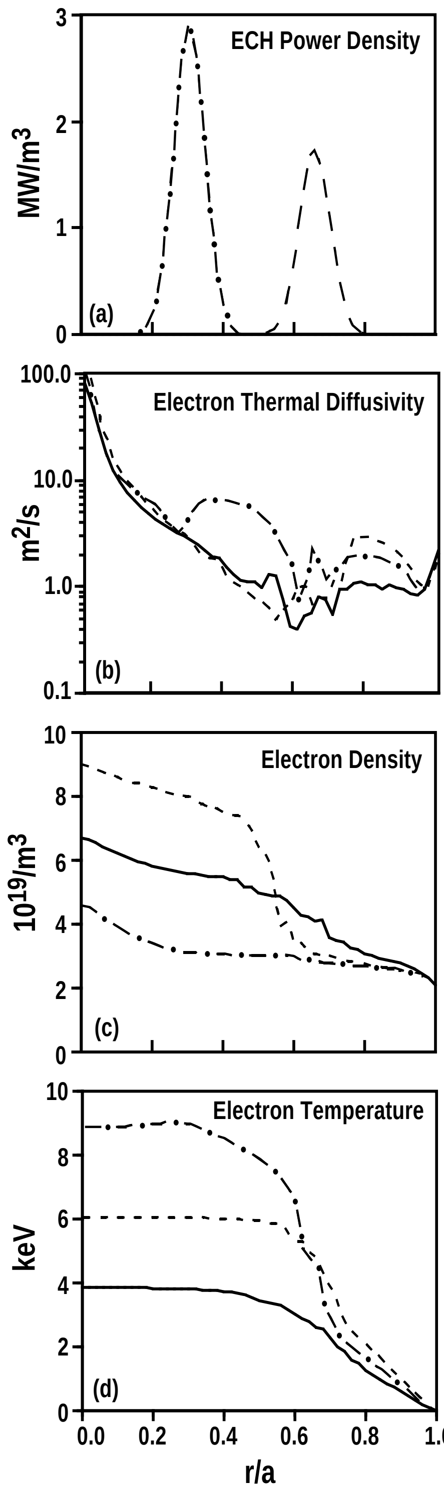

Fig. 13. ECH barrier control is illustrated by a three-case comparison: 6 MW NBI only (solid), 6 MW NBI + 6 MW ECH at r/a ~ 0.7 (dashed), 6 MW NBI + 6 MW ECH at r/a ~ 0.3 (dot dashed). Shown are profiles of (a) ECH power density, (b) model electron thermal diffusivity, (c) electron density, and (d) electron temperature.

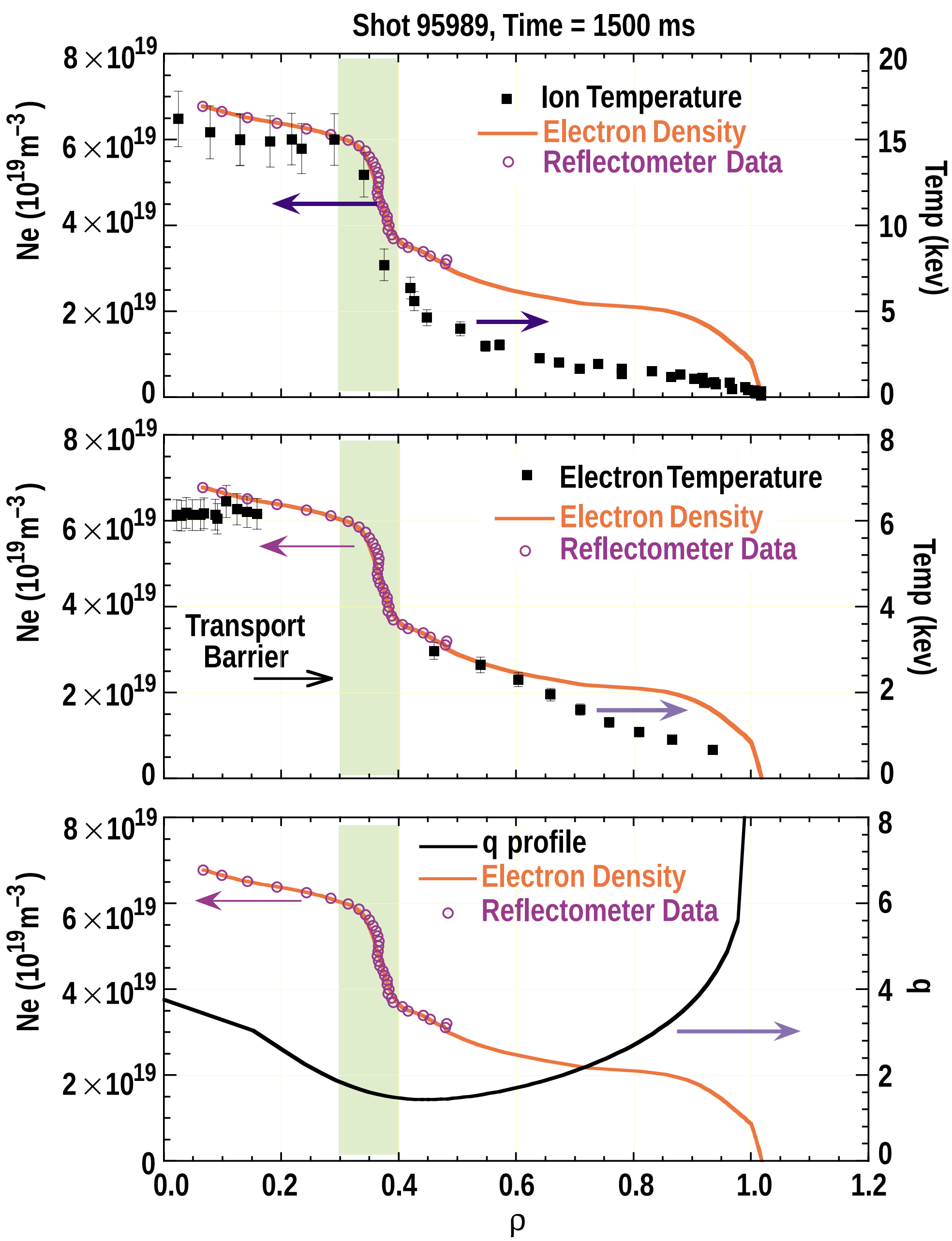

Fig. 14. Transport barrier in the density.

for barrier control. We found that ECH applied just outside the radius where a transport barrier was beginning to form would draw the transport barrier out to larger radius. Equally striking but not so positive was the effect of ECH when applied inside a formed transport barrier. The transport barrier was found to retreat to just inside of the ECH absorption layer. In the model this was due to the fact that the model growth rate increased with the electron temperature gradient but the E×B shear only depends on the ion temperature gradient. Thus, electron heating caused a loss of the E×B shear suppression. A retreat of an existing internal transport barrier with central ECH heating has been observed on DIII–D. Linear growth rate calculations suggest that the excitation of electron temperature gradient modes may be the cause. These modes are not expected to be stabilized by E×B shear since they have very large growth rates (and small wavelengths).

The physics picture mentioned above in which $\omega_{E\times B}$ pushes out radially against a radially rising turbulence growth rate suggests that the way to move the transport barrier out in radius is just to add power or momentum inside the formed transport barrier. However, because the transport coefficients are so low inside the barrier, increasing the power, especially localized power, can produce wild swings in local gradients affecting not only $\omega_{E\times B}$ but stability as well. The way through these complications is to increase power slowly. Using this approach, we were able in 1998 to make an internal transport barrier discharge that lasted the whole length of the neutral beam pulse (5 s). This was done at low current where the plasma was beset with Alfvén eigenmodes which had the beneficial effect of throwing out enough fast ions so that the central NBCD was weak and the central q stayed high. When such discharges were attempted at higher current, the Alfvén eigenmodes were eliminated but the central NBCD drove q_0 below one and instabilities terminated the high performance phase.

In the 1999 Thrust 7 campaign, counter-NBI was used as a means to achieve near stationary q profiles with elevated q_0 and to evaluate techniques to expand the ITB. With co-NBI, the sheared E_r from the plasma rotation and that from the pressure gradient are in opposition. This gives a sharp gradient in E_r (large local $\omega_{E\times B}$) but the dynamics are such to make it difficult to increase the radius of the large local $\omega_{E\times B}$. In contrast, with counter-NBI, the E_r from the plasma rotation and the pressure gradient are additive. The local values of $\omega_{E\times B}$ are not as large as for the co-NBI case, but as the beta increases, the region of large $\omega_{E\times B}$ expands and the ITB with it.

The various cases have varying assumptions about how low the transport rates become inside the transport barrier. In DIII–D we have already seen ion neoclassical transport rates all across the cross section so this assumption for the residual transport was made in all cases. But it is clear that similarly low levels for transport rates for electrons and particles in DIII–D are too good. Beta limits would be quickly exceeded. DIII–D does not presently see as much transport reduction in the electron and particle channels as in the ions and apparently will not require it to reach the scenarios shown.

These are some of the interesting phenomena we have seen in our initial exploration of the possibilities for AT physics in the plasma core. The simulations presented give a feeling for the parameter regimes achievable, the power levels in various systems to achieve them, the density and edge control that may be required. But the main value of such simulations is to open a wide vista of new phenomena that should open up as the auxiliary capabilities of DIII–D are developed toward the goal of long pulse sustainment of AT operating modes.

2.2.4. Recent ARIES-AT Scenarios

We have also explored optimization of AT scenarios as part of the ARIES-AT study. These studies have pushed conceptually and computationally closer to what might be the ultimate stability and transport potential of the tokamak. Here we have looked for pressure profiles consistent with very high bootstrap fractions (f_{BS} = I_{BS}/I_P > 0.9) and high beta values (wall stabilized). Equilibria are found with β_N = 5.6 (wall stabilized), q_{95} = 3.3 and f_{BS} = 0.92, as shown in Fig. 15. The high fraction of bootstrap current at such a low q value is a consequence of the large value of q_{min} ~ 2.5 and the large radius of q_{min}, ρ_{qmin} ~ 0.8. The key physics to such a scenario is the ability to form and control a transport barrier at large radius, ρ_{ITB}; with small gradients near the boundary. Analysis shows that sufficient sheared E×B flows to stabilize ITG modes in such a plasma are feasible. Understanding and controlling shorter wavelength micro-instabilities remains a challenge. The ARIES-AT study clearly defines a challenging approach for the optimization of DIII–D NCS plasmas — expanding and controlling the transport barrier at large radius and this effort is the focus of Thrust 7.

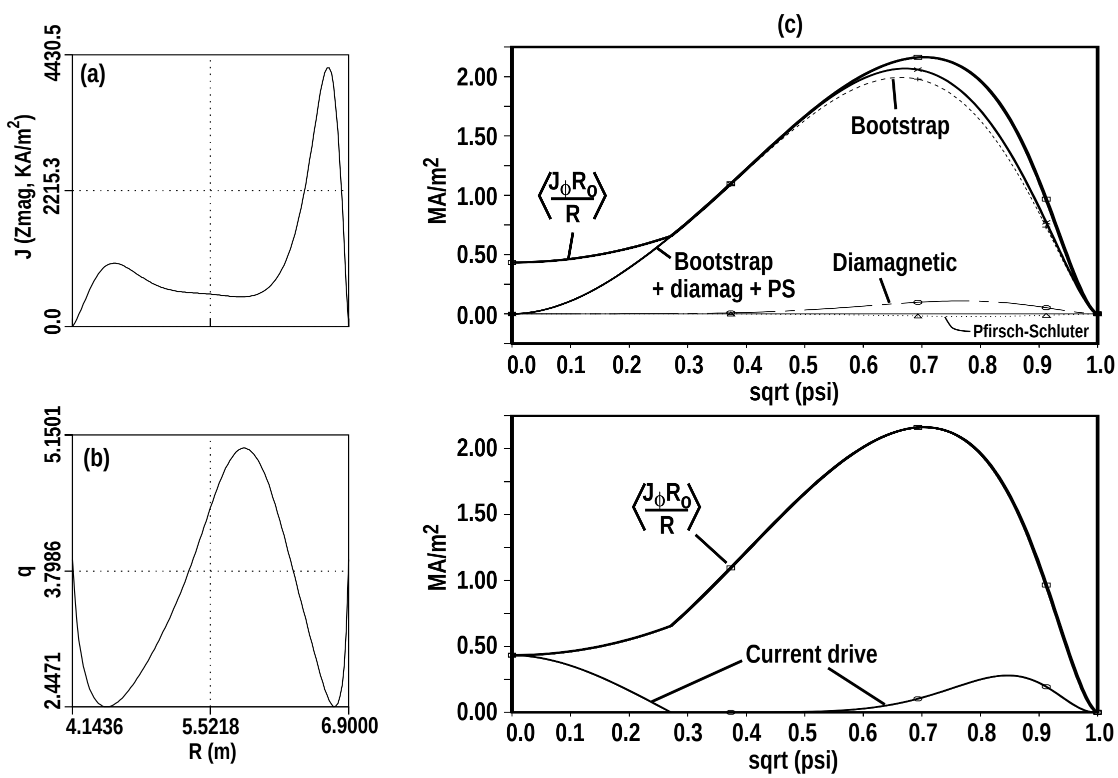

Fig. 15. High bootstrap fraction ARIES-AT scenario: (a) plasma current; (b) q profile; (c) total current (solid), bootstrap (dashed), and diamagnetic current (chain dashed).

2.3. THE HIGH INTERNAL INDUCTANCE SCENARIO IN DIII–D

The high internal inductance (high l_i) scenario is the second possible approach to AT performance being pursued in DIII–D research. This scenario is motivated by the well-established experimental observation that both the beta limit and the confinement multiplier increase approximately linearly with l_i. This scenario has the advantages that the current and q profiles are monotonic, requiring less precise tailoring, that the current density and pressure gradient at the plasma edge are not so large as to require wall stabilization to reach $\beta_N \approx 4$, and that the required external current drive would be peaked at the axis which is more efficient and easier to implement than in the NCS scenario.

In order to achieve high values of β_N, relatively broad pressure profiles are required. This places the regions of high pressure gradient toward the discharge edge and, in discharges with large bootstrap current fraction, produces relatively broad current profiles. So, operation at high β_N and high bootstrap fraction tends to lower the self-consistent value of l_i.

The achievable value of β_N is expected to be consistent with the empirical scaling Max(β_N) $\approx 4\, l_i$. Thus, a $\beta_N \approx 4$ operating point would have $l_i \approx 1$, a larger value than in the NCS scenario but smaller than the maximum values achieved in previous research on l_i scaling. Simulations have shown that bootstrap fraction in the range 50%–70% can be obtained self-consistently with $l_i \approx 1$. A sample equilibrium of this class is shown in Fig. 16. With strong shaping ($\delta \geq 0.7$) and flat J and q profiles in the center of the plasma, an optimized equilibrium can be found which is stable to n = 1 ideal modes and to $n = \infty$ ballooning at $\beta_N = 4$ without a conducting wall. This case has not as yet been examined for transport requirements although the bootstrap current profile is required to be consistent with the assumed pressure profile.

The achievable value of l_i for a given bootstrap fraction can be increased by reducing the value of the safety factor on axis. Reducing q_0 below 1 requires stabilization of the sawtooth instability. Previous work has indicated that sawtooth stabilization is possible with rf heating. A key question for the high l_i scenario is whether rf sawtooth stabilization can be done while maintaining the other requirements (high f_{BS} and β_N). Note that sawtooth stabilization should remove a primary source of perturbations which can initiate neoclassical tearing modes, which in turn may raise the beta limit. An example of this scenario is shown in Fig. 17. This example was developed with the same rules as the NCS example cited in Section 2.2.1, i.e., primarily to assess heating and current drive requirements.

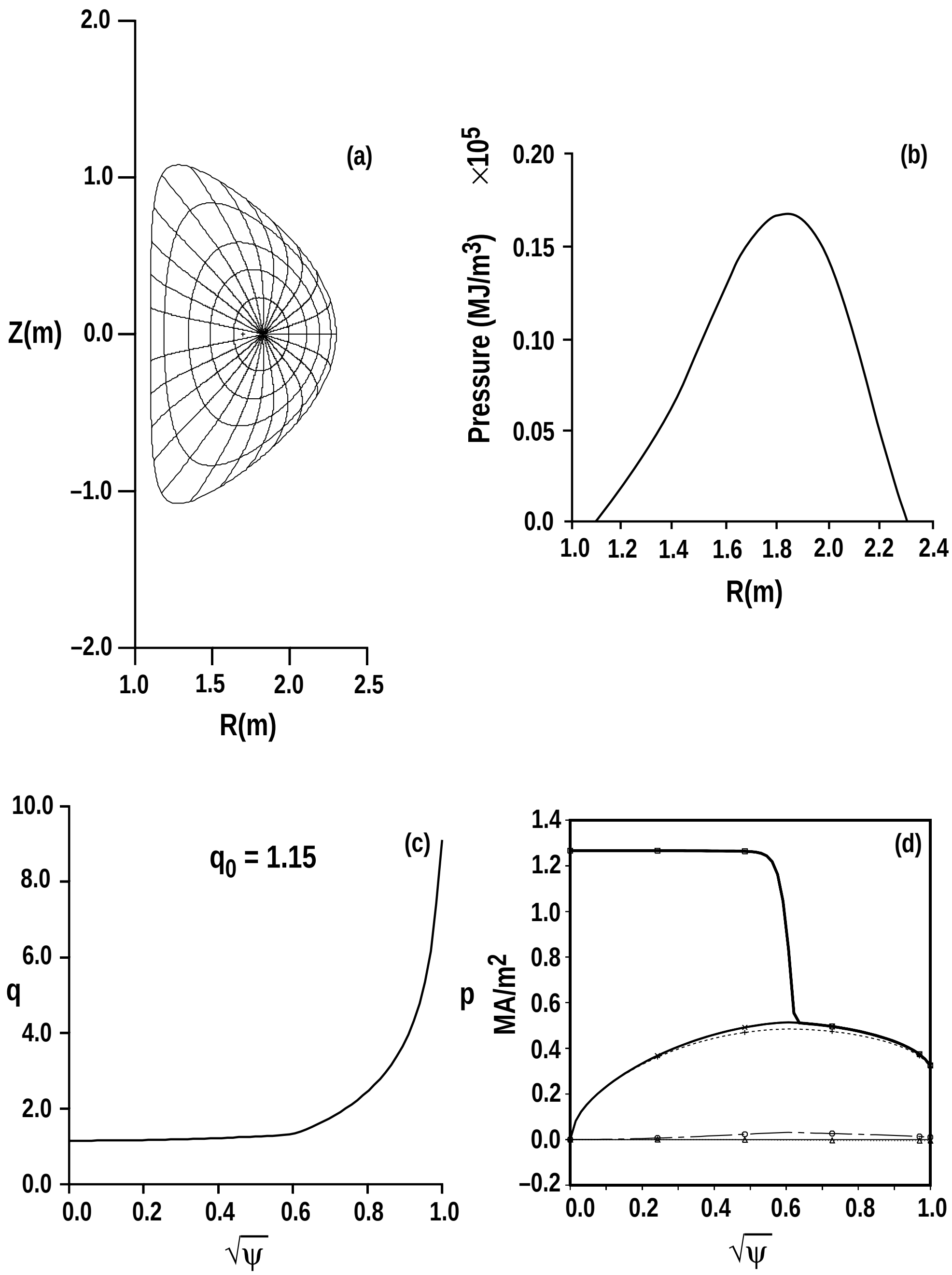

Fig. 16. Optimized l_i, high β_N, edge aligned bootstrap equilibrium in the full-size DIII–D configuration with R = 1.7 m, a = 0.6 m, κ = 1.8, δ = 0.7, B = 1.9 T, I_p = 1.1 MA, q_0 = 1.15, l_i = 0.92, $p_0/\langle p\rangle \sim 3.0$, β_N = 4.0, and f_{BS} = 70, q_{95} = 6.5. (a) Flux contours, (b) pressure profile across the midplane as a function of major radius, (c) q profile as a function of $\tilde{\psi}^{1/2}$, and (d) flux surface averaged toroidal current densities as function of $\tilde{\psi}^{1/2}$. Here, solid squares represent the total plasma current. The sum of bootstrap (dotted curve), diamagnetic (open circles), and Pfirsch-Schluter (open triangles) contributions is represented by crosses. parison: 6 MW NBI only (solid), 6 MW NBI + 6 MW ECH at r/a ~ 0.7 (dashed), 6 MW NBI + 6 MW ECH at r/a ~ 0.3 (dot dashed). Shown are profiles of (a) ECH power density, (b) model electron thermal diffusivity, (c) electron density, and (d) electron temperature.

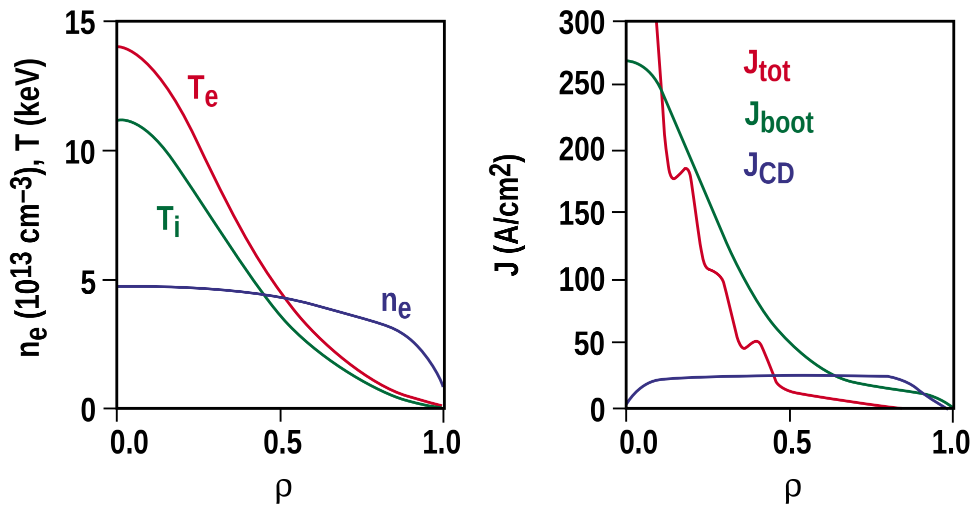

Fig. 17. A high l_i steady-state with $\beta_N H > 10$ can be sustained by a 3 MW ECH system. The parameters are: B = 1.9 T, l_i = 1.6, β_N = 2.5, I_{BS} = 0.41 MA, I = 1.0 MA, β_N = 4.0, P_{FW} = 3.6 MW, I_{FW} = 0.17 MA, q_0 = 0.55, H = 3.0, P_{EC} = 2.4 MW, I_{EC} = 0.14 MA, q_{95} = 5.6, n = 4.2×10^{19} m^{-3}, P_{NB} = 5.0 MW, I_{NB} = 0.27 MA.

Thus there are two distinct versions of the “high l_i” scenario, one requiring some current profile tailoring to maintain q_0 above 1 and sufficiently flat in the central region, and the other requiring effective stabilization of sawteeth.

One criticism of the high l_i scenarios has been that excessive external current drive power would be needed in a reactor. To examine this question explicitly, we have looked at spreadsheet modeling of three high l_i cases and compared them with ARIES-RS. Fixed parameters (with Aries-RS values in parentheses) are R = 5.0 (5.52) m, a = 1.8 (1.38) m, κ = 1.8 (1.7), δ = 0.7 (0.5), q_{95} = 6.5 (3.5), P_{fusion} = 2500 (2167) MW, and $n/n_{Greenwald}$ = 0.95 (1.78). Some of the results are summarized below.

	l_i = 1	l_i = 1.25	l_i = 1.5	ARIES-RS (l_i = 0.42)
β_N	4	5	6	4.84
q_0	1.15	0.85	0.55	2.78
B (T)	7.5	6.58	5.95	7.98
I (MA)	15	13.15	11.9	11.3
f_{bs}	0.61	0.67	0.60	0.88
P_{CD} (MW)	169	126	123	81
H_{89P}	2.1	2.44	2.65	2.35

The benefits of high ℓ_i operation are clear. If satisfactory sawtooth suppression is possible and the increase in β_N can be demonstrated, the q_0 = 0.55 case has significantly lower magnetic field than ARIES-RS, with roughly the same total current. Although the driven current fraction increases by 233%, from 0.12 to 0.40, the required external power increases by only 52%. This is because the current is driven at the axis, where T_e is high and trapping is small making the current drive much more efficient. Further, because the current is driven at the axis, a less complex profile control system is needed.

The multi-year goal of research for the high ℓ_i operating mode is to determine feasible scenarios for steady-state high ℓ_i discharges in DIII–D consistent with the available tokamak resources. A goal would be to maintain elevated ℓ_i values for twice the inductive decay time and confirm that the corresponding increase in confinement and stability is also maintained. The issues to be resolved over several years of work are:

1. Establish whether sawtooth stabilization is both possible and practical.
2. Establish the practical limits to β_N in the two high ℓ_i scenarios without additional wall stabilization. Do the linear relationships between β_N and ℓ_i, and between H and ℓ_i extend to $q_0 < 1$ cases?
3. Establish the current drive requirements for steady-state sustainment of these two scenarios. How much current profile control is needed for the $q_0 > 1$ case?
4. Development of entirely self-consistent scenarios to find the optimum combination of current, density, and temperature profiles.
5. Select the $q_0 > 1$ or the $q_0 < 1$ approach.

Regrettably, due to the intense competition for run time on DIII-D, we do not anticipate being able to allocate run-time to this research thrust until 2002.

To outline the possible content of a future plan to pursue the high ℓ_i scenario, we list here a simplified three-year view of the necessary research:

Goal: $\beta_N \bullet H_{89P} > 10$ with no inductive flux

<u>Year 1</u>

Demonstrate sawtooth stabilization for >1 s and validate the stabilization model. This includes modification and commissioning the ABB transmitters for operation at 60 MHz.

Develop the 3 MW ECH target scenario with $\beta_N \bullet H_{89P} > 10$ transiently. This includes FW coupling studies under the appropriate edge conditions and identification of core pressure limits.

Year 2

Demonstrate the 3 MW ECH integrated scenario. Develop a 6 MW ECH target scenario.

Year 3

Demonstrate the 6 MW ECH integrated scenario. Develop a 10 MW ECH target scenario.

2.4. RESEARCH THRUSTS — THREE-YEAR VIEWS

2.4.1. Edge Stability, Research Thrust 1 (Leader: J.R. Ferron, Deputy: L.L. Lao)

This thrust is aimed at solving a key problem in improving steady-state performance in DIII–D AT regimes: the termination of the AT high performance phase by instabilities that originate in the plasma edge. Previously, DIII–D discharges have been produced with transient phases with very high values of normalized beta, β_N and confinement factor H. Values of the performance product β_N H_{89P} as high as 20 have been obtained, where H_{89P} is the performance enhancement relative to L–mode. During 1999, longer duration high performance phases were produced at reduced plasma current and toroidal field. For example, a relatively long duration discharge with β_N H_{89P} = 9 lasted for approximately 2 seconds. While these values show great promise for the tokamak in its AT regimes, edge localized modes (ELMs) remain as an important limiting factor. This thrust is aimed at finding ways to stabilize these modes or to reduce their impact on the discharge performance.

Edge localized modes result from the large pressure gradient associated with the edge-localized transport barrier in H–mode. Large pressure gradients lead to significant bootstrap current being driven in the edge plasma. In shaped plasmas, this bootstrap current can open an edge-localized region with access to the ballooning mode second regime of stability. This enables the pressure gradient to increase above the calculated first ballooning regime limit. In this way a positive feedback loop is established between the edge pressure gradient, edge bootstrap current and the ballooning stability boundaries. Calculations and experimental results show that these conditions result in destabilization of low toroidal mode number coupled kink/ballooning modes. As a result of the low toroidal mode number, the radial extent of the unstable mode and the perturbation on the discharge can be significant. These instabilities serve as “soft” beta limits in that they cause a transition from an AT regime to an ordinary ELMing H–mode discharge.

We have shown that by closing access to the ballooning second stability regime, the positive feedback loop between the edge pressure gradient and edge current can be stabilized, resulting in less perturbing ELMs. However the increased edge pressure gradients allowed by second stable regime access also increase the edge pressure pedestal height and the overall confinement of the discharge. So, some compromise must be found between having the high edge pressure gradients and incurring instabilities severe enough to terminate the AT phase. It is the purpose of this thrust to find that balance.

Two approaches were explored in 1999. The first approach was to suppress second stable access in the edge region by choice of plasma shaping, seeking to build a high quality transport barrier inside the sufficiently stable, rapidly ELMing first regime edge plasma.Previous experiments had already shown that second regime access can be eliminated by either high or low squareness shaping of the discharge. In these experiments, an internal transport barrier was produced, but the results were dominated by locked modes apparently unrelated to ELMs. Further analysis of these results is required.

The second approach sought to retain the advantage in H-factor that results from edge region second stable regime access but to prevent or limit the consequences of the edge instabilities. Two approaches were planned. First, the growth of the edge pressure gradient (and therefore the resulting bootstrap current) was modified by impurity mantle radiation in order to keep the pressure gradient from reaching the unstable limit. These experiments were successful in preventing theoccurrence of ELMs but the discharges suffered from a radiative collapse resulting from buildup of the injected impurity. In the second approach the plan was to use edge-localized ECH to decrease the edge collisionality. The idea was to increase the ratio of bootstrap current to pressure gradient in order to increase the size of the region with ballooning mode second stable regime access. These experiments were ultimately postponed because of ECH availability. In other experiments, the triggering of ELMs by injection of deuterium pellets was studied. These experiments produced interesting data on the instability threshold as a function of pressure gradient and edge pedestal width. Finally, discharges useful for understanding edge instabilities were produced as part of the Thrust 2 effort. These discharges had relatively high performance during the initial portion of the ELMing phase. Analysis is required to understand why good performance was maintained during ELMs in these discharges in contrast to what is normally observed.

The focus during 2000 will be on analysis and developing a new lithium beam edge current density diagnostic. Data obtained during 1999 will be compared with theory to improve our understanding of the physics of edge stability. Extensions to the GATO code allowing analysis of higher toroidal mode numbers ($6 \le n \le 10$), and the ELITE code, which can evaluate stability of medium n coupled peeling/ballooning modes, will be utilized. One focus of analysis will be the relatively steady-state, high performance

ELMing discharges developed as part of Thrust 2 during 1999 to understand why the impact of ELMs on these discharges seems to be reduced.

One experiment on edge stability is planned for 2000 within the stability topical area to follow up on the results with impurity radiation by utilizing the RDP pump to control the impurity density. Finally, development of a diagnostic for improved measurement of the current density in the edge region is planned for 2000.

During 2001 and 2002, experiments on edge stability will resume. With the availability of improved edge current density measurements more accurate comparison of new experimental results with theory will be possible. Possible methods to modify the edge stability will be explored. Proposals that already exist include ECH in the edge region, various shape variations including a localized bump in the outer flux surface at the midplane to affect second stable regime access, and continuation of the use of impurity radiation and pellet injection. These experiments will follow up on the experiments that were begun during 1999. New experiments to make detailed comparisons to theory are planned, for instance the study of ELMs during limiter H–mode discharges for comparison with the theory implemented in the ELITE code. Experimental proposals generated during the 2000 year of analysis will also be explored.

2.4.2. AT Scenario, Thrust 2 (Leader: T.C. Luce, Deputy: M.R. Wade)

Three-Year Goal

Demonstrate normalized tokamak performance more than twice that of conventional ELMing H–mode with no inductive flux for a duration limited only by hardware constraints.

Goal: β_N*$H_{89P} > 10$ with no inductive flux.

Critical Path Items

Tool Development.

Gyrotron commissioning (up to six gyrotrons operational)
EC launcher commissioning
Validation of ECCD in ELMing H–mode plasmas
Particle (density) control
Feedback control with the PCS

Physics Issues.

Assessment of effects of q_{min} and q_{95} on bootstrap current fraction and alignment.
Assessment of confinement when T_e approaches T_i.

Assessment of impurity accumulation.
Assessment of resistive wall mode avoidance and suppression techniques.

Draft Three-Year Outline Plan

Issues to Address in 2000.

- Apply new RDP hardware for particle control.
- Commission new gyrotrons and new launchers.
- Validate ECCD in ELMing H–mode.
- Demonstrate PCS real-time q profile measurement.
- Assess impact on confinement of T_e approaching T_i.
- Assess difficulty in extrapolating performance to higher I, B.

Issues to Address in 2001.

- Demonstrate 3 MW ECH integrated solution.
- Develop 6 MW ECH target scenario.
- Commission 6 MW system.

Issues to Address in 2002.

- Demonstrate 6 MW ECH integrated solution.
- Establish basis for extrapolation.
- Develop 10 MW ECH target scenario.

2.4.3 Neoclassical Tearing Mode, Thrust 3 (Leader: R.J. La Haye, Deputy: C.C. Petty)

Two principal research lines are foreseen in a three year plan: (1) studies in H–mode with sawteeth present and (2) studies in an AT mode with raised q_{min} (Fig. 18).

H–Mode With Sawteeth

2000

Reduce the width of the 3/2 mode with ECCD.
Test physics of polarization threshold.

2001

Shrink the modes and/or prevent their onset with ECCD.

2002

Suppress the 3/2 and/or 2/1 modes separately using two ECCD systems.

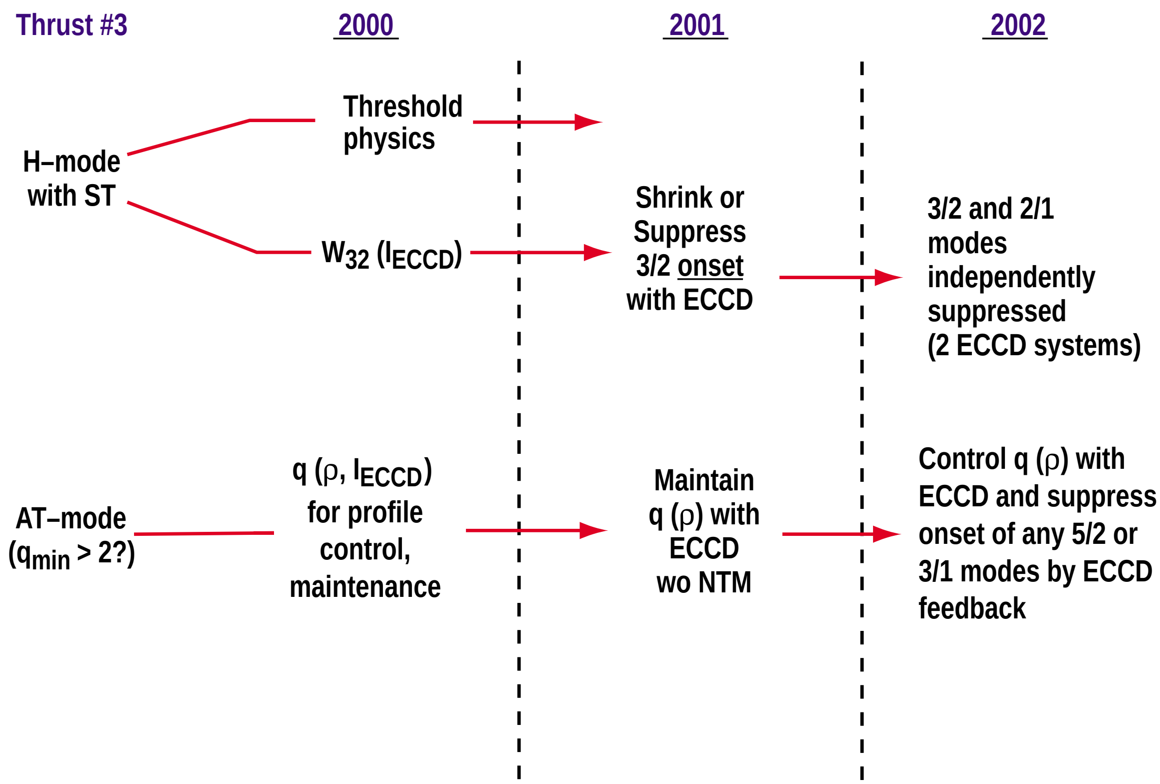

Fig. 18. NTM Research Plan.

AT Mode Line

2000

Study the variation of the q profile with ECCD.

2001

Maintain the q profile with ECCD so as to avoid NTM onset.

2002

Control the q profile and suppress any 5/2 and/or 3/1 modes by 2 ECCD systems.

2.4.4. Wall Stabilization, Thrust 4 (Leader: G.A. Navratil, Deputies: A.M. Garofalo, M. Okabayashi)

Validate the model of wall stabilization and begin feedback stabilization experiments. Overall Goal: Sustained operation at beta significantly above the no-wall limit.

Progress in 1999: Validate Models of Rotational Stabilization and Initial Experiments on Feedback Control

Physics of Wall Stabilization and Plasma Rotation.

- Three AT plasmas were developed for RWM Study: SND ($\beta_N^{no-wall}$ ~ 2); DND (q_{95} ~ 4.5); DND (q_{95} ~ 5.5; record long pulse β_NH ~ 9)
- The n=1 RWM limits the performance of low-l_i AT plasmas to $\beta_N \leq 4\, l_i$.
- Plasma rotation unable to completely suppress RWM for $\beta_N \geq 4\, l_i$.
- Plasma toroidal rotation strongly reduced whenever detectable RWM is present ($\delta B_r \geq 1$ Gauss).
- Test of q_{min} dependence of rotation threshold inconclusive: unable to vary q_{min} above and below 2 at RWM onset time.
- RWM "bursting" observed in DND plasmas near $\beta_N^{no-wall}$ limit.

Initial Feedback Control Experiments (PoP Test).

- Radial flux leakage of n=1 mode through the vacuum vessel can be compensated by the feedback system: test of basic "Smart Shell" algorithm.
- Three feedback algorithms were tested: "Smart Shell"; "Fake Rotating Shell"; and "Mode Control"
- "Fake Rotating Shell": co-injection direction favorable for stabilization.
- Smart shell control of low density locked mode was ineffective: tearing mode not sensitive to radial flux compensation on vacuum vessel wall.
- 3-D code VALEN improved to include GATO generated n=1 RWM current distribution in the plasma model: basic tool for design of an optimal C–coil extension for mode control.
- 2-D simulation of active RWM control by A. Bondeson [MARS] and M. Chance/M. Chu [PEST-VACUUM] is in progress.

Extend Lifetime of Plasma Above the No-Wall Limit.

- High β duration was extended with addition of "derivative gain" in feedback loop (both for "Smart Shell" and "Mode Control" algorithms).
- Modest improvement in high β plasma duration is consistent with VALEN predictions of control coil (C–coil) coupling to n=1 RWM.

2000: Validate Model for Active Control. Optimize Control With Six-Element C–coil.

- Validate quantitative 3-D model for n=1 feedback control.
- Extend the regime of improved stability with closed-loop feedback control, with higher power using three bipolar power supplies.
- Finalize design of upgraded external coil set for improved feedback control.

2001–2002: Feedback With Upgraded C–coil

- Install upgraded C–coil set.
- Demonstrate sustained operation significantly above the no-wall beta limit in high performance AT plasmas.

Proposed Experimental Plan for 2000

1. Active Control of the Resistive Wall Mode (5 days)

    - Test range of leading active feedback control algorithms:
      — Optimal Smart Shell
      — Soft Rotor Stabilization
      — Mode Control Algorithm
    - Explore range of RWM target plasmas: SND and DND
    - Lower δB_r detection threshold for the RWM:
      — Establish required level of mode delectability
      — Use the extended saddle coil sensor array
      — Use toroidal array of B_p for n=1 mode detection

2. RWM Physics Studies (2 days)

    - Effect of Plasma Rotation
    - Seed error field amplification above & below the no-wall limit
    - Effect of q_{min} on rotation threshold
    - Effect of rational flux surfaces at plasma edge on threshold
    - Improved soft x-ray measures of mode structure
    - Use C–coil system for improved error correction for present DND AT plasmas.

3. Active Control of Locked Modes (1 day)

    - Density Limit Locked Modes
    - Quasi Stationary Modes
    - Locked NTM control

2.4.5. Optimum Edge, Research Thrust 5 — Develop the Basis for Choosing Single- Versus Double-Null and the Optimum Triangularity of the Outermost Flux Surface in Future Machine Designs (Leader: M.E. Fenstermacher Deputies: T.H. Osborne, T.W. Petrie)

This thrust seeks to accumulate a large body of detailed systematic measurements and analysis aimed at building a deeper understanding of the physics of the coupled regions just inside the separatrix (the H–mode pedestal region) and the region just outside the separatrix (the SOL and divertor). In the FY99 experimental campaign this thrust implemented a set of systematic data scans to obtain detailed edge pedestal, divertor information, and other plasma performance measures versus the triangularity, the distance between the separatrices, and the volume of the divertors of a double-null. This information is expected to answer key questions of future machine design related to the best shape of the outermost flux surface, focusing on an edge physics point of view. Although the experimental portion of the thrust is complete, significant data analysis will continue in FY2000 leading to a final report and recommendations on how to revisit the question of the effect of plasma shape for an optimized advanced tokamak core with internal profile control.

Low Triangularity, High Density and High Confinement with Gas Fueling and Divertor Pumping (T.H. Osborne)

In the Thrust 5 experiments focussed on triangularity, discharges with $n_e/n_G = 1.4$, and energy confinement enhancement over L–mode scaling, $H_{ITER89P} = \tau_E/\tau_{ITER89P} = 1.9$ were obtained with gas puffing in combination with divertor pumping. Here n_G is the Greenwald density, $n_G = I_P/(\_a^2)$. Gas puff fueling of unpumped H–mode plasmas typically leads to loss of energy confinement when the electron density, n_e, approaches the Greenwald density. Divertor pumping acts to maintain the temperature in the X–point region as high as possible while the H–mode pedestal temperature, T^{PED}, decreases and the pedestal density, n^{PED}, increases with gas puffing at roughly constant p^{PED}, in the Type I ELM regime. Maintaining high X–point temperature may avoid a transition from the Type I ELM regime to L–mode or to the Type III ELM regime in which confinement is reduced.

The high density good confinement discharges on DIII–D show spontaneous repeaking of the density profile in the Type I ELM regime which, in the highest density cases, compensates for a reduction in p^{PED}. The usual decrease in energy confinement in the Type I ELM regime with gas puffing is associated with a reduction in p^{PED} and a broadening of the density. The reduction in p^{PED} begins in the range $0.6 < n_e^{PED}/n_G < 0.8$ and is a result of the decrease in edge pressure gradient at low temperature. The pressure gradient decrease is consistent with what would be expected for a transition from ideal to resistive tearing modes. The effect of the reduction in p^{PED} is through stiffness of the temperature profile which is apparent in the high density regime on DIII–D. The energy confinement is also reduced in discharges with stiff temperature profiles when the density profile broadens at fixed p^{PED}. The density profile peaking occurs under conditions that reduce the central temperature suggesting the neoclassical Ware pinch.

Effect of Variation in Up/Down Magnetic Balance (T.W. Petrie)

Thrust 5 experiments also systematically varied the magnetic balance of highly triangular ($\delta \approx 0.8$), unpumped H–mode plasmas. Changes in divertor heat loading and particle flux, energy confinement, and density operating range in H–mode were observed when the magnetic configuration was varied from a balanced double-null (DN) divertor to a slightly unbalanced DN divertor. To quantify "magnetic balance," we define a parameter dr_{SEP}, which is the radial distance between the upper divertor separatrix and the lower divertor separatrix, as determined at the outboard midplane.

For attached plasmas, the variation in heat flux sharing between divertors is large for small changes in dr_{SEP} near 0 (i.e., near double-null); the peak heat flux shifts predominantly from one divertor to the other divertor within ±5 mm of magnetic balance (Fig. 19, red curve). This sensitivity can be shown to be consistent with the measured scrape-off length of the parallel divertor heat flux, λ_q. Furthermore, λ_q can be approximated to within a factor of two with a simple model using only the midplane scrape-off lengths of electron density and temperature, suggesting that divertor processes (e.g., recycling) are not dominating the physics. At magnetic balance ($dr_{SEP} = 0$), we find that the peak heat flux toward the divertor in the grad-B direction is twice that of the other divertor. Most of the heat flux goes to the outboard divertor legs in a balanced double-null, where the peak heat flux in the outer divertor may exceed that of the inner divertor by tenfold. The variation of the peak particle flux between divertors is less sensitive to changes in magnetic balance, suggesting that divertor processes are much more important here than in the heat flux case. We believe that these divertor "asymmetries" are driven by E×B poloidal drifts. In detached plasmas, however, we find the heat flux split between divertors to be much less sensitive to dr_{SEP} (Fig. 19, green curve).

Variations in magnetic balance affect plasma performance in other ways. The density at the H-L back transition may be 15%–20% lower for an unbalanced double-null biased away from the grad-B direction, with most of this change occurring near magnetic balance. Regardless of how the divertors were magnetically balanced, however, D_2 gas puffing always degraded energy confinement to the range $\tau_E/\tau_{E89L} \approx 1.3$–1.6. When this point was reached, τ_E stayed nearly constant, even as these plasmas were fueled to near their respective density limits

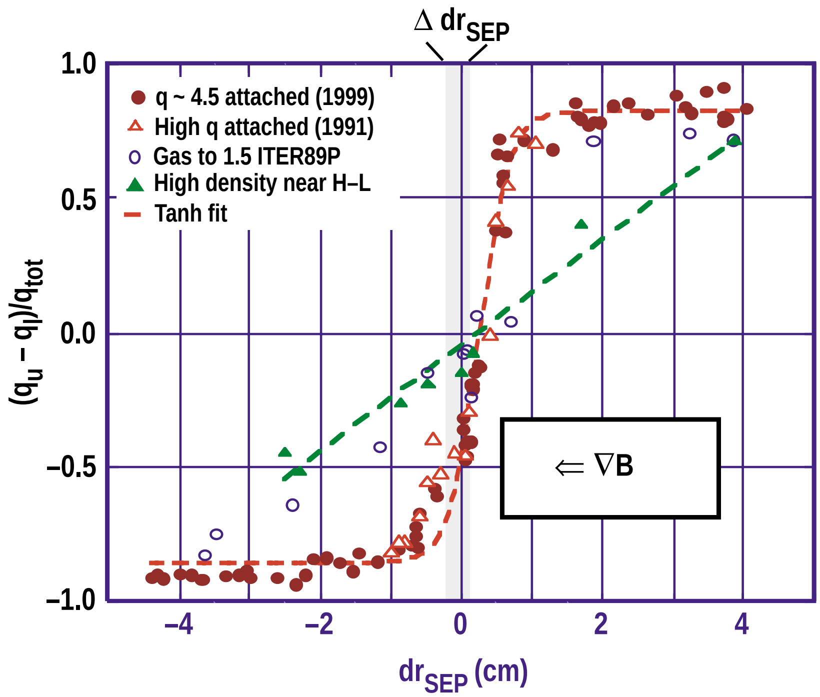

Fig. 19. Normalized peak heat flux balance as a function of magnetic balance parameter dr_{SEP}. Data from attached plasmas in the 1999 campaign at moderate q_{95} ~ 4.5 (red circles) and hyperbolic tangent fit (red dashed line) show a sharp transition from lower to upper heat flux dominance as dr_{SEP} is varied from slightly unbalanced lower single-null (dr_{SEP} = –0.5 cm), through balanced double-null (dr_{SEP} = 0) to slightly unbalanced upper single-null (dr_{SEP} = +0.5 cm). Uncertainty of dr_{SEP} is approximately 0.2 cm (grey bar). Data from a single swept shot in 1991 at high q_{95} (red trinagles) showed a similar transition. In high density (blue open circles) and partially detached operation (green triangles) the transition is much broader indicating the importance of local recycling effects in the divertor.

Effect of Variation in Divertor Volume (M.E. Fenstermacher)

The third subdivision of Thrust 5 attempted to address the desire to achieve the performance advantages of high triangularity (high–δ) operation with the core plasma volume maximized and the divertor volume minimized. At low δ in single-null divertor configurations, only the primary X–point is present inside the vacuum vessel. As δ is increased the location of the secondary X–point, which maps at the midplane to a flux surface radially outboard of the primary, moves from outside the vacuum vessel to inside and divertor physics (recycling, target heat flux etc.) becomes important in this secondary divertor. Since the secondary divertor takes up volume that could be used for the burning core plasma, the focus of these experiments was to determine the minimum secondary divertor volume consistent with good core, pedestal and divertor performance.

The sensitivity of edge pedestal and divertor performance parameters to reduction in secondary divertor volume was examined by varying the vertical distance of the secondary X–point from the target plate, 1 cm < Z_S < 16 cm, while holding the primary X–point height, Z_p = 16 cm, fixed. For these discharges the ion ∇B drift was in the direction of the primary divertor. Discharges with and without active primary divertor cryopumping were examined. The effective rate of rise of the core density at the L-H transition increased 60% as Z_S was reduced from 16 to 1 cm. At high density achieved by gas injection, the core line averaged density at the H-L back transition decreased 25% as Z_S was reduced. Both of these results indicate that performance may be affected when core plasma screening of neutrals in the secondary divertor is reduced as Z_S decreases. The peak heat flux in the secondary divertor $\left(P^s_{div}\right)$ was nearly constant for high Z_S. However, when Z_S was reduced from 3 cm to 1 cm, P^s_{div} increased a factor of 3 indicating that the secondary divertor target was beginning to act as a heat flux limiter as Z_S became comparable to the power scale length in the scrape-off-layer mapped to the secondary X–point location. Finally, for unpumped discharges the dependence of the maximum achieved edge pedestal temperature and pressure during the ELM-free period was nonlinear with Z_S. The dependence on Z_S was very weak for discharges with active pumping. Boundaries between Type-I ELMing and Type-III ELMing regimes in edge pedestal operating space also seemed to depend weakly on Z_S for unpumped plasmas. Although we attempted to hold as many control parameters fixed as possible, data showed that variation in wall conditions may also have affected the edge and divertor performance somewhat. Core transport and SOL/divertor fluid simulations are in progress to identify the mechanisms connecting secondary divertor volume variation to changes in performance.

2.4.6. High ℓ_i, Thrust 6

Work deferred until 2002. See end of Section 2.3 for the plan.

2.4.7. ITB, Research Thrust 7 — Expand the Spatial Extent and Time Duration of Internal Transport Barriers (Leader: C.M. Greenfield; Deputies: E.J. Synakowski, E.J. Doyle)

Goals

Control of internal transport barriers (ITB) has been identified as a high priority at the recent AT Workshop held at General Atomics as well as at the Snowmass meeting. Specifically, control of three different aspects of the ITB is needed in order to establish it as a viable confinement regime.

First, the spatial extent of the barrier must be extended in order to increase the energy content and the fusion output from within the barrier region (Fig. 20). The requirement that this be done in a manner consistent with MHD stability leads to a second area of control: the pressure gradient in the barrier itself must be maintained at a level below

MHD stability limits. Third, in order to maintain a steady barrier, the current profile must be maintained so that q_{min} remains elevated, with weak or negative shear in the core.

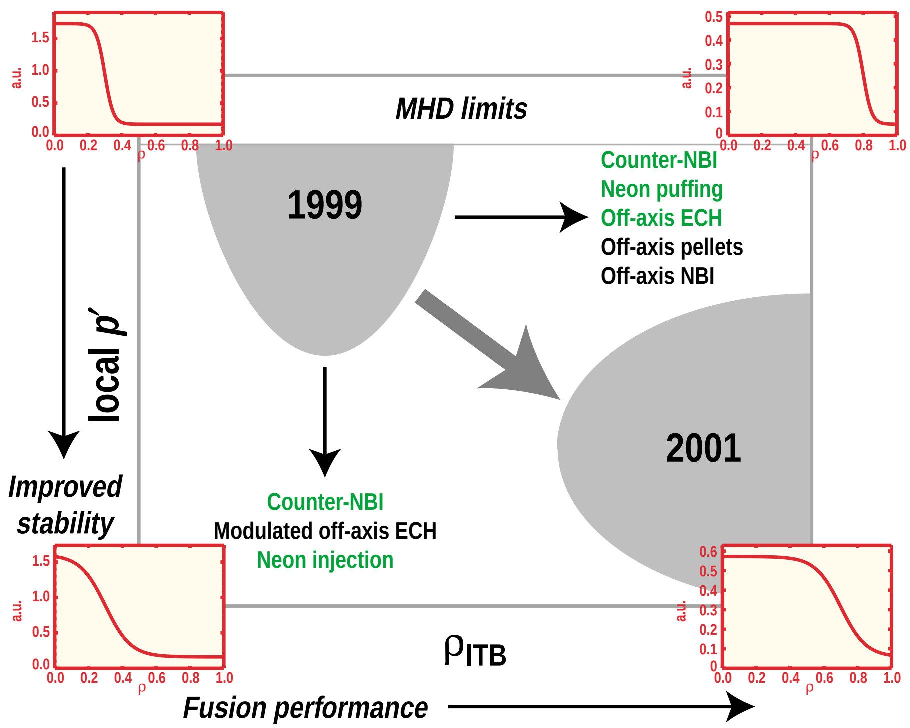

Fig. 20. Efforts in Thrust 7 are focused toward increasing fusion performance by expanding the transport barrier, while at the same time controlling the pressure gradient within the transport barrier to maintain MHD stability.

The plan for the 2000 campaign directly addresses open-loop tests of control of the first two of these requirements, with the third being addressed indirectly. Since the current three day plan does not allow for testing all of the proposed methods, the entire set of proposed open-loop tests will require two or more years. Successful completion of the proposed near-term program can lead to future closed-loop tests of ITB control with feedback.

A fourth requirement, relating to reactor relevance of the ITB regime (barring advances allowing a hot-ion mode in a reactor) is to extend the operating space toward $T_e/T_i \sim 1$. An experiment to explore a possible avenue toward this state is not included in the five day plan, but is included as a possible contingency experiment.

1999 Progress

Experiments in 1999 concentrated on studies of the ITB with counter-injected neutral beams. As might be expected with any new regime, development of the regime took most of the time allocated, with only a small amount of time left for actual optimization of study. Nevertheless, the experiments were successful in demonstrating that barriers can be formed with counter-NBI, and are broader than their co-injected counterparts. This is not surprising, since with co-injection, the diamagnetic and toroidal rotation terms of the E×B shearing rate oppose in such a way that broadening or increasing the pressure gradient will *decrease* the shearing rate, thereby allowing drift ballooning modes such as the ITG mode to become more unstable. With counter-NBI, the two terms are aligned so that increasing or broadening the pressure profile can actually be stabilizing to such microinstabilities [C.M. Greenfield, *et al.*, GA-A23305, submitted to Phys. Plasmas] (Fig. 21). Although progress was made in exploiting this feature of counter-NBI, it is believed that further optimization with counter-injection may allow further ITB broadening.

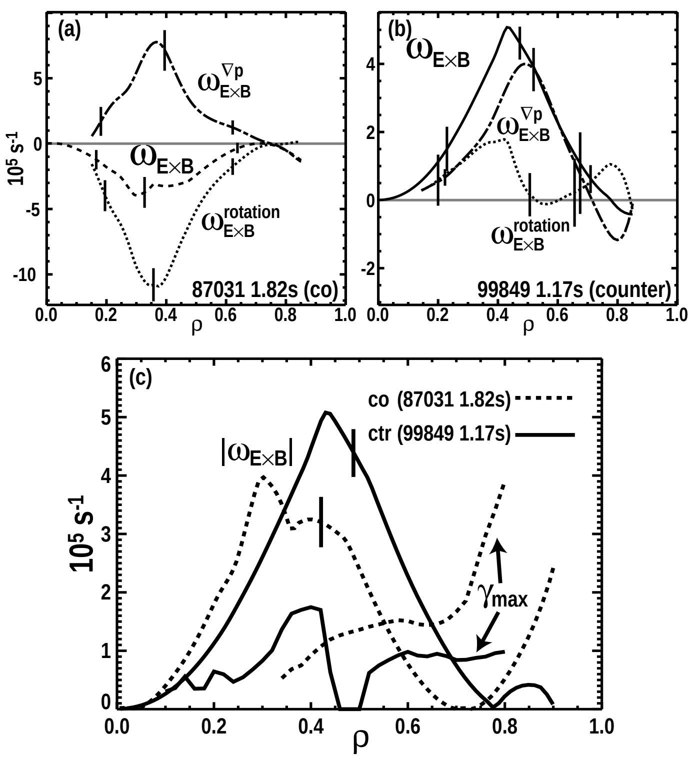

Fig. 21. Main ion pressure gradient and rotation terms of the E×B shearing rate are opposed with co-, and aligned with counter-injection so that increasing or broadening the pressure profile is stabilizing to drift-ballooning modes with counter-injection.

Another important feature of counter-injection is that counter-neutral beam current drive (NBCD) was successful in arresting the evolution of the current profile during the ITB phases of the discharge. With finer control of the neutral beam power, we believe there is a possibility of simultaneously exploiting both the favorable effect on the shearing rate and the counter-NBCD to expand and sustain the barrier.

First attempts at producing a transport barrier using high-field-side pellet-injection were also successful during the Thrust 7 experiments in 1999 [L.R. Baylor, *et al.*, submitted to Phys. Plasmas]. In these experiments, extremely steep barriers were produced in the electron density profile, with $T_e/T_i \sim 1.25$ achieved and maintained for hundreds of ms with counter-injection.

Although not carried out within Thrust 7, DIII–D demonstrated that impurity injection can produce transport barriers by decreasing the ITB growth rates [G.R. McKee, *et al.*, submitted to Phys. Plasmas]. This tool will be incorporated into our efforts within Thrust 7.

Finally, an experiment was carried out to determine the relationship between the transport barrier location and the location of the minimum safety factor ρ_{qmin} [M. Makowski, Bull. Am. Phys. Soc. **44**, 77 (1999). Paper CP1 87]. Incorporating a fast current ramp and high power neutral beam (co) injection very early in the discharge did this. Although discharges were produced with very large $\rho_{qmin} \leq 0.9$, the transport barrier was not formed at this large radius. It is felt that the aforementioned cancellation of terms of the shearing rate may be responsible for limiting the barrier location in such co-injected discharges. Although a proposal was made to follow this up with a similar experiment in a counter-injected plasma, it has not been included on the list of experiments for 2000 due to concerns that the beam ion confinement may be too poor when combining the large orbits produced with counter-injection and the very low poloidal field inherent to these plasmas.

Experiments Proposed for 2000 and Beyond:

In the year 2000, we proposed to continue development of barrier control tools, justified either by previous experiment or theoretical predictions, in an open-loop fashion. If one or more of these tools is extremely successful in modifying the barrier in the desired manner, we might choose to make an earlier transition to application in a closed-loop. Otherwise, the first phase of experiments (which will probably take 2 years or more depending on time allocations) will include open-loop tests of the following. Note that many of these tests are intended to be performed with barriers formed by both neutral beams alone and those with pellet triggers, in order to produce two very different data points:

1. **Continued Optimization of the Counter-Injected ITB**. Attempts have been made to use fine control of neutral beam power to control the barrier position in the past, but have not been successful. We now believe that this might have been at least partially due to the cancellation of the diamagnetic and rotation terms of the shearing rate, as previously mentioned, with co-injection. In those discharges, increasing the power would result in a steepened pressure gradient and eventually to an MHD event (which could lead to either disruption or an H–mode transition). We believe that similar efforts with a counter-injected target plasma should lead to broadening of the barrier through the mechansim described in the previous section.

   Further success in this area may motivate future consideration of modifying the neutral beam geometry in DIII–D by reversing the orientation of one of the beamlines.

   The plasmas produced by this optimization are expected to have broader barriers and be easier to sustain than we can achieve with co-injection, and so are proposed to be used as a target condition for several of the other areas listed below.

2. **Optimization of Impurity Injection**. Previous experiments with impurities, primarily neon, have demonstrated the production of an internal transport barrier at rather limited parameters. Experiments in the next phase of Thrust 7 will attempt to extend this improvement to barriers with similar local performance to those produced with high power neutral beams alone and exhibiting higher temperatures, densities, etc. Successful application of this technique should lead to broader barriers due to the favorable influence of the impurities on microinstability growth rates in the part of the plasma where they are usually expected to be largest.

3. **Off-Axis ECH**. ECH heating (radial launch) near the axis of beam-heated discharges has previously been shown to result in deterioration of the transport barrier [C.M. Greenfield, *et al.*, Nucl. Fusion **39**, 1723 (1999)]. Theoretical predictions [G.M. Staebler, *et al.*, EPS 1998] have been made which indicate that the same effect can be used in our favor, by injecting ECH outside the ITB, thereby causing the ITB to move toward the heating location. Further predictions [D. Newman, private communication (1999)] indicate that modulated ECH injected in two locations, just inside and outside the barrier, may be a useful too to

control the pressure gradient in the barrier. Tests of control of both the ITB position and strength are proposed using off-axis ECH in both ways. Future experiments may even be able to do both of these simultaneously.

4. **Off-Axis Pellet Injection**. Utilization of shallow pellet injection, just outside the barrier, may be another means of expanding the barrier in a similar manner as with off-axis ECH. The primary mechanism here is expected to be in the angular momentum, rather than a termal, transport channel.

5. **Magnetic Braking**. Magnetic braking may be used to remove momentum to simulate the case where balanced injection is used to maintain broader barriers, as in JT-60U [H. Shirai, *et al.*, H–mode Workshop 1999]. Although using field errors to brake the plasma may not ultimately be a desirable situation, this may also help to motivate future changes to beam geometry.

6. **Off-Axis NBI**. Shifting the plasma above the midplane of the tokamak can be used to move the neutral beam heating location significantly off-axis. This is expected both theoretically and experimentally to result in a broader barrier. Once again, this may not lead to an attractive scenario in DIII–D as it is presently configured, but may be used to motivate future considerations of modifications to the neutral beam geometry.

One other experiment is proposed for inclusion in this phase of the experimental program. Recently, ASDEX–U incorporated counter-ECCD in a beam-heated discharge to produce an internal transport barrier with $T_e(0) \approx T_i(0) \approx 12$ keV [F. Leuterer, *et al.*, EPS 1999; O. Gruber, *et al.*, H–Mode Workshop 1999; R. Wolf, *et al.*, submitted to Phys. Plasmas]. This regime is a challenge to our understanding and previous experience with the impact of electron heating in ITB discharges. However, if it can be duplicated, this regime offers perhaps a more reactor-relevant scenario than the hot-ion modes usually produced with an ITB. We propose to attempt to produce plasma in this regime both to demonstrate the regime itself and in an attempt to understand the underlying physics and how it differs with our previous experience.

Future experiments, nominally planned for the third year of this plan, will incorporate the most promising results of these closed-loop tests in a demonstration of a controlled barrier utilizing feedback control of one or more of these tools.

3. TOPICAL SCIENCE AREAS — THREE YEAR VIEWS

3.1. STABILITY TOPICAL AREA GOALS (3 YEAR VIEW)

1. Advance the physics understanding of resistive wall mode stability, including the dependence on plasma rotation, wall distance, and feedback stabilization.
   Develop sustained operation above the no-wall beta limit through passive or active stabilization of the resistive wall mode.

2. Characterize the physics of edge-driven instabilities in plasmas with a large (H–mode) edge pressure gradient and associated bootstrap current.
   Develop methods to avoid or reduce the impact of edge-driven instabilities through modification of the edge pressure gradient, collisionality, or shaping.

3. Advance the physics understanding of non-ideal plasma instabilities including neoclassically driven tearing modes, sawteeth, and fast ion driven instabilities.
   Develop sustained high beta operation free of sawteeth and neoclassical tearing modes, through profile control or active stabilization.

4. Advance the understanding of disruption physics in advanced tokamak discharges and improve the viability of tokamak reactor concepts by avoiding and mitigating disruptions.
   Develop methods of mitigating runaway electron, halo currents, and disruption heat loads, and disruption prediction and avoidance using real-time identification of disruption boundaries.

3.2. CONFINEMENT AND TRANSPORT TOPICAL AREA GOALS (3 YEAR VIEW)

Physics research aims at a level of understanding that allows quantitative predictions. In the transport arena in magnetic fusion research, this means the development of a predictive understanding of the energy, particle and momentum transport in magnetized plasmas. Achieving this goals requires the combined efforts of theorists, modelers and experimentalists to develop the fundamental theories, include them in numerical models, compare those models with the results of experiments and then iteratively improve them. Based on this ultimate goal, our three year goals for confinement and transport are:

1. Develop improved physics understanding and control of reduced core transport regions
   — Develop and exploit new tools for controlling core transport: Pellet injection, impurity injection, counter neutral beam injection, co and counter ECCD.
   — Broaden tests of the $\omega_{E\times B}$ versus γ_{MAX} comparison by using new tools to investigate effect of T_i/T_e ratio, impurities, density peaking, magnetic shear.
   — Increase emphasis on understanding electron transport.

2. Investigate fundamental nature of turbulent transport in tokamaks.
   — Is complex dynamics (avalanches) a better fundamental model than a theory in which fluxes depend continuously and smoothly on gradients?
   — Can we identify features in the data which are unique to the fundamental theoretical microturbulence modes (e.g. ITG, ETG, TEM)?
   — Compare measured turbulence characteristics with gyrokinetic and gyrofluid code predictions.

3. Carry out innovative experiments to make quantitative tests of predictions of (theory-based) transport models

4. Utilize nondimensional scaling approach to further elucidate tokamak transport
   — Use this approach to define an attractive next-step device based on ELMing H–mode.

5. Test theories of edge and divertor conditions needed to get H–mode
   — Quantitatively test the new set of analytic theories developed in Europe.
   — Encourage detailed comparison of US numerical work (e.g. Drake, Xu) with experimental results.
   — Determine if plasma parameters alone govern threshold or whether atomic physics (e.g. neutrals) is also important.

6. Investigate fundamental nature of L to H transition.
   — Physics of pellet triggered H–modes.
   — Effect of electron versus ion heat flux on transition.
   — Effect of current ramp on transition.

7. Study H–mode edge pedestal and investigate key physics controlling edge gradient and pedestal values.

8. Continue development of modeling capability in parallel with experimental tests.

Summary of 1999 Experimental Results in the Confinement and Transport Topical Area

Although lack of ECH reduced the number of experimental days devoted to this topical science area, significant experimental results were obtained in each of the five experimental days devoted to it in 1999. Perhaps the most impressive set of results were obtained in the experiment that investigated use of impurity injection to improve the core confinement (RI–mode). As was reported in G.R. McKee's invited talk at the APS DPP meeting in Seattle, neon, argon and krypton injection were used as part of this work with neon giving the best results. The impurity injection resulted in a substantial improvement in global confinement and in the local electron and ion thermal diffusivities with the ion improvement being the greater. The reduction in transport was clearly correlated with reduced density fluctuations as measured by beam emission spectroscopy and by far infra-red scattering. Comparisons between the E×B shearing rate and the gyrokinetically-determined turbulence growth rate showed that the E×B shearing rate was below the growth rate before impurity injection but exceeded it after injection. In other words, impurity injection reduced the turbulence growth rate so that the E×B shear feedback loop could result in reduced transport. Preliminary evidence was obtained of a change in the high-κ ($\kappa \sim 13\ \mathrm{cm}^{-1}$) fluctuations which correlated with the confinement improvement, suggesting that impurity effects on short wavelength fluctuations may be connected with the reduction in electron thermal transport. In addition to providing a wealth of fundamental physics, this experiment has given us a new tool for triggering core transport reduction.

In the H–mode physics area, we combined several experiments into one set of shots in order to maximize the amount of information that we could obtain. Two results from this day stand out. First, we used the beam emission spectroscopy system to obtain two dimensional turbulence data at the plasma edge across the L to H transition. Processing this data to produce a movie allows one to see the turbulent eddies convect past the field of view. These results were presented in R. Fonck's invited talk at the APS DPP meeting in Seattle. Second, we thoroughly documented the pellet-triggered H–modes which we had first identified on DIII–D in 1998. Both high and low field side launch pellets can trigger the H–mode with the power threshold reduction being greater for the high field side launch. The best result was a reduction in power threshold by about 2.5 MW (30%).

In addition to the planned experiments, we made a serendipitous discovery this year of a mode of operation with no ELMs and no sawtooth oscillation which had controlled, constant density and impurity levels. These discharges were created using counter neutral beam injection to plasmas where the density was lowered using cryopumping. The operational key was a line averaged density below $\lesssim 3 \times 10^{19}\ \mathrm{m}^{-3}$ and a neutral beam power above about 7.5 MW. The constant density and impurity levels are connected with the presence of low level MHD oscillations in the plasma edge which apparently increase the particle transport enough that cryopumping is still effective in spite of the absence of ELMs. These oscillations have little effect on the H–mode edge pressure profiles; the profile width is the same whether or not these modes are present. A key issue for divertor design for a fusion reactor is the pulsed heat load to the divertor plates caused by ELMs. The ELM-free operation seen in these discharges solves these problems by getting rid of the ELMs without paying the usual price of uncontrolled density rise in an ELM-free phase. If we can understand why this occurs and apply this in reactor plasmas, we will have solved a significant problem in fusion reactor design.

The Fundamental Turbulence Studies group performed an experiment whose primary goal was to provide a comprehensive test of whether ion temperature gradient (ITG) turbulence is the dominant microinstability and source of anomalous transport in DIII–D as predicted by theory. The experiment was performed by study the changes in turbulence during a density scan in Ohmic plasmas from the neoAlcator regime and into the saturated Ohmic confinement regime. Far infra red scattering measurements did see an enhanced low frequency feature in the scattered spectra at high density, consistent with the theoretical prediction that the ITG mode is more unstable there. Theory also predicts that the electron temperature gradient mode (ETG) is important at all densities; reflectometry measurements indicate the presence of two modes. More detailed comparisons with the predictions of gyrokinetic codes is in progress.

In 1999, nondimensional transport studies concentrated on the effect of rotation on confinement using counter neutral beam injection. A previous, co-injected ρ_* scan in ELMing H–mode plasmas was duplicated with all the dimensional parameters except the Mach number and Z_{eff}. The ρ_* scaling of global confinement was Bohm-like for counter injected discharges while the one for co-injected discharges was gyroBohm-like. Theory-based transport modeling is now needed to see if this change in the transport scaling can be explained either by the different Mach number and, hence, different E×B shearing rate or by the differing Z_{eff}.

In the area of core transport barrier physics and control, we investigated whether ICRF could be used to control the plasma toroidal rotation. Theoretical predictions indicate that spatial transport of resonantly heated ions could produce torques on the plasma which might alter the toroidal rotation. Previous DIII–D experiments in had also shown that electron heating from ICRF fast wave and ECH increased radial transport of angular momentum, also altering toroidal rotation. The goal of the experiment was to see which of these effects is dominant in our plasma. By utilizing counter neutral beam injected plasmas, we set up a condition where the postulated ICRF torque would increase the magnitude of the rotation while the electron heating effect would decrease it. The results were consistent with the increased transport being the dominant effect.

3.3. DIVERTOR/EDGE PHYSICS TOPICAL AREA GOALS (3 YEAR VIEW)

The main function of the boundary plasma is to control particle and power flux at the interface between the core plasma and the material walls. The long range goal of the DIII–D divertor and scrape-off layer science program is to: (1) use state-of-the art 2-D diagnostics to identify the relevant physical processes, (2) model these processes with computational models (e.g. UEDGE), and (3) sufficiently understand the relevant physical processes in the edge plasma so that computational models can predict operation for new operating modes on existing machines and for new machine designs.

We have identified and studied the radiative divertor or "detached" mode of operation which reduces the heat and particle flux in the divertor by deuterium puffing. Intrinsic carbon radiation is a key ingredient in this mode. We plan to extend the operating regime (i.e., operation at lower core n_e) for near-term AT operation by concentrating radiation in the divertor with injected impurities such as argon. The two tools to achieve this goal are so-called "puff and pump" techniques, (deuterium injection and pumping to provide a force on impurities towards the divertor) and divertor baffling (to better control neutrals). The baffling and pumping are also important ingredients in the control of density and impurities for the core plasma. We will also investigate the role of triangularity, single-null, and double-null on both divertor and AT conditions. Substantial progress has been made in the measurement (DiMES probe) and modeling (REDEP) of erosion and redeposition in the DIII-D divertor during detached operation. These studies will be continued during the next phase of impurity radiative divertor operation. They are also important in understanding the best means to control carbon radiation in an all-carbon machine like DIII–D.

3.3.1. 1999 Divertor/Edge Progress

The experiments in the Edge and Divertor area were executed both in the Divertor Topical Science area and Thrust 5; the latter work was focused on the effects of plasma shape in unbalanced double null plasmas. The experiments that were specifically done in the divertor area focused on plasma flows and carbon sources and transport. We obtained new flow data with both the Mach probes and the spectroscopic diagnostic in detached plasmas. Measurements with divertor biasing in ohmic plasmas showed that the divertor potential could be changed with biasing. DiMES measurements (DiMES is an impurity probe) showed that there was no appeciable net erosion in detached plasmas. Data also indicated that the net carbon source in DIII–D has been decreasing over the past seven years (presumably due to wall condition of the graphite), but the core carbon concentration has not changed appreciably. Carbon sources and transport will also be an important topic in the FY2000 campaign. Experiments at high core electron density (greater than the Greenwald density) were performed; degredation of confinement was not observed. We are now theorizing that divertor pumping may play an important role in this operation, and will be the focus of one run day in FY 2000.

3.3.2. 2000–2001 Work

At the start of the year 2000 we will have several new boundary research tools at our disposal which will significantly enhance our ability to conduct experiments in support of the DIII–D Advanced Tokamak and Boundary Physics program goals. The private flux cryopump-baffle system will be commissioned. The graphite armor tiles in the vicinity of the new divertor system will be improved so that they follow the field lines more closely, thereby reducing the number of sharp edges that can overheat. The new capabilities apply to single-null and biased double-null configurations while allowing a side by side comparison of the closed and open configurations.

With these modifications we will have the capability of independently pumping both legs of the divertor, reducing the core neutral source in single-null by an estimated factor of six relative to an open configuration, and sustaining AT plasmas up to the device volt-second limit before reaching the tile thermal limit. New research made possible by these modifications include:

1. Impurity control by the forced flow technique ("puff and pump") may be extended to lower density plasmas, and perhaps even to ELM-free plasmas. If successful, the technique will be used routinely to reduce carbon concentration in AT plasmas.
2. Research to expand the volume of radiative zone by convection.
3. Study feasibility of stable fully detached plasmas.
4. Investigate stability and confinement of density controlled rectangular cross-section plasmas.
5. Isolate the effect of neutrals on edge transport barrier and L-H transition.
6. Investigate heat flux control at densities compatible with AT scenarios using a combination of mantle and divertor radiation and application of convection.

The first order of business in the year 2000 is to evaluate the new system for these applications. The actual detailed experiments will be spread out through years 2000–2002. The commissioning work includes; evaluation of the result of improved wall armor on carbon content of the plasma, optimization and control of pumping configurations, preliminary evaluation of impurity reduction by bi-directional forced flow, and neutral density decrease due to the new baffle system. These preliminary rough measurements will be followed by more detailed focused experiments in years 2001 and 2002 as described below.

3.3.3. Details of the Year 2000 and 2001 Experiments

1. Determine conditions necessary for divertor impurity enrichment. Make extensive use of the full upper RDP.
2. Develop radiative mantle discharges.
3. Develop heat flux reduction techniques at AT-like edge conditions.
4. Determine steps required to minimize carbon influx in high performance plasmas.
5. Demonstrate predictive capability of erosion/redeposition pattern in the DIII–D tokamak.

3.3.4. 2002 Work

1. Continue to develop radiative divertor and mantle solutions compatible with the density operation needed for the (near-term) AT core plasma scenarios.

2. Attempt an integrated divertor/core demonstration as an element of the NCS scenario work.

3. Prove viability of poloidal tokamak divertor concept by demonstrating control of erosion and co-deposition.

The outcome of the years 2001 and 2002 AT and divertor experiments will guide us towards the future course of the divertor effort. The options in the near future are:

1. Accept the single-null/biased double-null configuration, perhaps with a number of refinements such an inner wall bump to increase the amount of baffling (but limit the shape flexibility).

2. Proceed to a full double-null divertor configuration.

3.4. HEATING AND CURRENT DRIVE TOPICAL AREA GOALS (3 YEAR VIEW)

1. Establish predictive capability for ECCD, including dependencies on density, temperature, Z_{eff}, geometry, power, trapping, and dc electric field.

2. Advance the physics understanding of FWCD, including effects of frequency, $n_{||}$, competing edge losses, high harmonic absorption on beam ions and thermal ions, rf-

induced resonant ion tranport, wave propagation, conservation of toroidal mode number.

3. Advance the understanding of NBCD, including the effects of fast particle modes and TAE modes. This would involve development of a model of fast ion transport.
4. Understand the effects of heating of electrons and/or ions on plasma rotation and transport, particularly transport barriers.
5. Develop long pulse discharges with full noninductive current drive, including discharges with very high bootstrap fraction as a step toward transformerless operation.
6. Develop routine electron heating using the ICRF system, through fast wave and/or second harmonic hydrogen minority heating (especially at high density where beam penetration is poor). Develop minority heating for sawtooth stabilization and minority or beam ion current drive.

4. SYNOPSIS OF THE 2000 DIII–D RESEARCH PLAN

The research campaign for 2000 has been organized into five research thrusts and a broader selection of experiments in four Topical Science Areas. Significant blocks of experimental time have been allocated to the research thrusts, since these activities are aimed directly at critical objectives for the DIII–D Program and for the tokamak research program generally. Additional experimental time in the topical areas maintains the breadth and scientific depth of the DIII–D Program. Below we convey the essential content of the various research thrust and topical science experiments and their goals and anticipated and hoped for results. The research described has been allocated to 55 run days out of a possible 69 run days in the 1999 campaign. Additional detailed information can be found on the Web locations:

http://fusion.gat.com/exp/
http://fusion.gat.com/exp/2000/
http://fusion.gat.com/exp/2000/thrusts.shtml
http://physics.gat.com/sched2000.asp
http://physics.gat.com/exp2000.asp

The experiment plan was put together with input and prioritization by the year 2000 Research Council. Based on the "DIII–D Five-Year Program Plan 1999–2003," August 1998, GA–A22950, the Research Council develops a three-year plan which is annually updated. The first of these Three Year Plans was made in 1999. Progress on the research thrusts and topical areas in the 1999 experiment campaign was reviewed at the Year End Review (http://fusion.gat.com/exp/2000/review.shtml, also broadcast on the internet) September 15–16, 1999. With input from that review and considering the three-year objectives, year 2000 research thrusts were identified. A call for ideas towards those objectives was issued and approximately 200 ideas were presented at a community "Brainstorming Meeting" of October 20–22, 1999 which was broadcast on the internet. The various thrust and topical area groups prioritized, combined, and otherwise sifted these ideas. The plans so arrived at were presented to the Research Council December 14 and the advice of the Research Council was used to set the final allocations of run time for the year 2000 campaign.

The 2000 experiment plan, summarized in Table 6, consists of efforts in five thrust areas and four topical areas. Owing to limited run time, it was not possible to allocate time to each of the thrusts which have been identified by the Research Council over the last two years. One thrust, the Optimum Edge Thrust, was completed in 1999. Others which did not receive an explicit allocation of time in 2000 will be part of the plan in future years. Each of the nine efforts has a responsible leader and deputy leaders. A brief synopsis of progess in the various thrusts in 1999 followed by year 2000 plans is given below.

Table 6
Run Time Allocations for the 2000 Experiment Campaign

No.	Acronym	Description	69-Day Plan	Thrust Leaders
1	Edge stability	Regulate the edge bootstrap current and/or the edge pressure gradient to extend the duration of AT modes. (Analysis, diagnostic in 2000)		J. Ferron (GA) L. Lao (GA)
2	AT Scenario	Progress toward a high bootstrap fraction AT plasma demonstration	9	T. Luce (GA) M. Wade (ORNL)
3	NTM	Stabilization of neoclassical tearing modes (Some work in Stability Area)		R. La Haye (GA) C. Petty (GA)
4	RWM	Feedback stabilization of resistive wall modes	8	G. Navratil (Columbia) A. Garofalo (Columbia) M. Okabayashi (PPPL)
5	Optimum edge	Develop the basis for choosing single versus double null and the optimum triangularity of the outermost flux surface in future machine designs. (Complete)		M. Fenstermacher (LLNL) T. Osborne (GA) T. Petrie (GA)
6	High l_i	Exploration of the high l_i AT plasma scenario		Deferred to 2001
7	ITB	Expand the spatial extent and time duration of internal transport barriers	3	C. Greenfield (GA) E. Synakowski (PPPL) E. Doyle (UCLA)
8	AT divertor	Explore closed, pumped divertor operation toward AT application	8	M. A. Mahdavi (GA) M. Wade (ORNL)
9	EC	ECH/ECCD validation	6	R. Prater (GA) J. Lohr (GA)
		Thrust Totals	34	
		Stability Topical Area	6	E. Strait
		Confinement Topical Area	10	K. Burrell
		Boundary Topical Area	5	S. Allen
		Heating and Current Drive Topical Area	0	R. Prater
		Topical Area Sum	21	
		Percentage of Total Days	38	
		Contingency	14	
		Sum	69	

4.1. RESEARCH THRUSTS FOR 2000

4.1.1. AT Scenario, Research Thrust 2 — Preparation for an NCS AT Plasma Demonstration (Leader: T.C. Luce, Deputy: M.R. Wade)

The high q_{min} approach is the primary AT scenario being pursued by DIII–D in its long term development of the AT potential. The key to realizing this scenario in steady-state is the maintenance of a hollow current profile using ECCD to prevent resistive diffusion of the off-axis current peak. Over the next three years, the EC power on DIII–D will be increased steadily from the present system to an eight-gyrotron system. More importantly, the five newest gyrotrons will be equipped with diamond windows to enable longer (10 s) pulses. Set against this background of a steady buildup in the necessary hardware, this thrust is aimed at a first demonstration in 2001 of a non-inductive high performance AT scenario. Once such a scenario has been demonstrated, optimization of normalized and absolute performance will be carried out. Both physics understanding and direct implementation on larger devices will be key to developing confidence for a true fusion power system.

Progress toward the AT demonstration discharge was significant in 1999. Guided by previous scenario modeling, exploratory experiments to determine the limiting β at parameters suitable for the demonstration (B = 1.6 T, I = 1.2 MA) were initiated. Surprisingly, these discharges made a smooth transition into an ELMing H mode while maintaining β near the maximum value. The longest duration discharge (β_N H_{89} ~ 9 for 2 s) of this type is shown in Fig. 22. This discharge exhibits the three typical features seen in most of these high performance discharges. First, the initial rapid increase in β during the ELM-free period is terminated before the first ELM and without the catastrophic loss of performance typical of previous high performance discharges. This saturation is attributed to bursting high frequency instabilities seen on external magnetic coils which appear to be Alfvénic and driven by the NBI fast ion population. Second, the small excursions in β_N (and large ones in H_{89}) are correlated with the growth of very low frequency (<100 Hz) n = 1 magnetic perturbations identified as resistive wall modes. These set the limit on β in the quasi-steady phase. Finally, due to resistive diffusion, the current evolves to where a resistive wall mode (in this case combined with a tearing mode) grows and irreversibly ends the high performance phase. This points to the focus of this year's campaign which is current profile control and sustainment with ECCD.

Analysis of the internal loop voltage in this type of discharge indicates that about 75% of the plasma current is supplied non-inductively, of which calculations indicate 50% may be attributed to bootstrap current. The analysis shows (consistent with the original scenario modeling) that the edge current is consistent with being entirely bootstrap current, the central current is overdriven by the NBI, and the remaining Ohmic

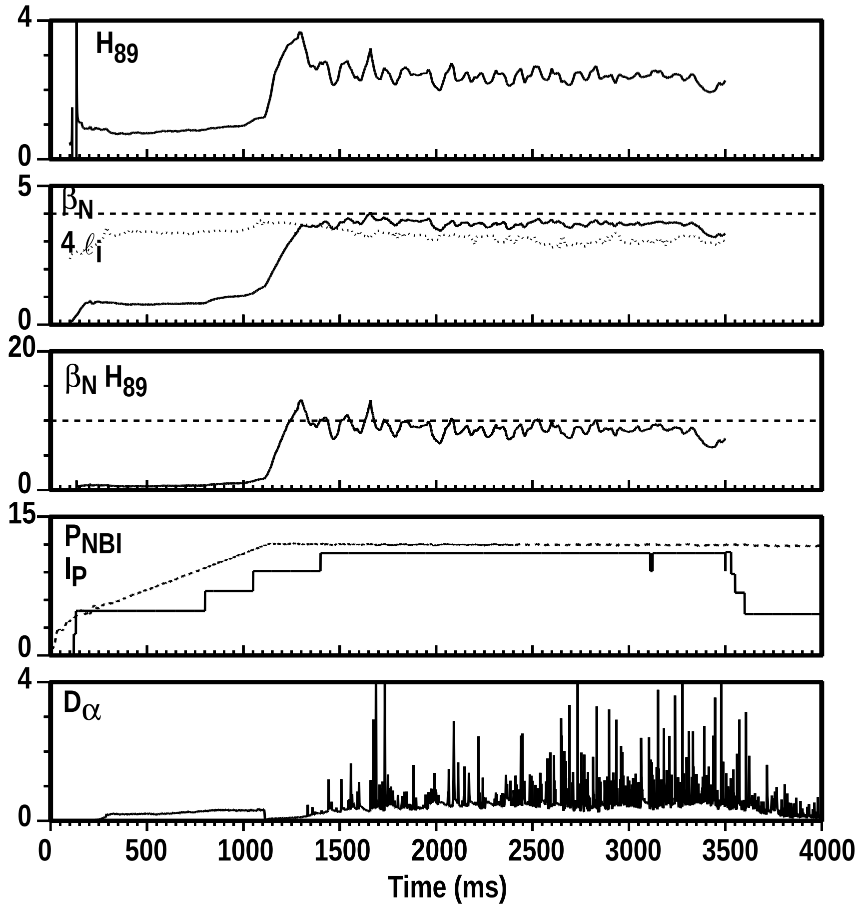

Fig. 22. $\beta_N H_{89}$ ~ 9 sustained for ~16 τ_E.

current is at the half radius. This implies that replacement of some of the NB power with off-axis ECCD should lead to a fully non-inductive current sustainment.

In order to achieve the goal of a demonstration discharge in 2001, three key tools must be commissioned and successfully applied in 2000. The new private flux cryopump is the newest part of the comprehensive particle control system required for a successful integrated scenario. The density must be held in the range of 50%–75% of the natural H–mode density for a effective current drive. The new ECCD systems are clearly an essential component of the scenario. Separate thrusts (#8 and #9) are responsible for the commissioning of these two systems. Application of these tools will occur at the earliest possible opportunity. The third tool is real-time control through the plasma control system. In addition to the significant shape control issues, algorithms will be implemented this year for β control for instability avoidance and q profile calculations for current profile control.

In 2001, the demonstration of non-inductive high performance will be the centerpiece of the plan. More gyrotrons for ECCD will be commissioned, which should allow optimization experiments involving current profile control, and higher absolute performance. In this time frame, it may also be possible to begin extending the maximum β by means of active feedback control of the resistive wall mode.

Beginning in 2001, but with increasing attention in 2002 will be experiments focused on placing this scenario on a sound theoretical and empirical basis for extrapolating to future fusion devices. The steadily increasing ECCD, diagnostic, and control capabilities should allow a window of high performance operation in contrast to the existence demonstration of 2001.

4.1.2. NTM, Research Thrust 3 — Validate Neoclassical Tearing Model and Begin Stabilization With ECCD (Leader: R. J. La Haye; Co-Leader: C.C. Petty)

After the edge instabilities that are the subject of Thrust 1, the next largest immediate stability concern for the AT work are the neoclassical tearing modes (NTMs). These modes have been seen to limit the performance in all our approaches to AT plasmas. Even in plasmas in which q_{min} has been raised above 2, NTMs have been observed. The purpose of this thrust is to gain further physics understanding of the neoclassical tearing modes and develop means of avoiding or stabilizing them.

This thrust has five highest priority tasks: use of unmodulated ECCD to stabilize NTMs, studies of the NTM critical β versus q-profile, studies of the ρ_{i*} and S scaling of the threshold β_N, tests of the physics of the polarization threshold, and studies of classical tearing mode stability.

Two principal research lines are foreseen in a three year plan: (1) studies in H–mode with sawteeth present and (2) studies in an AT mode with raised q_{min}.

H-mode With Sawteeth

The diagnostic set now available on DIII–D, in particular the MSE diagnostic for measuring the current profile, affords a scientific opportunity not previously available to measure all the quantities involved in tearing mode theory to verify that theory. Some effort will be devoted to this basic science verification. Work in 2000 will continue on our ongoing collaboration with JET, ASDEX Upgrade, JT–60U, and Alcator C–Mod on the scaling of NTMs. Tests of the physics of the polarization threshold will be made in DIII–D to confirm the theory or suggest any additional theoretical work needed. An active attempt will be made to modify the width of the 3/2 mode with ECCD. This work will lead to efforts in 2001 toward preventing their onset with ECCD. In the year 2002, we will be able to use two separate ECCD systems for suppressing the 3/2 and 2/1 modes simultaneously.

AT-mode Line

In 2000, we will continue to establish the critical β_N as a function of (q_0, q_{min}) for 5/2 or 3/1 modes. We will hope to continue to find that the NTM problem becomes less severe with higher q_{min}. We will also begin to study the variation of the q profile that can be achieved with ECCD so as to avoid NTMs. In the year 2001, we expect to have enough long pulse ECCD power to maintain a more stable q profile. In the year 2002, we will also seek to control the q profile and suppress the 5/2 and/or 3/1 modes by two ECCD systems.

Principal Goals for 2000

1. Test the physics of the polarization threshold for NTMs.
2. Show unmodulated ECCD shrinks NTM islands.

4.1.3. Wall Stabilization, Research Thrust 4 — Validate Model for Active Control and Optimize Control With Six-Element C–Coil (Leader: G. A. Navratil; Deputies: A.M. Garofalo, and M. Okabayashi)

The AT Program on DIII–D has shown from theory calculations that sustaining β_N greater than four requires stabilization by a nearby conducting wall. The two key elements of wall stabilization are the degree to which a conducting wall can look "superconducting" if the plasma rotates past the wall and the provision of suitable non-axisymmetric feedback to suppress the modes that grow locked to the wall. Recent theory work has suggested that even with a rotating plasma, a "resistive wall mode" can arise that is locked in position and does not rotate with the plasma. Experiments to date have provided support for both the existence of the resistive wall mode and transient evidence for the ability to operate plasmas above the no-wall beta limit as long as wall stabilization remains effective. Over the next three years, DIII–D plans to implement a set of non-axisymmetric coils to provide feedback stabilization of resistive wall modes. This thrust area has two main objectives:

1. Advance the physics understanding of resistive wall mode stability, including the dependence on plasma rotation, wall/plasma distance, and active feedback stabilization.
2. Develop sustained operation above the no-wall beta limit through passive or active stabilization of the resistive wall mode.

In 1999 significant progress was made in both the clear identification of the resistive wall mode in DIII–D high performance plasmas and the initial demonstration of active mode control using the existing C–coil set powered by three new 5000 Ampere/100 Hz amplifiers. A summary of the results of the 1999 experimental campaign for Thrust 4 is shown below:

Physics of Wall Stabilization and Plasma Rotation.

- Three AT plasmas were developed for RWM Study: SND ($\beta_N^{no-wall}$ ~ 2); DND (q_{95} ~ 4.5); DND (q_{95} ~ 5.5; record long pulse $\beta_N H$ ~ 9).
- The n=1 RWM limits the performance of low-ℓ_i AT plasmas to $\beta_N \leq 4\ \ell_i$
- Plasma rotation unable to completely suppress RWM for $\beta_N \geq 4\ \ell_i$
- Plasma toroidal rotation strongly reduced whenever detectable RWM is present ($\delta B_r \geq 1$ Gauss).
- Test of qmin dependence of rotation threshold inconclusive: unable to vary q_{min} above and below 2 at RWM onset time.
- RWM "bursting" observed in DND plasmas near $\beta_N^{no-wall}$ limit.

Initial Feedback Control Experiments (Proof-of-Principle Test).

- Radial flux leakage of n=1 mode through the vacuum vessel can be compensated by the feedback system: test of basic "Smart Shell" algorithm.
- Three feedback algorithms were tested: "Smart Shell"; "Fake Rotating Shell"; and "Mode Control".
- "Fake Rotating Shell" co-injection direction favorable for stabilization.
- Smart shell control of low density locked mode was ineffective: tearing mode not sensitive to radial flux compensation on vacuum vessel wall.
- 3-D code VALEN improved to include GATO generated n=1 RWM current distribution in the plasma model: basic tool for design of an optimal C-coil extension for mode control.
- 2-D simulation of active RWM control by A. Bondeson [MARS] and M. Chance/M. Chu [PEST-VACUUM] is in progress.

Extend Lifetime of Plasma Above the No-wall Limit.

- High β duration was extended with addition of "derivative gain" in feedback loop (both for "Smart Shell" and "Mode Control" algorithms).
- Modest improvement in high β plasma duration is consistent with VALEN predictions of control coil (C–coil) coupling to n=1 RWM.

Experimental Plans for 2000: Validate Model for Active Control and Optimize Mode Control Using the Existing Six-Element C–Coil

In the coming year we expect to significantly extend our understanding of active control using the existing C–coil set powered by three new 5000 Ampere/100 Hz amplifiers we installed and began using at the end on the 1999 experimental campaign. In addition, the saddle coil sensor array used for mode detection has been extended above and below the existing C–coil set with the addition of 24 new saddle coils providing for improved mode structure measurement and lower detection levels. Among the most important results we expect to achieve this year are:

1. Validate quantitative 3-D models now being developed for n=1 feedback control.

2. Extend the regime of improved stability with closed-loop feedback control and test a range of promising active feedback control algorithms.

3. Finalize design of upgraded external coil set for improved feedback control

Achieving these results will provide the basis for the installation and test of an upgraded C–coil system in DIII–D for mode control in 2001 and 2002. Feedback control model calculations indicate the prospect of stabilizing the RWM with an upgraded mode control coil set.in plasmas 50% to 80% above the no-wall beta limit. Successful demonstartion of theis upgraded mode control system would allow the exploration of the extremely important plasma regime approaching the ultimate AT wall stabilized beta limit of β_N in the range of 5 to 6.

4.1.4. AT Divertor, Research Thrust 8 — Explore Closed Pumped Divertor Operation Towards AT Applications (Leader: M.A. Mahdavi, Deputy: M.R. Wade)

The primary goal of the Thrust 8 is to develop density and particle control techniques for the AT plasmas, using the exiting and newly installed divertor tools. The new divertor enhancements will serve many other elements of the DIII–D program. Therefore, much of the work in this thrust will have applications to other research topics. As such, it is highly desirable to compress most of the Thrust 8 effort within the year 2000 campaign year, ahead of research topics which will utilize the new divertor capabilities.

Several years of divertor development for impurity and particle control in AT plasmas culminated with the recent successful installation of the final elements of the pumped divertor at the top half of the DIII–D vessels. The new systems consist of a cryopump at the inner-strike point, a private flux region baffle and high heat flux inner wall armor tiles. The new system combined with the outer upper cryopump and baffle system completes the package for impurity and particle control in single-null plasmas and should provide an adequate impurity and particle control tool for double-null plasmas.

Particle control requires placement of the divertor strike points accurately in prescribed positions near the cryopump pumping apertures. Furthermore, in order to regulate the plasma density at the desired value, the strike point positions have to be moved away from the pump apertures according to the density feedback command while maintaining many other plasma shape parameters fixed. What is more, introduction of the new divertor hardware into the DIII–D vessel imposed additional plasma shape constraints. Therefore, in addition to commissioning of the new divertor systems and development of impurity and particle control techniques, development of plasmas shapes for AT plasmas is integrated into the Thrust 8 activity. The Thrust 8 activities, nearly in the order that they will take place are shown as follows:

1. Develop shape control algorithms that allow precise strike-point positioning while maintaining freedom (albeit limited) in the choice of divertor geometry.

   Determine divertor configuration that provides the optimum exhaust efficiency (defined as the ratio of the exhaust rate to the particle flux incident on the divertor target) at density levels at least roughly consistent with the DIII–D AT target scenarios

   Document plasma conditions sufficiently well to allow detailed highly constrained modeling.

2. Develop a physics-based understanding of why the experimentally determined “best” divertor configuration is indeed the best through detailed modeling of the experimental data. With this knowledge, develop ideas for and test other divertor configurations with model.

3. Measure exhaust efficiency versus pumping configuration, flux expansion, and toroidal field direction.

4. Determine heat flux distribution on upper divertor at low density, and heat load and particle flux limits in best configurations.

5. Establish an ELMing H–mode scenario which can be used as a proxy for the Thrust 2 high-performance discharge and then systematically vary divertor and plasma conditions to study the effect of divertor symmetry (DRSEP scan), X–point height (rigid-body translation of shape), initial conditions on final density, and beam and carbon contributions to density.

6. Use improved exhaust and gas injection capabilities and the ability to pump the inner divertor leg to study effect of induced particle flows on core carbon buildup and trace impurity exhaust at low density.

4.1.5. EC, Research Thrust 9 — Electron Cyclotron Heating Physics Commissioning (Leader: R. Prater, Deputy: J. Lohr)

The ability to apply high power electron cyclotron heating (ECH) for localized heating and current drive is a key element of the AT program on DIII–D. The function of the localized current drive is to develop and sustain the desired current profile, thereby avoiding the decay in the central safety factor which leads to sawteeth and enhanced transport. In addition to the AT program, there are numerous experiments which either benefit from ECH or depend fully upon it. These experiments include studies of the heat pinch, locally measured transport, rf-assisted startup for optimized shear, studies of plasmas with equal electron and ion temperatures, edge heating or current drive for controlling ELMs, and many others.

The objective of this work is to bring the ECH system to the condition where power from at least four gyrotrons can be applied robustly to the plasma with high power and long pulse length. At present, three of the gyrotrons are made by Gycom, and their power and pulse length is limited by the boron nitride window to 0.75 MW for 2 s. Two of the gyrotrons are made by CPI, and they have diamond windows which can operate for longer pulses, nominally 10 s at 1 MW. Power supplies for these gyrotrons are also being developed at present.

The transmission lines for the ECH power follow designs well tested in past experiments. These evacuated transmission lines have been shown to handle high power with little difficulty. Grooved mirrors are used to generate the elliptical polarizations needed to launch pure X–mode power, and a code has been tested which calculates the grooved mirror settings needed for a particular equilibrium for given angles of incidence of the rays.

New this year is the ECH launcher designed and constructed by Princeton Plasma Physics Laboratory. This launcher differs from the previous launchers in that it has mirrors which can be tilted in the toroidal direction remotely through a vacuum feed-through. (Both types of launcher may be tilted in the vertical direction.) The PPPL launcher will facilitate tests of the physics of ECCD, since n-parallel can be varied from shot-to-shot. Co-current drive as well as counter-current drive can be carried out. This important flexibility will facilitate a number of exciting experiments.

One-Year Goal

Commission the 110 GHz ECH system to demonstrate reliable high power from four-gyrotrons with pulse lengths longer than 1 s, with well characterized launching direction and polarization of the waves.

Objective: Demonstrate that the four gyrotron ECH/ECCD system is ready for routine operation for performance of experiments on DIII–D which need high power electron heating or localized current drive.

Critical Path Elements

- High power long pulse operation of at least four gyrotrons
- Power supplies to power four gyrotrons simultaneously
- Operation of two gyrotrons from a single power supply
- Efficient transmission and polarization control
- Launchers with good optical properties

Approach

Apply modulated ECH power and use wave absorption measurements, as deduced from temperature fluctuations measured by electron cyclotron emission, to determine the wave propagation properties and mode content. This approach has been well developed in past applications.

4.2. PHYSICS TOPICAL AREAS

4.2.1. Stability — (Leader: E.J. Strait)

Stability Topical Area Goals (3 Year View)

1. Advance the physics understanding of resistive wall mode stability, including the dependence on plasma rotation, wall distance, and feedback stabilization. *Develop sustained operation above the no-wall beta limit through passive or active stabilization of the resistive wall mode.*

2. Characterize the physics of edge-driven instabilities in plasmas with a large (H–mode) edge pressure gradient and associated bootstrap current.

Develop methods to avoid or reduce the impact of edge-driven instabilities through modification of the edge pressure gradient, collisionality, or shaping.

3. Advance the physics understanding of non-ideal plasma instabilities including neoclassically driven tearing modes, sawteeth, and fast ion driven instabilities.
Develop sustained high beta operation free of neoclassical tearing modes, through profile control or active stabilization.

4. Advance the understanding of disruption physics in advanced tokamak discharges.
Develop methods of mitigating halo currents and disruption heat loads, and disruption avoidance using real-time identification of disruption boundaries.

The DIII–D Stability and Disruption Physics program addresses critical issues for both conventional and Advanced Tokamak (AT) plasmas. With recent advances in scientific understanding and technical tools, we are beginning to study plasmas compatible with steady-state operation, and to develop active means of controlling stability. Much of the fundamental stability physics involved also has wider application in other toroidal confinement devices. For experiments in 2000, resistive wall stabilization experiments (Goal #1) will be carried out under research Thrust #4, while the other goals will be addressed within the Stability topical science area.

Stabilization by a conducting wall is predicted to strongly enhance the ideal kink mode beta limit in AT plasmas with a broad pressure profile and broad, negative central shear (NCS) current density profile. However, the presence of a resistive wall is expected to destabilize a slowly growing Resistive Wall Mode (RWM). Experiments in 1999 showed that small-amplitude resistive wall modes can cause a significant slowing of plasma rotation, a potential problem for rotational stabilization of the RWM. An important goal for the coming year will be to improve our understanding of the relationship between RWM stability and plasma rotation, in comparison with recent theoretical models. Initial tests of active feedback control have been carried out using the existing C-coil, driven by three new power amplifiers provided by PPPL. These showed promising results, producing a modest extension of the duration at high beta. In 2000 we plan to continue the feedback experiments, making use of newly installed arrays of sensor loops, with the aim of validating feedback control models sufficiently to design an extension of the active coil set. The longer-term goal for the next three years is to use the additional active coils to achieve sustained operation significantly above the no-wall stability limit. Much of the physics understanding of rotation and feedback stabilization gained here should be applicable to other toroidal confinement concepts.

Experiments and modeling indicate that edge-localized modes (ELMs) are triggered by moderate-wavelength instabilities, driven in the H–mode edge pedestal by the steep pressure gradient and its associated bootstrap current. Recent experiments have succeeded in reducing ELM amplitudes by the use of discharge shaping to lower the stability limit for short-wavelength ballooning modes at the edge, thereby limiting the pressure gradient to the first regime ballooning mode limit. Preliminary experiments in DIII–D as well as other tokamaks have also shown promising results with the use of impurity radiation to reduce the edge pressure gradient and bootstrap current. These and other approaches for control of the edge will be pursued in future DIII–D experiments, toward the goal of an ELMing H–mode edge plasma compatible with an internal transport barrier (ITB). However, most experiments will be deferred until 2001, when better measurements of the edge current density should greatly aid our understanding of edge stability physics.

Neoclassically driven tearing modes (NTMs) are metastable modes, destabilized by the helically perturbed bootstrap current arising from a “seed island.” DIII–D experiments in 1999 have extended the range of data for scaling of the instability threshold. A multi-machine database incorporating the DIII–D data suggests that stability may improve at large magnetic Reynolds number S, due to reduced seed island amplitudes. Experiments in 2000 will aim to test theories for the damping of the NTM, a key physics element for predicting their stability. Experiments have also shown that current profile modification can be used to avoid triggering the instability, and in the future electron cyclotron current drive (ECCD) will provide a valuable tool for q profile control to improve stability. A major emphasis of future work will be the use of localized ECCD at the mode rational surface for direct stabilization of the NTM, as predicted theoretically.

Our program will continue to explore and validate basic MHD stability physics, making use of DIII–D's extensive set of diagnostics for precise, detailed measurements of the pressure and current density profiles and the internal structure of MHD modes. Investigation of the physics of the sawtooth crash will be continued, including the role of fast ions in sawtooth stabilization. Validation of resistive interchange mode theory in regions of negative magnetic shear will provide a test of basic stability physics which is also applicable to stability of stellarator plasmas. Preliminary experiments will be carried out in 2000 to measure the damping rate of stable MHD modes, using low-power signals launched from the ICRF antennas. This technique can provide valuable physics information on the driving and damping rates of kink modes, tearing modes, and fast ion-driven Alfvén eigenmodes, and has the potential to provide a warning signal for the approach to stability boundaries.

Disruptions are in principle predictable, occurring when a stability boundary is crossed, and much of the DIII–D stability program can be viewed as learning how to predict and avoid disruptions. However, some disruptions are inevitable due to unforeseen causes such as control system failure or unexpected impurity influx. The DIII–D program will continue to develop methods of mitigating the effects of disruptions using impurity pellets, hydrogenic pellets, and possibly liquid jets, as well as gas puffing. Important physics issues to be investigated in the next three years include the physics of non-axisymmetric halo currents, the role of avalanche processes in runaway electron generation, and the transport of impurity ions during disruption mitigation.

4.2.2. Confinement and Transport (Leader: K. H. Burrell)

This topical area has experiments under various headings:

In the area of **Fundamental Turbulence Studies**, we will perform an experiment investigating whether infrequent large transport events (avalanches) are an important part of the overall tokamak transport.

In the **H–mode Physics area**, two experiments are planned. First, we will investigate the relative importantance of electron versus ion heat flux in triggering the L to H transition. This experiment will also be used to provide information on the edge neutral density in L–mode and H–mode which will allow us to test a recent theory of the H–mode edge pedestal which includes neutral effects. Second, we will investigate further the effect of the ion grad B drift on the edge plasma prior to the transition. Analysis last year of two year old data showed that the edge electric field reversed sign when the direction of the toroidal field reversed. The key question to be investigated this year is whether it is the direction of the grad B drift relative to the divertor X–point which is the key parameter in this behavior. These shots will also be used for further studies of the pellet-triggered H–modes which were first investigated last year on DIII–D.

In the area of **Test of Transport Models**, an experiment will be done to demonstrate the existence of a heat pinch with outside launch, second-harmonic ECH and to determine if the heat pinch is dependent on the sign of the magnetic shear as predicted. The inward transport effect seen with the 60 GHz system remains a severe challenge to the theoretical community. One remaining mechanism could explain the observed profiles without requiring transport up the temperature gradient: the conversion of the fraction of ECH power which is not absorbed at the resonance to electron Bernstein waves at the upper hybrid layer. This mode conversion is not possible with second harmonic outside launch. The superior diagnostic set now available and the higher power densities possible with the 110 GHz ECH system could provide clear evidence of the mechanism responsible for the inward transport. Furthermore, the theoretical heat pinch model of coupled transport between Grad-J and Grad-T can be tested by comparing the non-diffusive electron transport for positive and negative shear plasmas.

A second **Test of Transport Models** experiment is planned to provide tests of turbulence simulations, tests of transport models with modulated ECH, a test of the predictive capability of turbulent transport models and a demonstration of marginal stability in the electrons (L–mode part only).

The experiment in the **Nondimensional Transport** area will investigate the changes in radial correlation length and decorrelation time as ρ_* is varied. Preliminary experiments suggested that the correlation length was proportional to ρ_* as expected from local turbulence models but that the decorrelation time varied in such a way that Bohm-like transport scaling resulted. However, the match of the other nondimensional parameters in this preliminary experiment was not good enough to produce a definitive result. A better match will be produced in the new experiment.

The **Core Transport Physics** area will have four experiments. First, we will do a more detailed investigation of the formation of regions of reduced core transport and the effect of the q profile on that formation. As part of this work, we will also use perturbative transport techniques to study the reduced energy and particle transport region. Modulated ECH will be used to investigate electron thermal transport while modulated gas injection will be used to study particle transport.

Second, we will investigate the controlled density, ELM-free H–mode that was discovered last year. This will be the first dedicated experiment in this area; previous work was done piggyback. The key for the new experiment is to utilize all the fluctuation diagnostics to determine the nature of the MHD modes at the plasma edge which provide sufficient particle transport to maintain density control without significantly degrading the edge pedestal. In addition, we plan to use pellet and neon injection both to provide perturbations for transport studies and also to attempt to trigger reduced core transport in these shots. An ELM-free, controlled density shot with reduced core transport would be of great interest to reactor designers.

Third, we will investigate further the fundamental physics of core transport reduction using impurity injection which was so successful last year. A prime goal this year is to obtain information on the electron thermal transport reduction and to attempt to correlate that with the changes seen in high-k turbulence ($k > 10\ cm^{-1}$). Indeed, by reducing the transport effects of ion temperature gradient modes to negligible levels, we are in a position to probe the fundamental physics of electron temperature gradient mode and high-κ turbulence.

Fourth, we will study the formation of core electron transport barriers using intense ECH directed to produce counter-ECCD. In experiments on DIII–D last year, ECH during the initial current ramp produced significant localized reductions in the electron thermal diffusivity. This is similar to effects seen several years ago on DIII–D with counter-FWCD and seen last year on ASDEX–U using counter-ECCD. This is contrary to results seen three years ago on DIII–D where application of ECH to a region where ion transport was reduced lead to increased ion transport. The key question here is to try to sort out what the competing effects are that have produced these disparate results.

4.2.3. Divertor/Edge Physics (Leader: S. L. Allen)

Divertor/Edge Physics Experimental Objectives for FY2000

The planned experiments, in rough order of priority, are described below. Some of the ideas were grouped by machine configuration (e.g., those with the upper divertor), and others were grouped by topic (e.g., understanding carbon transport).

A. (Configuration grouping) **— Upper Divertor Experiments at "high" density (2 days).** (Experiments that involve the upper pump that will not be done in Thrust 2, as they will focus on reducing the density).

1. Does the plasma detach at lower core density with the closed divertor, as predicted by UEDGE and observed by other machines?
2. Is the density limit reduced by the closed divertor?
3. Is the density limit reduced by the low x-point height above the floor (the dome)?
4. Characterize upper divertor with new diagnostics, both ELMing H–mode and detached plasmas (PDD) upper tangential TV camera (carbon and deuterium profiles), Langmuir probes (may require some sweeping to get good data), filterscopes (look at different lines).
5. What is the impurity enrichment with puff and pump of the upper divertor compared to the lower divertor?
6. Is a narrow divertor slot compatible with a radiative divertor?

An optimistic estimate is that these experiments will take 2–3 days, assign 2.

1. What is the effect of the ∇-B drift on the upper divertor detachment and density limits. (It is assumed that the experiments in section A above will be done with the ∇-B drift *towards* the upper divertor (opposite to that used in all but one day of Thrust 2 plans!). We would do one day with the ∇-B drift away from the upper divertor.

Assign one day. If we can somehow obtain data from Thrust 2 with ∇B away from the upper divertor, this day could be deleted.

B. (Topic grouping) **Improve understanding of carbon transport (1 day).**

1. Obtain carbon flow and carbon source data spectroscopically at high power and H–mode density (we currently have very little data in this regime, probes may not be able to take data under these conditions).

2. Do hot spots contribute significantly to the carbon inventory? Create discharges without hot spots (large gaps) and with (high power, focused on areas of the wall that are less-well aligned).

3. Is the main chamber wall a significant source of carbon? (some new diagnostic capability with filterscopes).

C. (Topic grouping) **Is pumping required for high density operation (near the Greenwald density)? (1 day).**

This is a one-day experiment to finish a topic from last year to allow a publication to go forward. Also, this will provide information on possible reasons why JT–60 and JET see degradation at high density.

1. The experiment is to examine in detail the divertor configuration required for high density operation (above the Greenwald density). We have recently realized that we think that nearly all of the high density results with good confinement have been obtained with pumping. We would like to confirm this by comparing high density shots on the same day, one set with pumping(e.g., private flux space pumping, normal pumping), and another set without pumping. A definitive result was not obtained on this topic last year in the high density experiments.

2. We would expect that we could also address some questions about pedestal parameters that were not completed last year. To our knowledge, the divertor science area is the “home” for the high density experiments.

D. (Configuration grouping) **DiMES impurity transport studies — 2 times (1/2 day) – 1 day** — plasma setup can often be done in piggyback mode, but actual data shots require that the strike point is positioned on the DiMES probe.

1. Transport of lithium. Preliminary experiments last year (1/2 day) have shown that a large amount of sputtering, erosion, and impurity transport

data can be obtained in these experiments. Introduce lithium into the plasma from the DiMES probe, and use spectroscopic diagnostics. (1/2 day)

2. Effect of impurities on sputtering rates. This experiment would introduce small amounts of impurities into the divertor to determine if the sputtering rates on the DiMES probe were affected by this. (1/2 day)

E. (Topic grouping) **Basic Divertor Physics Topics — 1 day (the group could not converge on which experiment was the highest priority, but the general feeling was that a careful comparison between experiment and theory should be done on the one-day level. However, with the alllocated time, these experiments will have to either be deferred or done in piggyback mode.)**

(NOT in order of priority) —

1. *Measurement of "sheath factor", using drsep to vary parameters*. We currently observe that the peak divertor heat flux is a very strong function of drsep close to magnetic balance, and the particle flux is a much broader function. Careful experiments (optimizing the signals on the langmuir probes and IRTV) can help us understand the "sheath" transmission factor.

2. *Measurement of fluctuations in PDD*. We have a new probe head which can be used to measure temperature fluctuations in the divertor (i.e., we can move the probe heat from the midplane to the X–point probe). Several theoretical hypothesis are being tossed around that turbulence may play an important role in PDD discharges (in addition to charge exchange in the divertor). Comparisons with the BOUT code may be possible.

3. *High time resolution measurements of ELMs* — This year, we will have several new diagnostics that will be able to measure ELM quantities in more detail. A new, high speed intensified tangential camera will be used in the divertor; this can be triggered by photodiodes (ELMs) upstream and can obtain snapshots of impurity and deuterium radiation. A new high-speed IRTV will be in use to measure the heat flux from ELMs. We will also have new probe capabilities to measure ELM properties. All these new diagnostics can be brought to bear on the study of ELMs.

F. (Topic grouping) **Does puff and pump cause a measureable plasma flow towards the divertor? Improved measurement of flow during puff and pump — 1 day requested, we will try to complete some part of these experiments in "piggyback" mode.**

1. We feel that the experiment done in 1999, which showed no evidence of plasma flow on the Mach probes during puff and pump, could be improved by a lower deuterium flow rate, and perhaps some improved spectroscopic diagnostics.

2. We are developing improved flow diagnostics, and we need discharges to test out these techniques. Specifically, we are searching for lines to pump with a laser to do fluorescence measurements in the divertor. A fiber and spectrometer have been added to the divertor Thomson scattering system. Also, R. Isler has some ideas about using high ionization states of impurities for flow measurements.

G. **X–point physics.** Last year, we found several interesting phenomena near the X–point, which will be presented in an invited PSI paper. There are several details that need to be completed. Some of these issues involve changing the potentials near the X–point by biasing — in this case, however, we would try to apply the external potential closer to the X–point

H. (Topic grouping) **C–Mod and DIII–D edge "simularity" comparison — 1 day. After discussions with the C–Mod group, it was agreed that this topic was very important, but we could not agree on exactly what experiment should be performed. These discussions will continue.**

Several divertor/SOL parameters are quite different on the two machines, including: 1) midplane pressure is high on C–Mod, low on DIII–D, 2) ionization source is believed to be primarily from the divertor on DIII–D, the main chamber is thought to be a large source on C–Mod, 3) a baffled divertor on DIII–D reduced the core ionization by about a factor of 2–3, baffles did not make large changes on C–Mod.

Exact experimental conditions are yet to be determined, but the idea is to try to obtain some overlap of conditions (particularly main chamber edge pressure) so that SOL and divertor parameters can be compared.

4.2.4. Heating and Current Drive — 3 Days Work in Thrust 9 (Leader: R. Prater)

Three-Year Goals

1. Establish predictive capability for ECCD, including dependencies on density, temperature, Z_{eff}, geometry, power density, trapping, and dc electric field. Determine the effect of H–mode and ELMs.

2. Advance the physics understanding of FWCD, including effects of frequency, $n_{||}$, competing edge losses, high harmonic cyclotron absorption on beam ions and thermal ions, rf-induced resonant ion transport, wave propagation, conservation of toroidal mode number.
3. Complete the understanding of NBCD, including the effects of fast particle modes and TAE modes.
4. Develop long pulse discharges with full noninductive current drive, including discharges with very high bootstrap fraction as a step toward transformerless operation.
5. Develop routine electron heating using the ICRF system, through fast wave and/or second harmonic hydrogen minority heating (especially at high density where beam penetration is poor.)
6. Develop minority heating for sawtooth stabilization and minority or beam ion current drive.

Prioritized List of Experiments for 2000

In the 2000 experiment campaign, the focus of effort is on ECH/ECCD, which is the first goal. New capabilities in the ECH area (tested in Thrust 9) and needs in the program for a predictive capability for ECH/ECCD drive this appraoch. The two highest priority activities in this topical area are the study of the effect of collisionality and power density on ECCD (2 days) and the study of ECCD in H–mode plasmas (1 day).

1. **Effect of collisionality and power density on ECCD.** This experiment on the effect of collisionality on ECCD will help explain the surprising results found in last year's experiments, that the decrease in the efficiency of ECCD due to electron trapping as the driven current is moved further off-axis is much weaker than theoretically expected. An understanding here is needed in order to support the application of ECCD to objectives like stabilization of neoclassical tearing modes or sustainment of off-axis plasma current for AT program purposes. (2 days)

2. **Validation of ECCD in ELMing H–Mode.** Validation of ECCD in ELMing H–mode plasmas is needed to resolve the issue of the degree of achievable power deposition localization in the presence of ELM effects on ray trajectories. Since the AT target plasmas will typically be in ELMing H–mode, an understanding of the ray propagation properties under these conditions is important. (1 day)

If contingency time becomes available, the first experiment to be added to the list is:

3. **Neutral Beam Current Drive.** NBCD is needed for realization of the AT scenarios. The actual profile of NBCD appears to be broader than predicted. Experiments are needed to clarify the mechanism by which the broadening takes place in order to increase the confidence in the models. (1 day)

4. **Transformerless Startup.** Transformerless startup is needed by low aspect ratio tokamaks since space near the centerpost is too valuable for a ohmic heating coil. Two experiments are proposed. In the first, the outer poloidal field coils are used to provide an electric field which drives the plasma current to intermediate values of current, around 150 kA. The experiment is to validate the models which have been developed and to study the transition to a magnetic configuration like that of a conventional tokamak equilibrium. (1 day) The second experiment is to apply strong electron heating from the ECH system to drive a large electron temperature gradient, which in turn generates a strong bootstrap current. Under some conditions, the bootstrap fraction may be larger than unity, and the total current increases. (1 day).

4.3. DETAILED SCHEDULE OF EXPERIMENTS

Date	Time	Exp Number	Description	Author
2/7/00	0800	2000-08-011	Shape Control Development for AT Divertor Day 1	Hyatt
2/8/00	0800	2000-22-031	Edge Er Structure and GradB effect on L->H	Carlstrom
2/9/00	0800	2000-08-012	Shape Control Development for AT Divertor Day 2	Hyatt
2/10/00	0800	2000-08-021	Quantify Upper Pump Exhaust Efficiency Day 1	Mahdavi
2/10/00	1700	2000-09-011	ECH System Conditioning - Day 1	Prater
2/12/00	0800	2000-97	Weekend	
2/14/00	0800	2000-08-022	Quantify Upper Pump Exhaust Efficiency Day 2	Mahdavi
2/15/00	0800	2000-22-051	NonDimensional Scaling of Turbulence - Day 1	McKee
2/16/00	0800	2000-08-023	Quantify Upper Pump Exhaust Efficiency Day 3	Mahdavi
2/17/00	0800	2000-23-011	Upper Divertor Experiments at High Density - Day 1	Allen
2/17/00	1700	2000-99-011	T.B.D.	
2/19/00	0800	2000-97	Weekend	
2/21/00	0800	2000-21-011	NTM Threshold and Polarization Drift	LaHaye
2/22/00	0800	2000-02-011	Re-establish 1999 High Performance Scenario	Luce
2/23/00	0800	2000-08-031	Optimize Density Control in DND Day 1	Mahdavi
2/24/00	0800	2000-98-011	Scheduled Contingency Day	
2/25/00	0800	2000-98-011	Scheduled Contingency Day	
2/26/00	0800	2000-96	Maintenance Period	
3/13/00	0800	2000-04-011	Active Control of the RWM - Day 1	Navratil
3/14/00	0800	2000-08-032	Optimize Density Control in DND Day 2	Mahdavi
3/15/00	0800	2000-04-012	Active Control of the RWM - Day 2	Navratil
3/16/00	0800	2000-08-041	Puff and Pump at Low Density	Wade
3/16/00	1700	2000-09-011	ECH System Conditioning - Day 1	Prater
3/18/00	0800	2000-97	Weekend	
3/20/00	0800	2000-23-012	Upper Divertor Experiments at High Density - Day 2	Allen
3/21/00	0800	2000-22-061	Core Barrier Formation - Day 1	Burrell
3/22/00	0800	2000-02-021	Density/Impurity Control with AT Pumping - Day 1	Wade
3/23/00	0800	2000-02-022	Density/Impurity Control with AT Pumping - Day 2	Wade
3/23/00	1700	2000-09-011	ECH System Conditioning - Day 1	Prater
3/25/00	0800	2000-97	Weekend	
3/27/00	0800	2000-04-013	Active Control of the RWM - Day 3	Navratil
3/28/00	0800	2000-23-031	Pumping Necessary for Greenwald?	West
3/29/00	0800	2000-04-014	Active Control of the RWM - Day 4	Navratil

Date	Time	Exp Number	Description	Author
3/30/00	0800	2000-21-031	Controlled Kr Radiation and ELMs	
3/30/00	1700	2000-09-011	ECH System Conditioning - Day 1	Prater
4/1/00	0800	2000-97	Weekend	
4/3/00	0800	2000-23-021	Carbon Sources and Transport - Day 1	West
4/4/00	0800	2000-22-081	RI-mode Physics	Murakami
4/5/00	0800	2000-98-011	Scheduled Contingency Day	
4/5/00	1300	2000-98-011	Scheduled Contingency Day	
4/6/00	0800	2000-98-011	Scheduled Contingency Day	
4/6/00	1300	2000-98-011	Scheduled Contingency Day	
4/7/00	0800	2000-98-011	Scheduled Contingency Day	
4/8/00	0800	2000-96	Maintenance Period	
5/1/00	0800	2000-04-021	Lower DeltaB_r Detection Threshold	Navratil
5/2/00	0800	2000-09-012	ECH System Conditioning - Day 2	Prater
5/3/00	0800	2000-04-031	RWM Physics; Rotation Effects - Day 1	Navratil
5/4/00	0800	2000-23-041	DIMES (two 1/2 days requested)	Whyte
5/4/00	1300	2000-09-012	ECH System Conditioning - Day 2	Prater
5/6/00	0800	2000-97	Weekend	
5/8/00	0800	2000-09-013	ECH System Conditioning - Day 3	Prater
5/9/00	0800	2000-04-032	RWM Physics; Rotation Effects - Day 2	Navratil
5/10/00	0800	2000-09-021	Effect of Collisionality on ECCD - Day 1	Luce
5/11/00	0800	2000-09-022	Effect of Collisionality on ECCD - Day 2	Luce
5/13/00	0800	2000-97	Weekend	
5/15/00	0800	2000-21-091	MIMO! - Request 6 X 2 hour increments	Walker
5/15/00	1300	2000-23-041	DIMES (two 1/2 days requested)	Whyte
5/16/00	0800	2000-09-031	ECCD in H-mode Petty	
5/17/00	0800	2000-02-031	Current Profile Sustainment and Control - Day 1	Luce
5/18/00	0800	2000-98-011	Scheduled Contingency Day	
5/19/00	0800	2000-98-011	Scheduled Contingency Day	
5/20/00	0800	2000-96	Maintenance Period	
6/5/00	0800	2000-21-021	Active ECCD Stabilization of NTM - Day 1	LaHaye
6/6/00	0800	2000-02-032	Current Profile Sustainment and Control - Day 2	Luce
6/7/00	0800	2000-21-022	Active ECCD Stabilization of NTM - Day 2	LaHaye
6/8/00	0800	2000-21-041	Rapid Impurity Transport in Disruption	Whyte
6/8/00	1700	2000-09-013	ECH System Conditioning - Day 3	Prater
6/10/00	0800	2000-97	Weekend	

Date	Time	Exp Number	Description	Author
6/12/00	0800	2000-02-033	Current Profile Sustainment and Control - Day 3	Luce
6/13/00	0800	2000-02-051	Scale-Up to 1.6MA/2.1T and Edge Stability	Luce
6/14/00	0800	2000-04-041	Active Control of Locked Modes	Navratil
6/15/00	0800	2000-21-061	Validate Resistive Interchange Mode Theory - Day 1	
6/15/00	1700	2000-09-013	ECH System Conditioning - Day 3	Prater
6/17/00	0800	2000-97	Weekend	
6/19/00	0800	2000-22-011	Avalanches in L-Mode	Politzer
6/20/00	0800	2000-22-041	Heat Pinch Physics	Petty
6/21/00	0800	2000-22-021	Electron vs Ion Physics in H-Transition	Thomas
6/22/00	0800	2000-98-011	Scheduled Contingency Day	
6/23/00	0800	2000-98-011	Scheduled Contingency Day	
6/24/00	0800	2000-96	Maintenance Period	
7/14/00	0800	2000-99-011	T.B.D.	
7/17/00	0800	2000-07-011	Optimize Counter NBI Generated ITBs - Day 1	Greenfield
7/18/00	0800	2000-22-071	Controlled Density ELM-free H-mode	Burrell
7/19/00	0800	2000-07-012	Optimize Counter NBI Generated ITBs - Day 2	Greenfield
7/20/00	0800	2000-07-021	Neon-Puffing to Improve ITB - Day 1	Greenfield
7/21/00	0800	2000-98-011	Scheduled Contingency Day	
7/22/00	0800	2000-97	Weekend	
7/24/00	1300	2000-99-011	T.B.D.	
7/25/00	0800	2000-22-091	Test of Transport Models with Modulated ECH	DeBoo
7/26/00	0800	2000-22-101	experiment tbd	Burrell
7/27/00	0800	2000-98-011	Scheduled Contingency Day	
7/27/00	1700	2000-09-013	ECH System Conditioning - Day 3	Prater
7/29/00	0800	2000-97	Weekend	
7/31/00	0800	2000-02-041	Real-Time Beta and/or q Control	Luce
8/1/00	0800	2000-02-061	Integrated High Performance AT Demo	Luce
8/2/00	0800	2000-98-011	Scheduled Contingency Day	
8/3/00	0800	2000-98-011	Scheduled Contingency Day	
8/4/00	0800	2000-98-011	Scheduled Contingency Day	
8/5/00	0800	2000-96	Maintenance Period	

4.4. THE 2000 OPERATIONS SCHEDULE

The operations schedule is designed for efficient and safe use of the DIII–D facility. Sixteen weeks of plasma physics operations is scheduled for the calendar year 2000. The plan is to have five 3- or 4-week run periods. The operations schedule is shown in Fig. 23. Operations are carried out on either 4 or 5 days per week for 8.5 hours. Typically on four-day weeks, on one day operations are extended for 10.5 hours to allow longer experiments to reach completion.

The plan takes into consideration factors such as efficient matching of the machine run time with the availability of hardware and data analysis capabilities. Above all, the DIII–D program is carried out to keep radiation exposure to employees and to the general public. As Low As Reasonably Achievable (ALARA) and still carry out the research program.

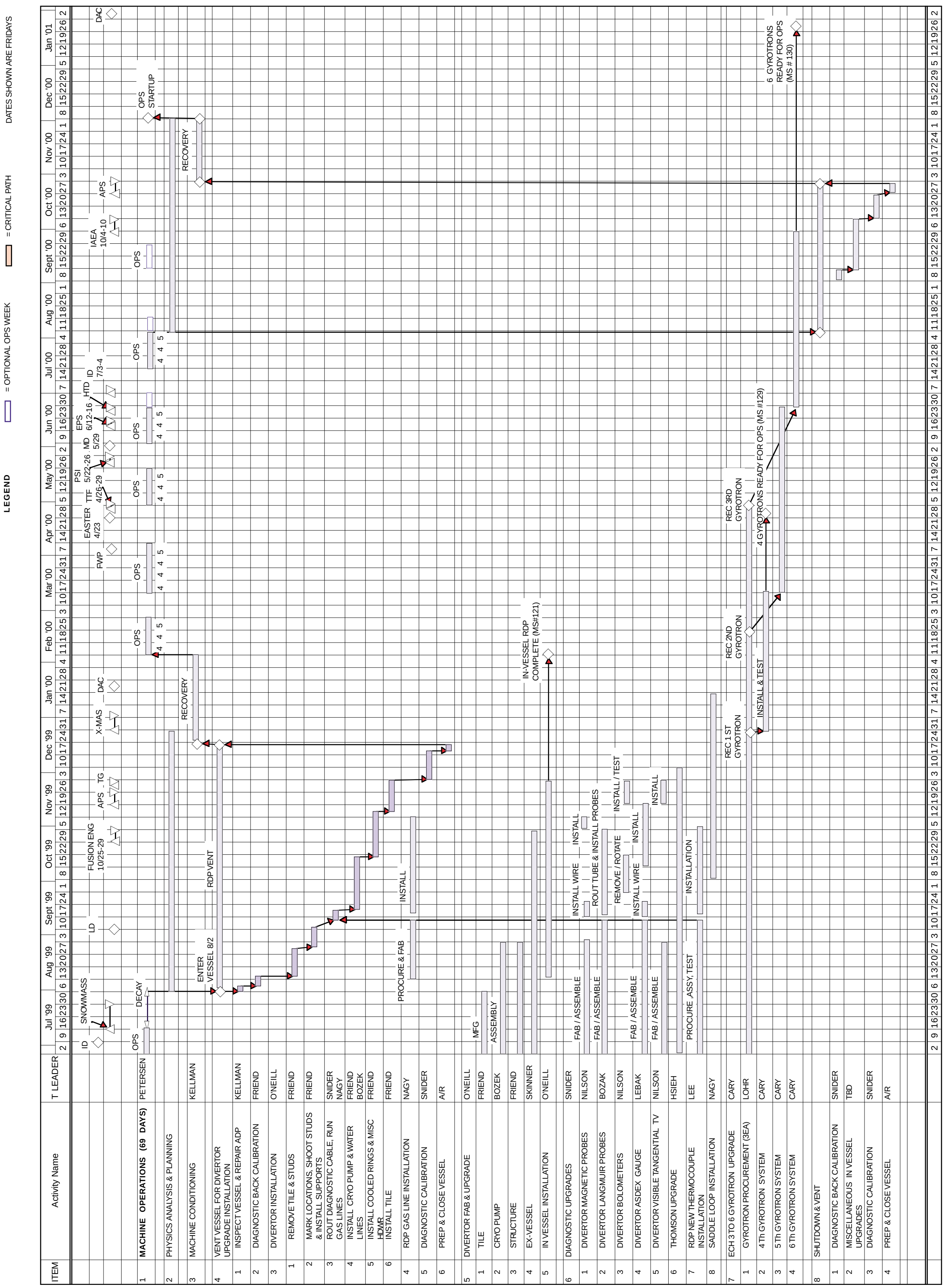

Fig. 23. DIII–D Master Schedule CY2000 16 Week Plan (With 18 Week Option).

ACKNOWLEDGMENT

This is a report of work supported by the U.S. Department of Energy under Contract No. DE-AC03-99ER54463.

APPENDIX A: RESEARCH COUNCIL LIST

Research Council Membership
2000 Campaign

July 1999 to July 2000

R. Stambaugh (Chair)
J. deGrassie (Experiment Coordinator)

At-Large Members
J. DeBoo
R. Groebner
C. Greenfield
L. Johnson
L. Lao
R. Moyer
M. Murakami
R. Perkins
C. Petty
P. Politzer
C. Rettig
A. Turnbull
R. Waltz
P. West

Thrust Leaders
E. Doyle
J. Ferron
A. Garofalo
R. La Haye
J. Lohr
T. Luce
M.A. Mahdavi
J. Navratil
M. Okabayashi
E. Synakowski
M. Wade

Standing Members
S. Allen
D. Baldwin
K. Burrell
V. Chan
R. Callis
A. Hyatt
A. Kellman
J. Luxon
P. Petersen
R. Prater
D. Schissel
R. Snider
E. Strait
T. Taylor
T. Simonen